Using Surface Geopolymerisation Reactions to Strengthen Athabasca Oil Sands Mature Fine Tailings

by

Saeed El Khair Nusri

A thesis submitted in partial fulfillment of the requirements for the degree of

Master of Science

in

Chemical Engineering

Department of Chemical and Materials Engineering
University of Alberta

Abstract

Bitumen extraction from oil sands operation in Fort McMurray, Canada produces an immense quantity of slurry waste that is discharged to tailings ponds. These ponds now stretch over a region which is roughly 1.5 times the area occupied by Vancouver city mainly due to slow consolidation process of the mature fine tailings (MFT). The MFT comprises of a mixture of water and fine solids that is characteristically known for very low shear strength. While the current research on tailings consolidation has been focused on removing water from the settled tailings sludge, there is presently no known technology to effectively consolidate tailings and strengthen it for land reclamation.

This dissertation describes a novel method to address the oil sands tailings reclamation problems using surface geopolymerisation reactions. Geopolymerisation involves dissolution of aluminosilicates and re-solidification reactions that result in the formation of three dimensional inorganic polymers, which have significant strengths. Since the fine solids in oil sands mature fine tailings (MFT) mainly consist of aluminosilicate minerals (clays), it is hypothesized that by adding appropriate reagents, the surfaces of the clay minerals can be activated to go through geopolymerisation reactions. The resulting geopolymers formed on the surfaces of the clay minerals bind the clay particles together and strengthen the tailings even without further dewatering and consolidation.

Characterizations conducted on kaolinite samples, which was chosen as model solids for MFT, showed that under the test conditions the geopolymerisation reactions only occurred on the surface of the kaolinite mineral. The “surface geopolymers” held the kaolinite particles together leading to an increase in shear strength.

The results also indicate that shear strength of MFT is considerably increased on addition of NaOH and Na_2SiO_3, or alkali activators, at the optimum dosage. When a 51 wt% solids centrifuged MFT was treated with 1 mole/L sodium hydroxide and 0.5 moles/L sodium silicate, it was found that the shear strength increased from 115 Pa to 4,880 Pa after 90 days. At the same activator concentrations, the original un-centrifuged MFT (37.9 wt% solids) saw an increase of its shear strength from 19 Pa to 1,245 Pa. Similarly, the shear strength of a 48 wt% solids MFT sample flocculated by adding 1000 g/t of A3335 polymer flocculant increased from 395 Pa to 3,950 Pa 90 days after the addition of the same concentration of alkali activators. Addition of A3335 polymer flocculant to the MFT is observed to hamper the surface geopolymerisation process leading to a lower than expected increase in shear strength. However, low capillary suction time is seen when coupling flocculation with surface geopolymerisation, indicating that the treated MFT is amenable for water release.

To mom, dad, Anne and Naamah

Acknowledgement

To begin with, my deepest gratitude goes to my supervisor, Dr. Qi Liu, for his invaluable guidance and support throughout the course of my research. I would also like to thank my co-supervisor, Dr. Phillip Choi, who always had his office doors open for immediate assistance and advice.

In addition, Dr. Xiaoli Tan has been most instrumental in guiding me through the technicalities of my research. His amicable personality and his readiness to engage in a variety of new experimental ventures made my research experience a truly memorable one. I genuinely thank him for his advice, guidance, and help.

In addition, I am downright grateful to Mirjavad Geramain, who took out time from his busy schedule to assist me in the sample preparation and analysis of quantitative XRD characterization. I am also thankful to the lab technicians, Jeremiah Bryksa and Lisa Brandt, for providing me with the necessary training and instruments to successfully run my experiments.

I would also like to acknowledge the financial support from Canada's Oil Sands Innovation Alliance (COSIA), and the Institute for Oil Sands Innovation (IOSI). The provision of mature fine tailings from Syncrude Canada Limited from its Fort McMurray operations is acknowledged too.

I am also very grateful to all my fellow graduate students. Their companionship made graduate school a fun and a stimulating place to be. However, I express my special gratitude to Sarang Gumfekar for his camaraderie and his integral support in providing me with valuable insights to my research and thesis.

Finally, I thank Mubaraka Husain, whose friendship, love and support helped me through the course of my masters. And above all, I thank my doting parents, Umme Hani and Najmuddin Nusri, and my sisters, Anne and Naamah. Their confidence in me has been paramount to all the accomplishments in my life. To them, I dedicate this thesis.

Table of Contents

List of Figures

List of Tables

Chapter 1

Introduction

1.1 General statement

Canadian oil sands deposits of northern Alberta consist of vast hydrocarbon deposits that occupy an area of around 142,000 km^2. While this amounts to 293.1×10^9 m^3 of bitumen in-place, only 28.1×10^9 m^3 of the crude bitumen have been deemed as economically recoverable based on current unconventional oil production technology (AER, 2014). Currently, bitumen is extracted through either in-situ method or open pit mining method.

In open pit mining method, the oil sands ores are mined and processed to extract bitumen and remove sand, water, mineral particles and other materials. The extraction of bitumen from oil sands through surface mining results in slurry tailings with high water content that are pumped in large quantities to surface tailings ponds. The tailings are composed mainly of sands, clays and other minor minerals, water, and unrecovered bitumen. Upon discharging to the tailings ponds, the sand aggregates settle quickly, while the fine particle slurry, also called the thin fine tailings (TFT), moves towards the center of the tailings ponds (BGC Engineering Inc., 2010). After 2 to 3 years, the tailings gradually settle to the bottom of the tailings ponds from 8 percent solid content to 30 percent solid content to form the mature fine tailings (MFT). MFT is characteristically known for its poor water release ability, poor consolidation, low permeability and low shear strength.

It is because of this nature of the MFT that has ensued in the inevitable growth of the tailings ponds across the Fort McMurray region where the oil sands operations are taking place,

such that now they cover a total area of more than 176 km^2 (CAPP, 2015). This has caused serious environmental concerns regarding their effects on public health, land use, water supply and air quality. Subsequently, various regulations and requirements have been put in place. One of the most significant regulations pertinent to this thesis research is the Alberta Energy Regulators Directive 074 established in 2009 (Alberta Energy Regulator, 2009).

The main objectives of oil sands tailings management is to consolidate MFT such that its load bearing surface is trafficable and the dedicated disposal areas (DDAS) are substantially reduced. In order to determine the ideal technique for tailings management, it is imperative to gauge the consolidation rates and shear strength of MFT before and after treatment. At the same time, treatment time and expenses are two important factors that should be taken into consideration during the evaluation process for the consolidation and strengthening techniques.

1.2 Objective and scope of Thesis

The purpose of the present study is to determine the feasibility of a novel method for consolidating and strengthening MFT using geopolymerisation so that it meets the requirements of Directive 074. Geopolymerisation has been used in past to treat copper mine tailings but the concept is relatively new for Albertan oil sands tailings.

Hence, the first objective will be to determine if geopolymerisation would work on oil sands tailings. This will require adding reagents, or alkali activators, that will initiate geopolymerisation in MFT and recording the increase in strength. Once determined, the next step would be to optimize the concentration of the activators so that an acceptable strength can be achieved. This will ensure that the requirement of Directive 074 is met with the best economics.

Besides, in order to understand the strengthening mechanism, a simplified model system for MFT will be chosen. Fundamental characterization will be carried out with the model system to understand the behavior of the geopolymerised sample.

Finally, in order to simulate industrial scenarios, geopolymerisation will be carried out on different types of MFT, with varying solid content and with or without polymer treatment, to gauge the load bearing performance of the reacted MFT.

In order to achieve the objectives of this thesis, sodium hydroxide and sodium silicate are determined as alkali activators. Also, kaolinite is chosen as a model solid to emulate MFT because it is the most abundant aluminosilicate mineral found in MFT. Shear strength is measured for both the model system and MFT samples. The shear strength measurements are carried out using ASTM D2573 standard. Fourier transform infrared spectroscopy (FT-IR), inductively coupled plasma spectrophotometer with optical emission spectroscopy (ICP-OES), laser particle size distribution, quantitative X-ray diffraction (XRD), and transmission electron microscopy with selective area electron diffraction and energy dispersive X-ray (TEM/SAED/EDX) are used to examine and understand the behavior of the formed geopolymers from kaolinite. Dewaterability of the treated MFT is also studied using capillary suction time apparatus. Experimentation and most characterizations are carried at the Institute for Oil Sands Innovation at the University of Alberta.

1.3 Organization of thesis

This thesis is divided into five chapters. While Chapter One gives an introduction to the thesis, Chapter Two focuses on literature review. Eight sections are included in Chapter Two: Section One discusses the Canadian oil sands resources; Section Two introduces currently used

oil sands extraction technologies; Section Three provides an introduction to tailings surface ponds, MFT and their characteristics; Section Four discusses Alberta's regulatory requirement for tailings management; Section Five provides an overview of current challenges and opportunities in tailings management; Section Six elaborates exclusively on geopolymerisation; Section Seven mentions the aluminosilicate minerals present in oil sands tailings; and finally, Section Eight briefs on how geopolymerisation can be applied to oil sands tailings.

Chapter 3 elaborates on the Materials and Experimental method. Section one states the materials used and Section Two details on the experimental method. Subsequently, Section Three explains the various analytical techniques used in strength measurement and characterization.

Chapters 4 then discusses the results obtained from shear strength measurements of both MFT and kaolinite, and expounds on the results of characterization of kaolinite. Also, Section 2 of this chapter further elaborates on the difference in shear strength measurement between different types of MFT and briefly discusses their dewaterability.

Finally, conclusions and scope of further research have been discussed in Chapter 5 and Chapter 6, respectively. Table of shear strength measurements, preliminary compressive strength measurement data and other relevant photos from the study have been included in Appendix B.

Chapter 2

Literature Review

2.1 Canadian oil sands

Oil sands resources of Canada comprises of a significant proportion of unconventional oil reserves in the world, with deposits covering over an area of 142,000 km^2 (NEB, 2004). These reserves are spread over northern Alberta region and, based on their geology, geography and bitumen content, are mainly located in three principal areas: Athabasca, Peace River and Cold Lake.

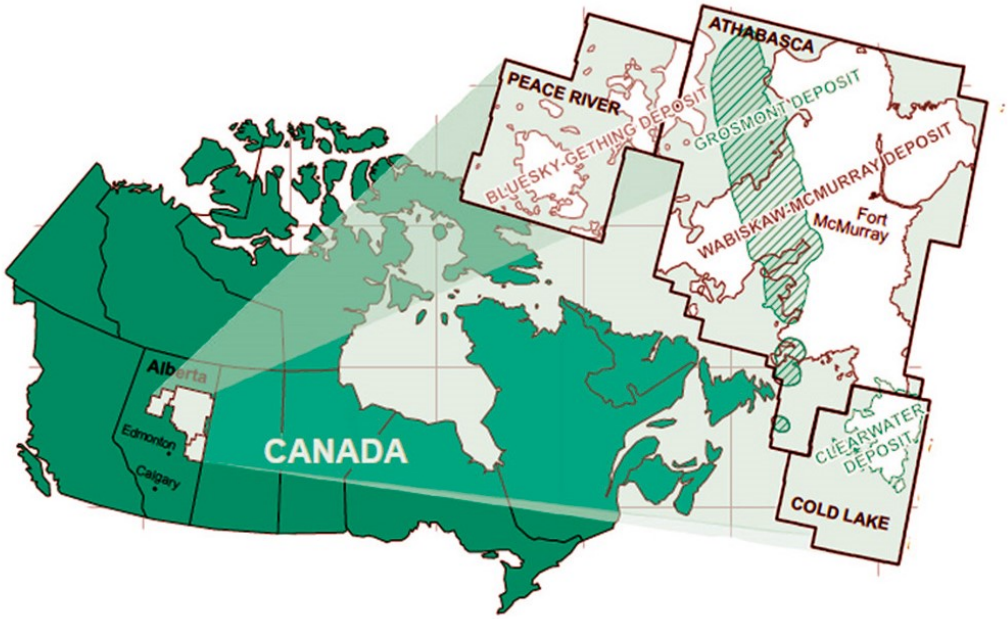

Figure 1: Areas in Northern Alberta with oil sands deposits (AER, 2014)

Alberta Energy Regulator (AER) has estimated the total initial volume in place for oil sands to be 293.1 billion cubic metres, from which 20.8 billion cubic metres can be surface mined and the remaining 272.3 billion cubic metres are categorized as amendable to in situ

recovery methods. Deposits are classified as in situ or mineable based the thickness of the overburden above the deposits (Masliyah et al., 2011). Oil sands operation first started in 1967 with the Great Canadian Oil Sands project. Today, it has become one of the biggest bitumen extraction industries in the world with a myriad of companies directly or indirectly involved in operations. It has been forecasted that the production would increase from 1.9 million barrels per day (MBPD), as recorded in 2012, to 3.7 MPBD by 2020 (Chalaturnyk et al., 2002). Table 1 shows the amount of initial volume of bitumen in place, established reserves and production change highlights of crude bitumen reserves at the end of 2013 (AER, 2014).

Table 1: Initial volume In-place, established reserves and production highlights of crude bitumen reserve at the end of 2013 (unit: million m^3) (AER, 2014)

Resource type	Initial Volume in Place	Initial Established Reserves	Cumulative Production	Remaining Established Reserves	Annual Production
Mineable	20,800	6,157	931	5,226	57
In situ	273,300	21,935	596	21,339	64
Total	293,000	28,092	1,527	26,565	121

Rich grade oil sands ores comprise of approximately 85 wt% solids, which include sands and fine clays, and 8-14 wt% bitumen, with a small amount of water. The water in oil sands is likely present either as clusters or as 10 nm thin film covering the sand particle (NEB, 2000; Shaw et al., 1996; Takamura, 1982). Figure 2 illustrates a diagram of the Athabasca oil sands structure.

The oil sands bitumen is trapped among the sand particles that are surrounded by a film of water. This water film is stabilized by an electrical double layer between water-bitumen and sand-water. However, the bond between water and bitumen is weaker compared to that between sand and the water film, allowing the bitumen to be recovered by the use of water-based extraction process (Shaw et al., 1996).

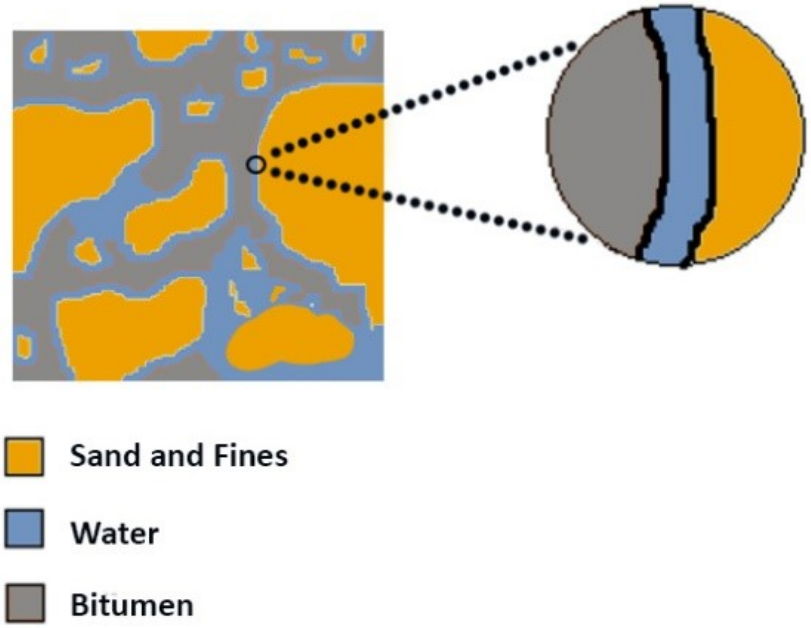

Figure 2 : A representative illustration of Athabasca oil sands (Takamura, 1982)

The quality of oil sands deposits are based on its bitumen content and can be classified into three main categories (Ng et al., 2000):

- Rich grade: 13-16 wt% bitumen
- Medium grade: 10-12 wt% bitumen
- Low grade: 7-9 wt% bitumen

Bitumen content lower than 7 wt% is not considered ore-grade as the production is not considered to be economically viable.

The oil sands bitumen is very heavy and has a higher specific gravity than water, unlike other types of oils (Chastko, 2004). The scale for density measurement for oil in the petroleum industry is defined by ^{o}API given by Equation (1) (ASTM-IP D1250, 1952):

$$°\text{API} = \frac{145}{\text{specific gravity at } 15.6°\text{C}} - 131.5 = \frac{1.415 * 10^5}{\rho(\text{kg} * \text{m}^{-3})} \quad (1)$$

Bitumen with high °API is ideally desired. If it has high dynamic viscosity (> 100 cP) and °API lower than 22.3, it is considered to be heavy (Masliyah et al., 2011).

The Canadian bitumen is about 6 to 12 °API and is highly viscous in nature. But its viscosity drops immensely with temperature (Figure 3). The dynamic viscosity (μ) of bitumen is about 10^6 cP at reservoir temperature making it practically immobile, but this also gives oil sands enough strength to make it mineable. Also, to make bitumen easy to transport, bitumen is diluted using natural gas condensates such as naphtha. The diluted bitumen is also referred to as dilbit.

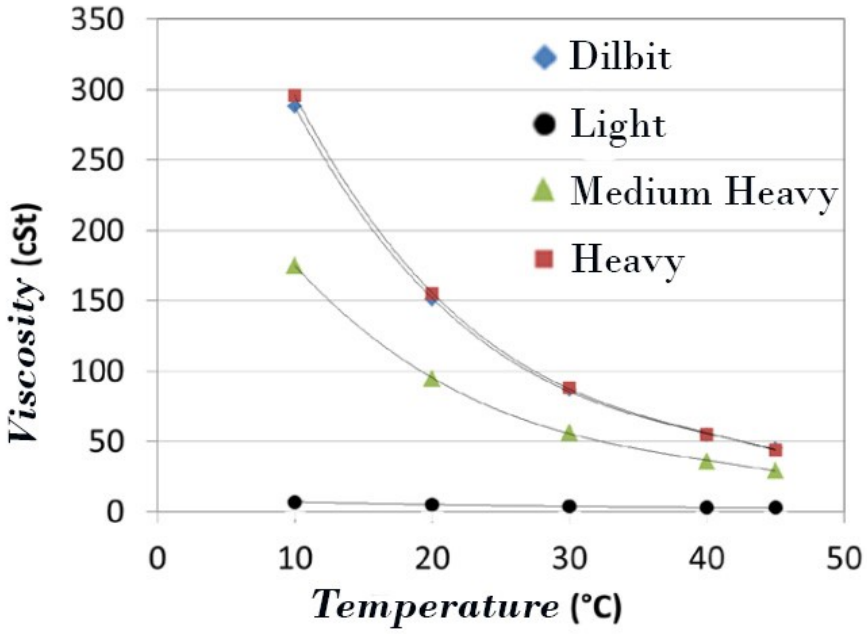

Figure 3: Comparison of temperature dependent viscosity in centistokes (1cSt = specific gravity of bitumen * cP) of dilbit with light, medium-heavy and heavy conventional oil (Tsaprailis & Zhou, 2013)

The Canadian Association of Petroleum Producers (CAPP), which represents member companies responsible for producing about 90 per cent of Canada's natural gas and crude oil, claim that the blend made from bitumen and a diluent should have a density less than 800 kg/m^3 to meet the pipeline viscosity and density specifications (CAPP, 2015). Figure 3 displays a graph of dynamic viscosity of dilbit as a function of temperature and compares it to other conventional crude oil (Tsaprailis & Zhou, 2013).

2.2 Surface mined oil sands extraction

Oil sands deposits having less than 75 meters of overburden are excavated by open pit surface mining, and then bitumen is extracted using Clark Hot Water Extraction (Masliyah et al., 2011). Once the deposit is designated for open pit mining, layers of muskeg and surface vegetation are first removed. Then the overburden under the muskeg, consisting of rocks, sands and clay, are removed to reveal the oil sands deposit underneath (NEB, 2000). The mined ores are transported to massive double roll crushers using large transport trucks and power shovels, where the ore is crushed to about 45 cm. A typical transport truck has the capability of carrying as much as 400 tonnes of oil sands in a single trip. The crushed ore is then transferred to a storage silo using capacity conveyor belts and later mixed with warm water (45°C to 55°C) at a pH between 7 and 8.5 in rotary drum blenders. The resulting slurry is then hydrotransported to the extraction facility. The concept of mixing the oil sands ore with water and caustic comes from the Clark Hot Water Extraction (CHWE) process, developed by Karl Clark, who started experimenting the process from the 1920s (Clark & Pasternack, 1932).

At the extraction facility, the conditioned ore mixture is then stored in large separation vessels, called primary separation vessels (PSV), where the various components of oil sands ore are separated. The heavier components along with any sediment such sands and rocks settle to the bottom of the vessel while the bitumen, floats to the top. At the same time, a layer consisting of a mixture of clay, sand, water and bitumen, called the middlings, sits in the middle of the PSV. To quicken the separation process, air is sparged through the PSV, allowing bitumen droplets to attach with the air bubbles and travel upwards. The separated bitumen sits at the top of the PSV with the froth, which is skimmed off and treated further. The froth typically contains 60 vol% bitumen, 30 vol% water and 10 vol% solids. The bitumen froth is treated with solvents, like naphtha or paraffin, to separate the bitumen from water and solids.

The coarse effluent and middlings from the separation cells are sent for tailings oil recovery (TOR) where the residual oil trapped in the tailings are recovered before being directed towards large containment areas called the tailings ponds. Tailings are also generated from the froth treatment process, but has different composition and properties compared to the tailings generated from the PSV. The froth treatment tailings are rich in titanium and zirconium minerals and can be a potential source for these commodities (Liu et al., 2006). However, they comprise of water, unrecovered solvent and fine solids and are also discharged to the tailings ponds.

Though oil sands extraction is a fairly effective process with bitumen recovery exceeding 90%, the efficiency of extraction is dependent on several factors including the water chemistry, mineralogy of the ore, and bitumen chemistry (Kasperski, 2001). Figure 4 depicts a generalized process flow sheet for the warm-water extraction process used in open pit mining.

The bitumen after froth treatment is then sent for upgrading where it is refined into high quality synthetic crude. This is achieved by coking, desulphurization and hydrogen addition to the tar-like viscous bitumen (Masliyah et al., 2011). The extraction process is very water-intensive; for every barrel (0.16 m^3) of oil produced, two tonnes of ore and 2.6 m^3 of water are required. While approximately 2 m^3 of water is eventually recovered as free recycled water, the remaining water is trapped in the waste, or tailings, generated by the extraction process (MacKinnon, 1989).

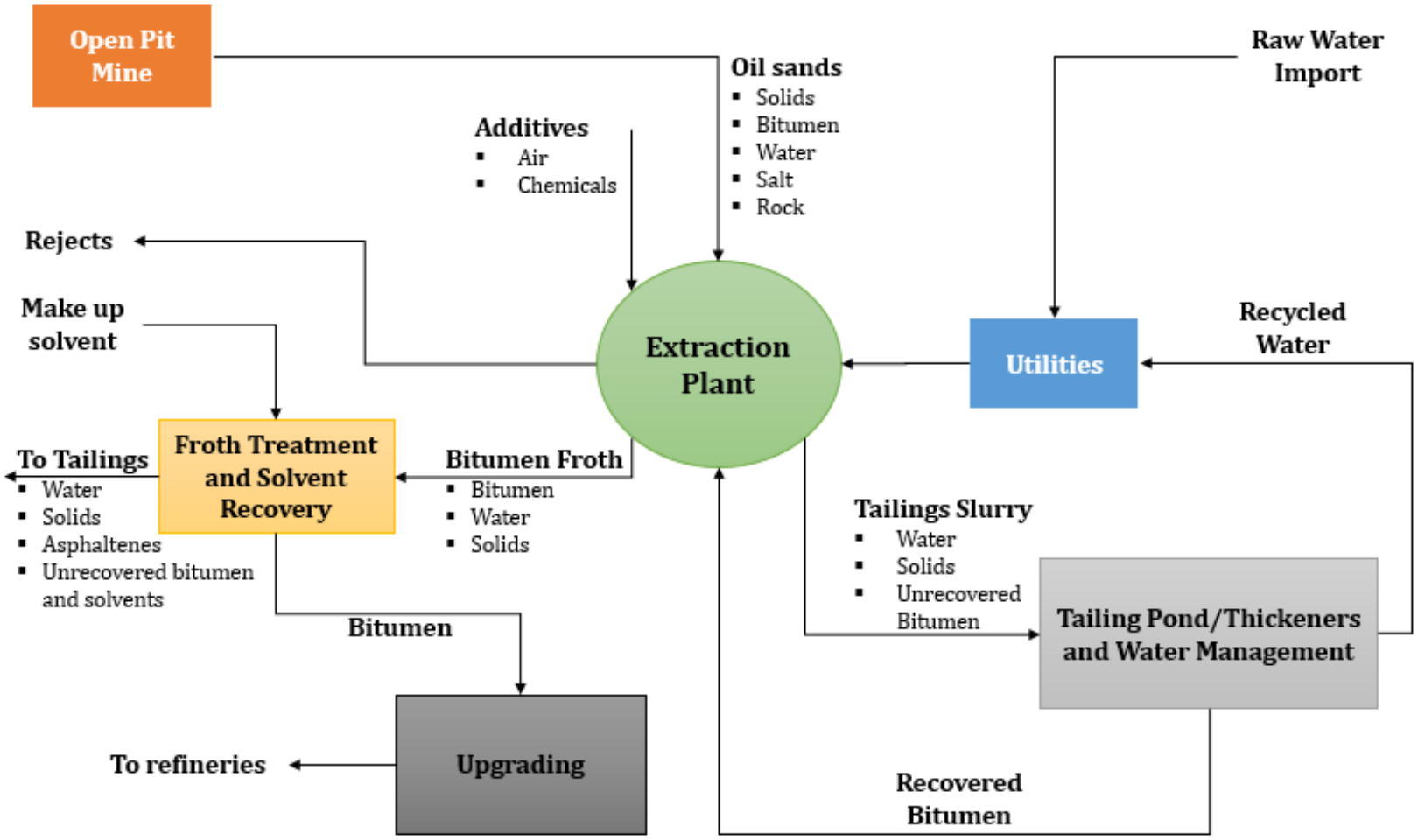

Figure 4: Generalized scheme for oil sands processing using CHWE bitumen extraction process (Masliyah et al., 2004)

2.3 Tailings ponds and mature fine tailings

As mentioned in the previous section, tailings, which are mixture of water, solids and fugitive bitumen remaining after recovery process, are referred to as tailings are discharged from the extraction plant to large containment areas referred to as tailings ponds.

The typical tailings pond is depicted in Figure 5. The coarse sands in the tailings are used in construction of the dykes and beaches of tailings ponds since they deposit rapidly. On the other hand, the fines and clays (<44 μm fraction) flow to the center of the pond as a relatively dilute slurry of approximately 8 wt% solids (BGC Engineering Inc., 2010). It takes approximately ten years for these fines to settle to about 30 wt% solids until no further consolidation takes place (Carter, 2009). Once the tailings have reached this state they are referred to as mature fine tailings (MFT). Such tailings have been found to remain stable for several decades and are characteristically known for their poor water release ability, poor consolidation, low permeability and low strength (Scott et al., 1985).

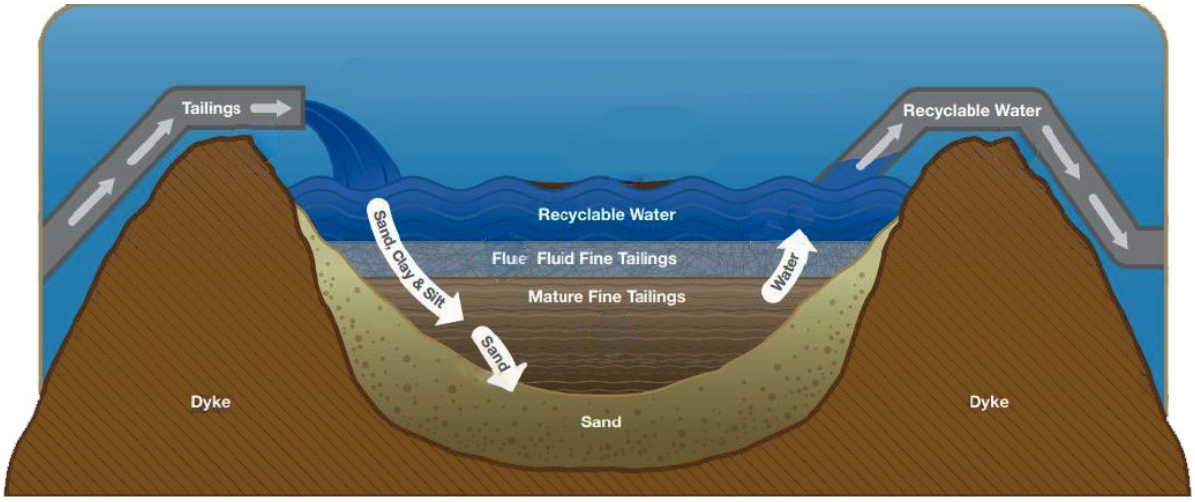

Figure 5: Typical oil sands tailings pond denoting different layers present in the pond (Government of Alberta, 2009)

It has been estimated that to produce each barrel of bitumen, 1.5 barrels of tailings wastes are generated, leading to an estimated 950,000 m^3 of tailings produced daily (Flanagan & Grant, 2013; MacKinnon, 1989). Furthermore, the slow consolidating properties of the MFT causes the accumulation of substantial volumes of fluid tailings. As of 2011, tailings ponds have displaced almost 170 km^2 of former boreal forest (WWF-Canada, 2010).

The mineralogy of MFT is an important attribute that helps to predict their behavior under different conditions. MFT consist of sand, clays, amorphous oxides, and trace metals (Mikula et al., 1996). The sand in MFT comprises 97.5-99% quartz, 0.5-0.9% of aluminum hydroxide, and 1-0.9% of iron. Clay minerals found in MFT include kaolinite and illite, with traces of smectites, chlorite, vermiculite, and mixed layer clays. The amounts and types of these clay minerals in tailings ponds may vary considerably but kaolinite and illite are the ones predominantly present. Some of the heavy metals detected in the oil sands tailings of Alberta include Ti, Zr, Fe, V, Mg, Mn, Al, Pb, Zn, Nb, and Mo. (Mikula & Omotoso, 1996)

2.4 Regulatory requirements

The water in the tailings pond contains a myriad of pollutants which are acutely toxic to the environment. Some of these pollutants include naphthenic acids, polycyclic aromatic hydrocarbons, benzene and toluene as well as inorganic elements such as lead and arsenic (Allen, 2008). Furthermore, there have been serious concerns with the expanding size of the tailings ponds which are increasingly making these areas uninhabitable (Ferguson et al., 2009). Hence, remediating the tailings problems has become necessary. In 2009, the Alberta Energy Regulator issued the Directive 074, mandating oil sands operators to reduce their tailings generated and convert the fluid tailings into trafficable deposits suitable for reclamation of the landscape. In brief, the directive states the following objectives (Alberta Energy Regulator, 2009) :

- To create trafficable landscape from the area occupied by the current ponds. The landscape should have at least 5 kPa of undrained shear strength at the end of first year and 10 kPa in 5 years
- To reduce and eventually eliminate the storage of tailings to facilitate progressive reclamation of land occupied by tailings ponds
- To maximize the water recycling and decrease freshwater consumption
- To reduce contaminants from tailings operations and reduce the impact of the pollutants on water storage areas
- To ensure that the liability is managed by oil sands operators

With Directive 074, the AER has a stringent supervision over all mining operations to eliminate growth of tailings ponds.

This has led to the active development and implementation of new tailings treatment technologies. Although many tailings treatment technologies have been studied, there has not been a single technology to completely address the tailings problem. Recently, a comprehensive report, the Oil Sands Tailings Technology Deployment Roadmap (TTDR), which listed more than 500 technologies aimed to remediate the tailings problem, was presented to Alberta Innovates Energy and Environment Solutions (AI-EES) by six leading industry consulting firms (Sobkowicz, 2012). Out of the list, only few were deemed useful and even fewer have been recently been implemented as pilot projects (BGC Engineering. July 2010). Also, to proactively address the tailings problem, seven major oil sands operators, namely Total E&P Canada, Imperial Oil, Shell Canada, Syncrude Canada, Teck Resources, Suncor Energy, Canadian Natural Resources Limited, formed the Oil Sands Tailings Consortium (OSTC) in December 2010. The focus of OSTC is to work with universities, research institutions and consultant

companies to find innovative solutions for tailings issue (Sobkowicz, 2013). Moreover, another alliance of 13 oil sands producers known as Canada's Oil Sands Innovation Alliance (COSIA) was formed in March 2012 to solve the issues of tailings, land reclamation, and greenhouse gases (GHGs) emission. The original OSTC was merged into the Tailings Environmental Priority Area of COSIA and it is now commonly referred to as COSIA Tailings EPA.

2.5 Present tailings treatment technologies

Over the years, various methods have been developed to reduce the impact of tailings and tailings pond. While many of them have remained at the laboratory scale due to certain limitations, some of them have been implemented and are currently being used to treat tailings. These techniques are categorized into five different groups (BGC Engineering Inc., 2010):

1. Physical or mechanical processes
2. Chemical or biological amendments
3. Natural processes
4. Mixtures/co-disposal
5. Permanent storage

The following are a brief description of some of the prominent tailings treatment technologies.

2.5.1 Physical or mechanical processes

2.5.1.1 Centrifuged Fine Tailings

This process uses centrifugation to separate the particles from liquid and involves two steps of separation. Firstly, an industrial centrifuge is used along with flocculants to produce two

streams: very high water content slurry with 0.5 to 1 wt% slurry and a cake with up to 60 wt% solids. The cake then undergoes further natural dewatering process, such as evaporation and freeze/thaw (BGC Engineering Inc., 2010).

The results of the laboratory and bench scale tests have turned out to be promising. Therefore, commercial-scale demonstration of the centrifuged fine tailings technology was started by Syncrude in 2012 and full-scale commercial plant is anticipated to start operations in 2015 (Syncrude, 2012).

2.5.1.2 Filtration

Filtration is one of the simple solid-liquid separation technologies and can take place using pressure or a vacuum. Filtration results in the generation of a filter cake with a significantly high solid content. The hydraulic conductivity and permeability of the cake are important variables that determine the quality and duration of the filtration. At the end of the filtration process, the filter cakes are removed for disposal or reuse in a site (BGC Engineering Inc., 2010).

The main challenge of this method is that the filter cake typically has extremely low hydraulic conductivity. However, this issue can be resolved by the addition of coagulants or flocculants. Also, filtration of tailings depends on the fine content of the tailings, with lesser fines favoring better filtration. It has been estimated that the filtration of original tailings with more than 4 wt% fine particles is industrially not practical (Xu et al., 2008).

Despite several tests and studies aimed to improve the filterability of tailings, filtration of tailings method has never been carried out to maturation due to inefficiency of the designed systems in dealing with large amounts of tailings (BGC Engineering Inc., 2010).

2.5.2 Chemical treatment (thickened tailings)

Another commonly used technology is the Thickened Tailings (TT) Technology, which is also known as gel technology. In this method, chemical additives, called flocculants, are used to flocculate the fine fractions in the tailings and release water that can immediately be reused in the extraction process. TT technology takes very little time to increase the solids content of fine fractions of the extraction process effluent to 30 wt%.

Flocculation is used to describe the process by which certain polymers can adsorb on different particles simultaneously, causing it to aggregate as loosely-bound agglomerates called floccules or flocs. Generally, flocs that are produced by polymers are strongly held together. On a microscopic level, flocculation causes fine colloidal particles to agglomerate and settle down as suspension (Xu & Hamza, 2003). However, this treatment still does not meet AER requirements and further treatment is needed. Also, the high cost and large number of educated operators are desirable. Another technical drawback is the accumulation of coarse materials at the thickeners feed well which can dramatically affect the efficiency of the process with time (BGC Engineering Inc., 2010).

2.5.3 Natural process (freeze and thaw)

Freeze-thaw dewatering is a natural process that occurs throughout Alberta's summer and winter cycles. Thin layers of MFT are frozen at low temperatures and on thawing the water separates and drains from it. The first ice aggregates that form result in negative pressure and

produce a strong suction which drives the water from tailings towards the newly formed ice. This occurs because of compaction of the solids within the ice network formed as water expands before freezing. Simultaneously, the moving mass of water creates a network of path through which the water drains while thawing (Proskin et al., 2010; Dawson et al., 1999; Johnson, 1993).

The freeze-thaw process is reported to result in low strength deposits of up to 14kPa in one year, which opens up this technology for land reclamation purposes. The process, however, is labor intensive and requires a large area to deposit the thin layers due to the long periods of each freeze/thaw cycle.

2.5.4 Mixtures/co-disposal (composite tailings process)

In the composite tailings (CT) process, a coagulant, typically gypsum is added to a mixture of coarse sand and fine tailings to form a mixture which rapidly dewaters into a dense deposit. This process has been quite effective in treatment of MFT (Mikula & Omotoso, 2006).

A possible modification to the existing CT process is to add CO_2 along with typical coagulants to further enhance the consolidation of the tailings and, simultaneously, sequester CO_2 emissions. The enhancement of consolidation by CO_2 is primarily due to the decrease in pH resulting in a reduction of zeta potential of the fine clays (Mikula et al. , 2004).

Equation (2) shows the chemical reaction that takes place on addition of CO_2 to tailings mixed with gypsum (Chalaturnyk et al., 2002):

$$Ca(OH)_2 + CO_2 \rightarrow CaCO_3 + H_2O \quad (2)$$

$CaCO_3$ would adsorb the ultrafine particles suspended in the liquid and precipitates.

Despite its efficiency, CT process has been reported to have a negative impact on the quality of water released from the tailings. The added gypsum increases the amount of calcium ions in the recycled water which is detrimental to bitumen recovery (BGC Engineering Inc., 2010).

2.5.5 Permanent storage (water capping)

Water capping involves pumping fresh water over the deposits of fine tailings to form a lake. The MFT is capped with a layer of water with a sufficient depth to prevent the layer from mixing and allowing the formation of a self-sustaining lake ecosystem.

Figure 6: Ponds utilized by Syncrude over the last two decades to test water capping technology (Syncrude, 2012)

Research has pointed out that these lakes have the capability to evolve into natural ecosystems, and support healthy communities of aquatic plants, animals and fish (BGC Engineering Inc., 2010). Figure 6 shows the image of water capped ponds developed by

Syncrude to test this technology. In 2012, demonstration of the water capping technology was commissioned in the former West Mine area (Syncrude, 2012).

Studies done in laboratories and the field scale have pointed out water capping as an efficient remediation method for addressing the issue of MFT. However, one of the disadvantages include the emission of gas by biological activity that can result in mixing of fluid tailings and overlying water (BGC Engineering Inc., 2010).

2.6 Geopolymerisation

Having been studied for only around three decades, the concept of geopolymerisation is a relatively new topic. Since this thesis focuses on assessing the feasibility of geopolymerisation in MFT, it is important to provide an introduction to geopolymers and aluminosilicate minerals, discuss the relation between the two and point out their significance to treating mature fine tailings. The following sections give an introduction to geopolymerisation and the common aluminosilicate minerals present in MFT. Also, the chemistry involved in geopolymerisation reaction has been briefly discussed to help understand the work described in this thesis.

2.6.1 Introduction to geopolymerisation

Geopolymer, a term first coined in 1976 by Joseph Davidovits, is a kind of inorganic polymer with AlO_4 and SiO_4 structurally linked in tetrahedral configuration (Davidovits, 1988). These inorganic polymers show a high potential to substitute traditional cement in the near future due to their excellent mechanical strength and fire, acid and bacterial resistance properties (Davidovits, 1991, 1994). Besides, geopolymers can be produced from waste materials like fly ash, furnace slag, construction waste and, more importantly, tailings. Because of this attribute,

manufacturing of geopolymer can be environmentally friendly because it can help with waste management and, simultaneously, reduce greenhouse gas emission by cutting down the CO_2 produced from the manufacture of Portland cement (Duxson et al., 2007). Because of these advantages, geopolymerisation have been studied for past few years and the techniques of manufacturing geopolymers have moved from using solely kaolinite and metakaolinite as source material to any material containing silicon and aluminum. Naturally occurring aluminosilicate minerals are the most abundant Al and Si sources existing in the world.

2.6.2 Aluminosilicates and geopolymers

Both silicon and aluminium are the most common elements existing on earth comprising of more than three quarters of the continental crust (Dietrich & Skinner, 1979). Silicon has the oxidation state +4 which means that each silicon atom is nearly always found bonded to four oxygen atoms under normal conditions of temperature and pressure. Thus, a single unit of Si found in silicates and aluminosilicates simply exists as SiO_4. The tetrahedral units of Si have a strong tendency to polymerise each other by eliminating one oxygen and sharing another one to form silicate minerals.

Aluminium is a highly electropositive element and it occurs exclusively as Al^{3+} in combination with oxygen atoms (Cox, 1995). As the covalent radii for silicon is smaller than aluminium (1.17 Å and 1.26 Å, respectively), it is possible for Si atoms to be replaced by Al atoms during polymerisation of SiO_4 from the view point of the atomic size (Atkins, 2010). However, the negative charge will increase; for instance the layer $[Si_2O_5]^{2-}$ becomes $[Si_3AlO_{10}]^{5-}$ when one in four silicon atoms is substituted by aluminium. In this case, other positive metal

ions are needed to balance the net charge, giving aluminosilicates an enormous variety of formulae and structures.

Loewenstein has indicated (Lowenstein, 1954) that the substitution of silicon in three-dimensional frameworks and plane networks of tetrahedral aluminosilicate oxide by aluminium cannot exceed 50%. Hence, aluminosilicate minerals with tetrahedral framework and plane network structured are always silicon rich minerals.

Silicon is always tetrahedrally structured as SiO_4^-, while aluminium can exist in tetrahedral or octahedral configuration. For most of octahedral structured aluminosilicate minerals, for instance, andalusite (Al_2SiO_5), and mullite ($Al_6Si_2O_{13}$), there can be more Al than Si atoms (Deer et al., 1992).

Aluminosilicate minerals are a large group of minerals that comprise Al and Si oxides, but possess differences in chemical composition, crystal structure, density and hardness. Basically, aluminosilicate minerals can be classified on the basis of their structural groups as: ortho- and ring, chain, sheet and framework groups (Deer et al., 1992)

A first detailed introduction on geopolymerisation, geopolymeric products and their properties and structures was presented by Davidovits based on his studies which covered geopolymeric matrices, resins and composite materials (Davidovits, 1991). These geopolymeric binders were aluminosilicates made up of poly-sialate (silicon-oxo-alumintae) network that consists of SiO_4 and AlO_4 tetrahedra linked by sharing oxygen atoms. Positive ions such as Na^+, K^+, Ba^{2+}, Ca^{2+}, H_3O^+, NH_4^+ are present in the framework to balance the negative charge of AlO_4^- with the representative empirical formula being:

$$M(-(SiO_2)_z - AlO_2-)_n . wH_2O \quad (3)$$

z here can be either 1, 2 or 3, n is the degree of poly-condensation and M is the monovalent cation such as K^+ and Na^+ (Barbosa et al., 2000). Apart from poly-sialate (-Si-O-Al-O-), poly-sialate-siloxo (-Si-O-Al-O-Si-O-) and poly-sialate-disiloxo (-Si-O-Al-O-Si-O-Si-O-) are also possible structural units for geopolymers when the amount of silicate reactants increases in the reaction system.

The development in the field of geopolymerisation and geopolymeric products over the years has changed the meaning of terminology specified initially by Davidovits, which only included geopolymeric binder. A geopolymeric binder is a specific kind of geopolymer which is synthesised by complete transformation of metakaolinite (calcined kaolinite) from the solid phase to gel phase. Such geopolymer has a certain stoichiometric composition like poly-sialate, poly-(sialate-siloxo), or poly-(sialate-disiloxo) and possesses amorphous to semi-crystalline structure.

Nevertheless, the meaning of geopolymer nowadays not only encompasses geolymeric binders but also includes any mixtures comprising of geopolymeric gel and solid source Al and Si materials (van Jaarsveld et al., 2000; Xu & Van Deventer, 2000). Equation (4) describes what geopolymerisation means nowadays. Here, M is a monovalent cation.

$$Al - Si \text{ materials} + nMOH + M_2SiO_3 \xrightarrow{\text{Mixing, setting \& hardening}} \text{Geopolymer or Geopolymeric Product} \quad (4)$$

2.6.3 Chemistry involved

Geopolymerisation involves reactions that forms tri-dimensional aluminosilicates by naturally occurring aluminosilicates at low temperature and relatively short time (Khale &

Chaudhary, 2007; Silva et al., 2007; Xu & Van Deventer, 2002) . Geopolymeric products do not have stoichiometric composition and comprise of a mixture of amorphous to semi-crystalline structure Al-Si particles. In general, geopolymerisation reaction involved leaching, diffusing, condensation and hardening steps. When aluminosilicate materials come in contact with alkaline solution, leaching of both Al and Si starts. The extents of leaching for both Al and Si are dependent on factors like concentration of the alkaline solution, alkali metal cation in alkaline solution, stirring speed, leaching period as well as the structure and composition of source materials (Davidovits, 1991, 1994). However, the properties of the source materials and the concentration of alkaline solutions are believed to be dominant out of all these stated factors. After being leached, Al and Si species diffuse into the gel phase, which reduces the concentrations of Al and Si species on aluminosilicate surface resulting further leaching of Al and Si. During the diffusion step, the time and intensity of stirring are dominant factors. Hence, the removal of dissolved Al and Si complexes can be maximized by longer leaching period and a more intense stirring. This helps to kinetically break the barrier between the Al-Si particle surface and the gel phase so as to accelerate diffusion of Al and Si complexes.

Additional silicate (whether solid or liquid) is used to enhance geopolymerisation as it makes Si complexes more amenable to polymerisation with aluminate. Since the activation energy for forming an Al-O-Si linkage is lower than that of Si-O-Si linkage, polymerisation between Al complexes and Si complexes is preferred over the polymerisation between Si complexes (Barrer, 1982). Therefore, a simultaneous condensation between Al and Si complexes occurs along with leaching and diffusion of Al and Si complexes from the source materials.

It is reported that temperature, pH and cations are three main factors affecting the condensation stage during geopolymerisation. Higher temperature, higher pH (or higher

concentration of alkaline solution) and alkali metal cation with a larger atomic size favor the condensation step and hence promote the geopolymerisation to a complete stage.

Finally, during the hardening of geopolymerisation, temperature and air circulation are two main factors determining whether geopolymeric products have higher mechanical strength or possess cracks. Another depiction of the geopolymerisation process has been illustrated by Yao et al. (2009) as shown in Figure.7.

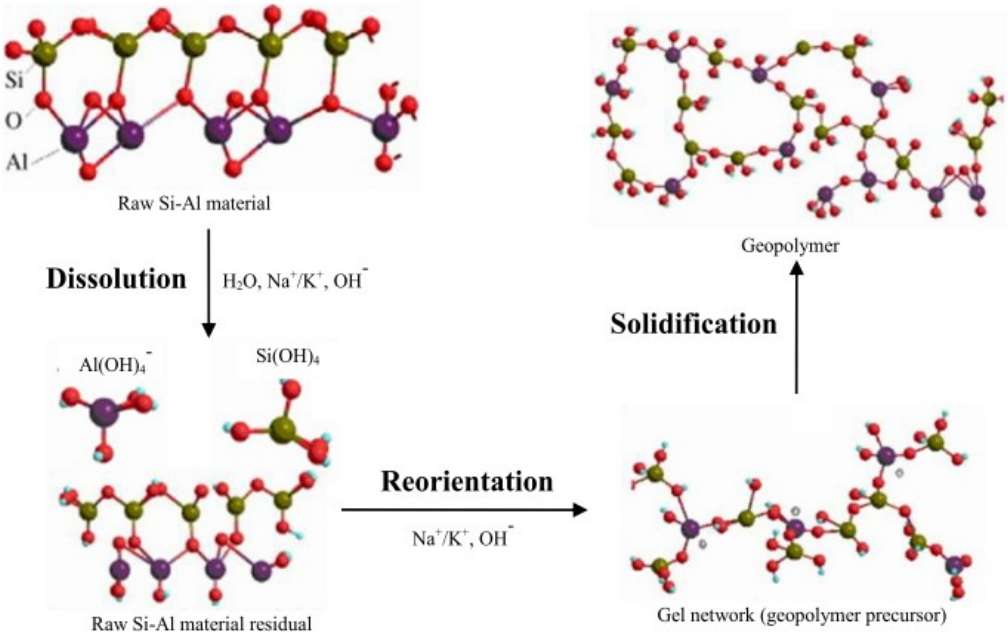

Figure 7: Simple breakdown of geopolymerisation into three stages: Dissolution of Si-Al source material, reorientation of silicate and aluminate precursors and solidication of the final geopolymer network (Yao et al., 2009)

Here, geopolymerisation process has been simplified into three main stages: dissolution, reorientation and solidification.

2.7 Aluminosilicate minerals in MFT

The MFT contains a variety of alumninosilicate minerals as illustrated by Table 2. However, out of all these aluminosilicates, clay minerals are most abundant source of Si and Al present in MFT. The focus of this research is to induce geopolymerisation in MFT with clay minerals as the Al and Si source for this process.

Clay minerals consists of repeating sheets of silicon bonded to oxygen in a tetrahedral arrangement and aluminum bonded to oxygen and hydroxyl groups in an octahedral arrangement as shown in Figure 8. The clay type depends not only on the chemical composition of its layers but also on the ratio of octahedral to tetrahedral layers. Kaolinite, for instance, has a 1:1 ratio of tetrahedral to octahedral layers, while illite and smectite clays have a 2:1 ratio. Clays with 2:1 ratios such as illite and smectite also have a layer of cations between each of the clay layers. The layered structure of clays results in clay particles having flat, plate-like structure with distinct edges and faces (basal planes) with differing surface properties (van Olphen, 1977).

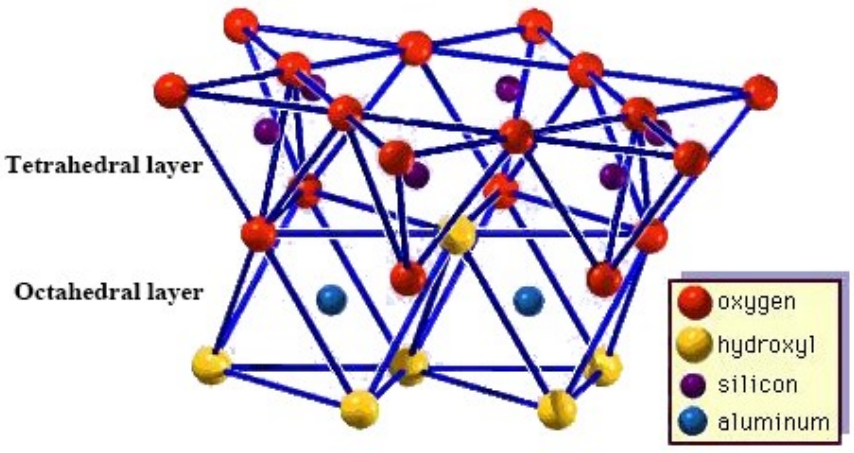

Figure 8: Illustration of the layers present in kaolinite (Britannica, 2015)

Mixed-layer minerals, such as illite-smectite, are minerals where the interlayer or layer type differs within the mineral (Srodon, 1999). When naming mixed layer minerals, the minerals are named by the mineral types of the two components; the mineral with the smallest d-spacing is named first (Srodon, 1999). The surface area and cation exchange capacities of these minerals are similar to a mixture of the mixed layer minerals. However, other geotechnical properties are very different from those predicted from a physical mixture of minerals, indicating that the mixed-layer minerals do indeed form a unique structure.

Imperfection in the crystal lattice can result in silicon or aluminum atoms being replaced by lower valence cations (Na^{+}, K^{+}, Mg^{+2} and Ca^{+2}) in a process called isomorphic substitution. Due to the deficit in positive charges, the lower valence of the cation leads to a permanent negative charge on the clay basal plane (Zbik & Smart, 1998). On the edges of clay, lattice bonds are broken to form silanol and aluminol sites which react with water. This gives the clay surface a pH dependent charge characteristic (Masliyah et al., 2011).

Since clay particles in water can have a different charge on their edges compared to their faces depending on the pH of the suspension, under the right conditions it is possible for the edges of clays to have a charge opposite to that of the clay faces. Under these conditions it can be expected that clay edges and faces will attach to one another, forming a porous "house of cards" structure which can result in the gelation of the suspension (van Olphen, 1977).

An important property of clays is the cation exchange capacity (CEC), whereby the cations in the interlayer that balance the net charge on the clay mineral, due to isomorphic substitution, are exchangeable. For example, clay minerals such as kaolinite have low CEC because there is a low degree of ion adsorption corresponding to a lower degree of isomorphic

substitution. In illite, however, charge is balanced by potassium which fits perfectly between the oxygen atoms that make up the base of a tetrahedron in the tetrahedral sheet (Mitchell & Soga, 2005). This excellent fit, coupled with the local charge created by tetrahedral substitution, ensures that the potassium is tightly bound within the structure, giving illite a low CEC.

Table 2: Silicates and aluminosilicates reported in the oils sands literature. Adopted from Kaminsky (2009).

Mineral Group	Mineral Name	Chemical Formula	Reference
-	Andalusite	Al_2SiO_5	Hepler & Hsi (1989)
-	Kyanite	Al_2SiO_5	Hepler&Hsi(1989)
-	Sillimanite	Al_2SiO_5	Bichard(1987)
-	Staurolite	$Fe_2Al_9Si_4O_{22}(OH)_2$	Bichard(1987)
Amphibole		$XY_2Z_5(Si, Al, Ti)_8O_22(OH,F)_2$	Bichard(1987)
Analcime	Wairakite	$CaAl_2Si_2Si_4O_{22}(OH)_4$	Hepler&Hsi(1989)
Chloritoid	Chloritoid	$Fe_21.2Mg_{0.6}Mn_{2+}0.2Al_{14}Si_2O_{10}(OH)_4$	Bichard(1987)
Clays	Kaolinite	$Al_2(Si_2O_5)(OH)_4$	Mercier et al. (2008)
	Illite	$K_{0.65}Al_2[Al_{0.65}Si_{3.35}O_{10}](OH)_2$	Mercier et al. (2008)
	Chlorite	$(Mg,Fe,Li)_6AlSi_3O_{10}(OH)_8$	Omotoso et al. (2006)
	Vermiculite	$Mg_{1.8}Fe^{2+}0.9Al_{4.3}SiO_{10}(OH)_2$	Omotoso et al. (2006)
	Montmorillonite	$(Na,Ca)_{0.33}(Al,Mg)_2(Si_4O_{10})(OH)_2$	Omotoso et al. (2006)
Epidote	Clinozoisite	$Ca_2Al_3Si_3O_{12}(OH)$	Hepler&Hsi(1989)
	Epidote	$Ca_2(Al, Fe)_3(SiO_4)_3(OH)$	Bichard(1987)
	Zoisite	$Ca_2Al_3(SiO_4)_3(OH)$	Bichard(1987)
Feldspars	Albite	$NaAlSi_3O_5$	Hepler&Hsi(1989)
	Anorthite	$CaAl_2Si_2O_8$	Hepler&Hsi(1989)
	Microcline	$KAlSi_3O_8$	Hepler&Hsi(1989)
Feldspathoid	Nepheline	$NaAlSiO_4$	Hepler&Hsi(1989)
Garnet		$(Ca,Fe,Mn,Mg)_3(Al,Fe,Cr,Ti)_2(SiO_4)_3$	Bichard(1987)
Lawsonite	Lawsonite	$CaAl_2Si_2O_6(OH)_4$	Hepler&Hsi(1989)
Mica	Paragonite	$NaAl_3Si_3O_5(OH)_2$	Hepler&Hsi(1989)
	Biotite	$K(Mg,Fe)_3(Al,Fe)Si_3O_{10}(F, OH)_2$	Hepler&Hsi(1989)
	Glauconite	$(K,Na)(Al,Fe,Mg)_2(Al,Si)_4O_{10}(OH)_2$	Bichard(1987)
	Muscovite	$KAl_3Si_3O_{10}(OH)_2$	Hepler&Hsi(1989)
Nepheline	Kalsilite	$KAlSiO_4$	Hepler&Hsi(1989)
Pyrophyllite-talc	Talc	$Mg_3Si_4O_{10}(OH)_2$	Hepler&Hsi(1989)
Pyroxenoid	Wollastonite	$CaSiO_3$	Hepler&Hsi(1989)
Quartz	Quartz	SiO_2	Hepler&Hsi(1989)
Titanite	Titanite (Sphene)	$CaTiSiO_5$	Bichard(1987)
Zeolites	Analcime	$NaAlSi_2O_5(OH)_2$	Hepler&Hsi(1989)
	Laumontite	$CaAl_2Si_4O_8(OH)_8$	Bichard(1987)
	Phillipsite	$KAlSi_2O_6.4H_2O$	Hepler&Hsi(1989)
Zircon	Thorite	$ThSiO_4$	Alberta Chamber of Resources(1996)
	Zircon	$ZrSiO_4$	Bichard(1987)

However, for smectite clays there is a greater degree of substitution in the octahedral layers which allows ions to be readily exchanged. Since cations are often hydrated by a layer of water molecules, the high CEC of smectite clays causes significant amounts of water to enter into the interlayer spaces causing the clays to swell (Brady & Krumhansl, 2001). Beside, due to the increased ion concentration in the interlayer spaces, osmotic pressure causes more water to enter the clay. These types of clays can absorb water and swell to double their original volume (van Olphen, 1977). Such clays are known to have poor settling rates and poor sediment consolidation, thus hindering remediation of tailings containing these types of clays (McFarlane et al., 2008).

2.8 Geopolymerisation in oil sands tailings

The idea of employing geopolymerisation on oil sands tailings shows a lot of promise, especially when compared to technologies like Composite Tailings (CT) and Thickened Tailings (TT). Also, technologies like CT and TT have been in the industry for decades. Because of such a prolonged presence, a lot of research efforts have already gone into improving these technologies, leaving very little scope for further improvement (Mikula & Omotoso, 2006). Long et al. (2006) demonstrated the importance of colloidal interaction in CT and TT but had, in fact, not proposed any important optimization parameter that could improve these methods of oil sands tailings treatment . They only elaborated on the importance of colloidal interactions in oil sands tailings treatment.

It is important to point out that geopolymerisation achieves consolidation of tailing through a totally different concept in comparison to TT and CT. CT and TT rely on aggregation of particles, which are predominantly determined by intermolecular forces predicted by the

DLVO theory (Long et al., 2006). But in the case of geopolymerisation, an entirely new species is formed by using the aluminosilicate sources inherently present in MFT.

So far the research on using geopolymerisation on tailings has been restricted to copper mine tailings and reservoir sludge (Lee et al., 2014; Zhang et al., 2011; Phair & van Deventer, 2002; van Jaarsveld et al., 2000). Application of geopolymerisation concept on Athabasca oil sands tailings has been reported in the open literature as patents (Canadian Patent No. 2873992., 2014; US Patent No. 20130019780, 2013; Canadian Patent No. 2684155A1 , 2013). But their approach is completely different from one proposed here. The idea here is to add the optimal amount of alkali activators so that geopolymerisation in the clays present in MFT only progresses to a small extent to prevent the formation of very high strength material similar to concrete.

Hence, this study investigates the feasibility of 'surface' geopolymerisation of Athabasca oil sands tailings sludge of three different categories: 40 wt% solids untreated mature fine tailings, 50 wt% solids centrifuged MFT and 50 wt% solids polymer flocculated MFT. The rationale behind this is to gauge how the water content and flocculant polymer affect the geopolymerisation process. Since the Fort McMurray bitumen extraction operation uses large amount of caustic soda for its operation, the following study has been limited to using sodium hydroxide (NaOH) and sodium metasilicate (Na_2SiO_3) as alkali activators to produce the intended geopolymer binder. Many studies cite the importance of M_2O:SiO_2 molar ratio (where M is either Na or K) in the activation solution. Swaddle (2001) state that the M_2O:SiO_2 ratio affects the degree of polymerization of the dissolved species and Provis and van Deventer (2007) report that a variation in silica content can be used to optimize the rate of geopolymersation. However, varying this ratio in the silicate solution is beyond the scope of this study. A simplistic

approach is used which involves varying monosilicate to NaOH ratio and the concentration of these alkali activators to determine the optimal technique.

Chapter 3

Materials and Experimental Methods

In order to investigate geopolymerisation in MFT, kaolinite was chosen as a model solid system. The methods used in characterisation include, FTIR, particle size distribution, ICP-OES, powder XRD, TEM/EDX/SAED. Solid content in MFT was calculated after Dean Stark extraction. The extracted solids were sent for quantitative XRD characterization to gauge the mineral content in MFT. Dean stark analysis and moisture analyzer were used to measure the solid content and moisture content, respectively, in different types of MFT. Also, shear strength measurements of all the samples were carried out using ASTM D2573 standard. Preliminary tests were also done using a field penetrometer to measure the compressibility of the reacted samples. The explanation of the method used and the results of preliminary compressibility measurements are included in Appendix B. Dewaterability of different types of MFT was determined using capillary suction time apparatus.

This chapter provides a detailed discussion on materials, instruments and methodologies used to carryout out and understand surface geopolymerisation in model kaolinite system and mature fine tailings (MFT).

3.1 Materials

3.1.1 Kaolinite

In order to understand the mechanism of geopolymerisation in MFT, a simplified model system is required. MFT is a mixture of various chemical species which makes it difficult to study specific reaction pertaining to one chemical group, which in this case is aluminosilicates. Because of its predominant presence as a clay mineral in MFT, kaolinite is deemed as the

appropriate model material to simplify this complex system of solid aluminosilicates present in MFT (K. L. Kasperski & Mikula, 2011).

Kaolinite was obtained as kaolin from Ward's Science (Twigg County, Georgia, USA) and was used to emulate the solids in MFT. The kaolinite sample has a high purity and crystallinity, as shown by XRD and TEM analyses in Figure 9.

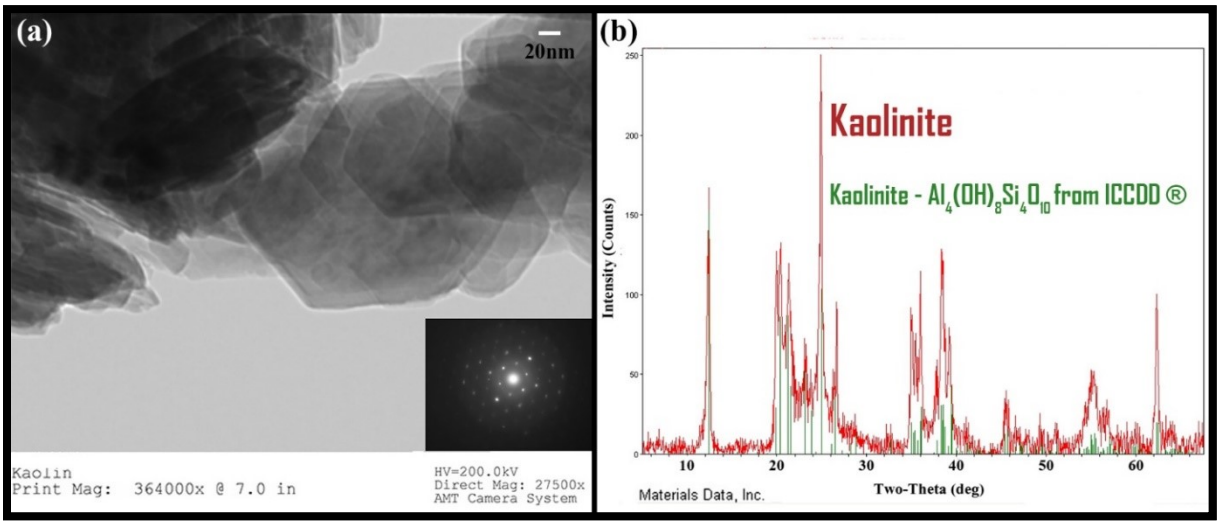

Figure 9: (a) TEM/SAED of Ward's kaolin showing its crystallinity (b) XRD of Ward's kaolin matched with kaolin peaks from the ICDD® database in JADE™.

3.1.2 Mature fine tailings (MFT)

MFT was obtained from Syncrude Canada Ltd. in its operations in Fort McMurray, Alberta, Canada. The solid content of the MFT sample was measured to be 37.9 wt% using Dean Stark analysis. Table 3 shows the mineralogical composition of the MFT sample determined by quantitative XRD.

The MFT samples used for geopolymerisation reactions was either as is, after centrifugation, or after flocculation by a 30% anionic polyacrylamide commercial flocculants

(A3335). First, the MFT sample was homogenized and sub-sampled into 1,500 gram batches which were stored in polypropylene containers.

Table 3: Mineralogical composition of mature fine tailings from Syncrude Canada Ltd. determined by quantitative XRD

	Minerals	Wt%
Non-Clays	K-feldspar	2.6
	Quartz	27.4
	Siderite	3.2
Clays	Illite	30.7
	Kaolinite	36.0

Centrifuged MFT samples were prepared by centrifugation of the subsampled MFT at 3000 G for 60 minutes using Avanti J-30 I centrifuge (Beckman Coulter, USA). The centrifuged MFT was found to contain 51 wt% solids using Dean Stark analysis. The flocculated MFT sample was obtained by treating the MFT with A3335 at a dosage of 1000 g/t. The treated MFT was left to settle for 48 hours, and the released water was decanted. The final settled sludge was found to contain 48 wt% solids.

3.1.3 Chemicals

Since the Fort McMurray extraction operation uses large amount of caustic soda for its operation, the following study has been limited to using sodium hydroxide (NaOH) and sodium silicate (Na_2SiO_3) as alkali activators to produce the intended geopolymer binders.

Sodium hydroxide (NaOH) and sodium silicate (Na_2SiO_3) are reagent grade chemicals (> 95% purity) purchased from Fisher Scientific. The reagents were dissolved in de-ionized water into various concentrations and varying NaOH:Na_2SiO_3 ratios, and used for the surface

geopolymerisation of kaolinite. For the geopolymerisation reactions of MFT samples, the reagents were added directly to the MFT samples as powders accompanied by vigorous mechanical stirring. Analytical grade chemicals and distilled water were used throughout the geopolymerisation and chemical analyses. A3335 is an anionic polyacrylamide macropolymer obtained from SNF, with an average molecular weight of 17 x 10^6 g/mol.

3.2 Methods

3.2.1 Sample preparation

3.2.1.1 Kaolinite

As stated before, mild conditions are required to carry out this reaction because the intention is to achieve geopolymerisation on the surface with shear strength much lower than that of construction grade geopolymer. Two categories are classified. Category A-1 evaluates the effect of varying NaOH:Na_2SiO_3 ratio on the shear strength and category B-1 assesses the increase in the concentration of the alkali activators while the NaOH:$NaSiO_3$ mass ratio is kept constant. Details of the samples in each category have been presented in Table 4. Each kaolinite sample was prepared by placing 100 g of kaolinite in 250 mL polycarbonate jars and adding 100 mL of solution mixture of NaOH and Na_2SiO_3 to the solids. The resulting slurry was mixed using Heidolph™ Electronic Overhead Stirrer (RZR 2052 Control) with a stainless steel impeller at 1000 rpm for 5 min to ensure the alkali activators properly mixed with the kaolinite.

Once the optimum ratio of the NaOH: Na_2SiO_3 was determined in category A-1, twelve kaolin samples were prepared with the optimum concentration of the alkali activators using the procedure mentioned above. Periodic shear strength measurements were carried out separately

on the samples over a span of 90 days. Each sample was discarded after the measurement because shear strength measurement is a destructive measurement.

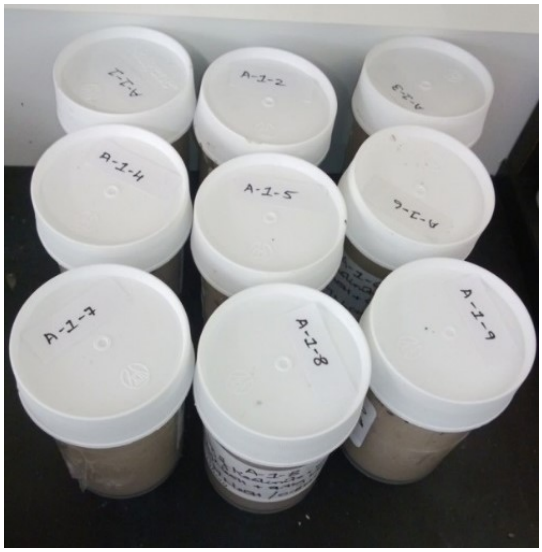

Figure 10: Sample set A-1 screw capped and labelled in polycarbonate containers.

3.2.1.2 Mature Fine Tailings

Similar investigation on MFT was carried out to determine the effect of changing NaOH and Na_2SiO_3 ratio and the effect of increasing concentration of these activators. Hence, two categories are set up: A-2 and B-2. An additional category, C-1, are also set up for MFT samples to demonstrate the influence of the absence of sodium silicate. For consistency in solid to liquid ratio with the kaolinite categories, 50 wt% centrifuged MFT is chosen for this preliminary study. Table 4 displays all the preliminary samples that were prepared with MFT.

After the subsampled MFT were centrifuged, the samples were placed in 2 propylene containers and thoroughly mixed to remove all lumps and produce a homogenous mixture. The final moisture content was measured to be 47 wt%. Figure 11 depicts the subsampling process.

200 g of MFT was weighed out in Thermo Scientific polycarbonate jars and crushed NaOH and Na_2SiO_3 solids were directly added to the samples under the assumption that 94 g of the MFT comprises of water.

Figure 11: Subsampling procedure of MFT in which MFT is mixed thoroughly using a mechanical impeller mixer to remove lumps and produce a homogenous mixture. One kilogram of MFT is then weighed into plastic containers similar to the one shown in the image.

Samples with the alkali activator concentrations denoted by Table 4 were prepared accordingly. All the samples were mixed at 1000 RPM for 10 min. The containers were screw capped tightly and left undisturbed for 90 days.

On determination of the optimum ratio, 12 samples with this concentration were prepared using the optimum concentration. The shear strength of these samples were recorded separately

at regular time intervals over a span of 90 days. Each sample was discarded after respective measurements.

Table 4: Kaolinite and centrifuged MFT sample concentration of alkali activators in test series A-1, A-2, B-1, B-2 and C-1.

Sample Name	Test Material	Moisture	NaOH		Na_2SiO_3	
			mol/L of water	kg/t of dry material	mol/L of water	kg/t of dry material
A-1-1	Kaolinite/Water	50.0%	1	40	0	0
A-1-2	Kaolinite/Water	50.0%	1	40	0.15	18.3
A-1-3	Kaolinite/Water	50.0%	1	40	0.2	24.4
A-1-4	Kaolinite/Water	50.0%	1	40	0.25	30.5
A-1-5	Kaolinite/Water	50.0%	1	40	0.33	40
A-1-6	Kaolinite/Water	50.0%	1	40	0.5	61.0
A-1-7	Kaolinite/Water	50.0%	1	40	0.65	79.3
A-1-8	Kaolinite/Water	50.0%	1	40	0.8	97.6
A-1-9	Kaolinite/Water	50.0%	1	40	1	122.2
A-2-1	Centrifuged MFT	47.3%	1	37.8	0	0
A-2-2	Centrifuged MFT	47.3%	1	37.8	0.15	17.3
A-2-3	Centrifuged MFT	47.3%	1	37.8	0.2	23.1
A-2-4	Centrifuged MFT	47.3%	1	37.8	0.25	28.8
A-2-5	Centrifuged MFT	47.3%	1	37.8	0.33	37.8
A-2-6	Centrifuged MFT	47.3%	1	37.8	0.5	57.7
A-2-7	Centrifuged MFT	47.3%	1	37.8	0.65	75.1
A-2-8	Centrifuged MFT	47.3%	1	37.8	0.8	92.3
A-2-9	Centrifuged MFT	47.3%	1	37.8	1	115.5
B-1-1	Kaolinite/Water	50.0%	0	0	0	0
B-1-2	Kaolinite/Water	50.0%	0.01	0.38	0.0033	0.4
B-1-3	Kaolinite/Water	50.0%	0.1	3.8	0.033	3.8
B-1-4	Kaolinite/Water	50.0%	0.5	18.9	0.16	18.9
B-1-5	Kaolinite/Water	50.0%	1	37.8	0.33	37.8
B-2-1	Centrifuged MFT	47.3%	0	0	0	0
B-2-2	Centrifuged MFT	47.3%	0.01	0.4	0.0033	0.4
B-2-3	Centrifuged MFT	47.3%	0.1	4	0.033	4
B-2-4	Centrifuged MFT	47.3%	0.5	20	0.16	20
B-2-5	Centrifuged MFT	47.3%	1	40	0.33	40
C-1-1	Centrifuged MFT	47.3%	0	0	0	0
C-1-2	Centrifuged MFT	47.3%	0.01	0.38	0	0
C-1-3	Centrifuged MFT	47.3%	0.1	3.8	0	0
C-1-4	Centrifuged MFT	47.3%	0.5	18.9	0	0
C-1-5	Centrifuged MFT	47.3%	1.0	37.8	0	0

3.3 Characterization techniques

3.3.1 Shear strength measurements

Shear strength is the stress required to inelastically deform settled solid into viscous flow and this resistance of the solids to motion can be quantified through shear strength testing. The vane shear test is used to measure the shear strength of clay and soil samples (Dzuy & Boger, 1985). As illustrated in Figure 12, a four bladed vane is immersed in undisturbed solid sample and rotated at a constant speed to determine the torsional torque. The measured force is then used to calculate the shear stress.

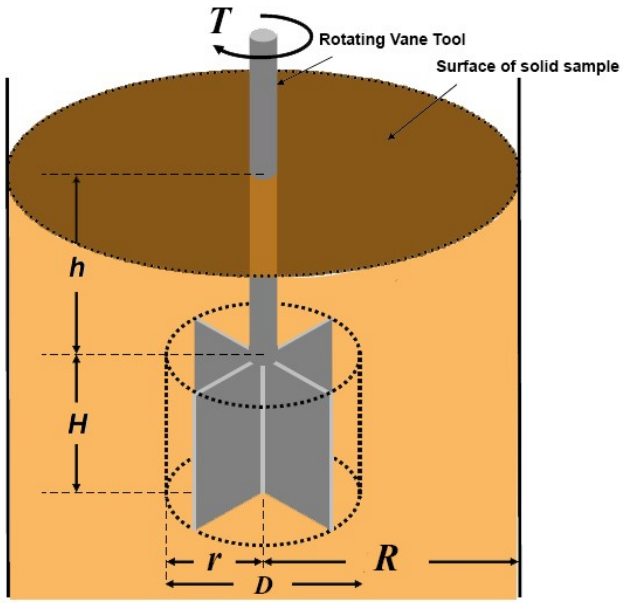

Figure 12: Schematic of shear strength measurement using vane tool (Burns et al., 2010)

Sludge or slurry sample is placed in a container of radius R and a vane tool is immersed into the solid portion of a sludge or slurry to a depth, h. The vane blades have a radius, r, and a height, H. The stress is then determined by continuously monitoring the torsional torque as a

function of time. The shear strength of the material is then associated to the maximum torque measured once a steady-state vane rotation has been achieved. This is under the assumption that there is uniform stress distribution on the known vane tool geometry.

An example shear stress against time curve is shown in Figure 13. The peak of this plot corresponds to the onset of plastic deformation in the solid sample. The maximum torque required for plastic deformation is dependent on vane geometry.

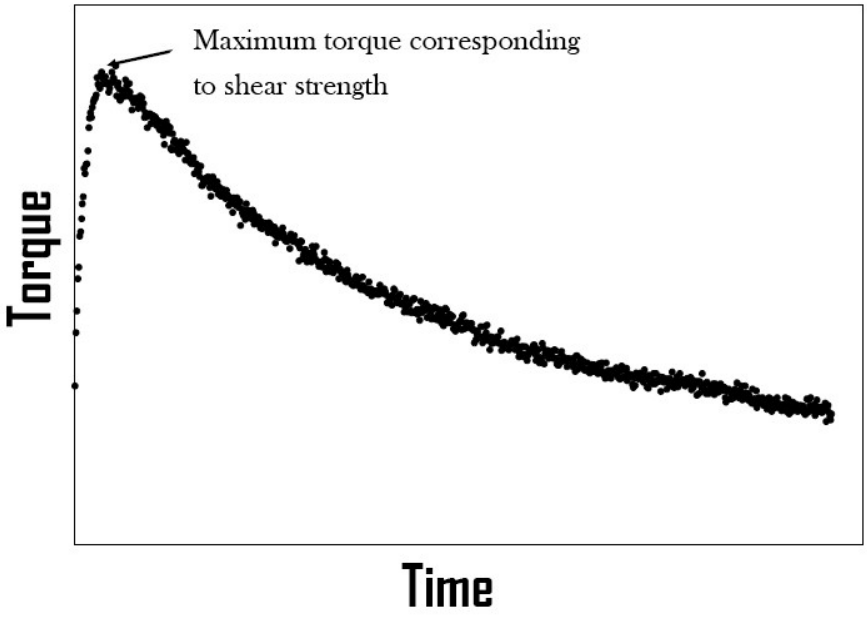

Figure 13: Torque versus time plot which can be used to obtain shear strength of solid samples (Burns et al., 2010)

To account for vane geometry effects, the shear strength is expressed as an isotropic and uniform stress acting over the entire surface area of the cylinder of rotation swept out by the vane. This shear strength is related to the maximal torsional torque during the steady state motion given by Equation (5), (6) and (7) (ASTM Standard D2573, 2002):

$$T_{max} = s_{max} * K \tag{5}$$

$$\text{K(Cylindrical Vane)} = \frac{\pi}{10^6} * \left(\frac{D^2 H}{2}\right) * \left[1 + \frac{D}{3H}\right] \tag{6}$$

$$\text{K(Tapered Vane)} = \frac{1}{10^6} * [\pi D^3 + 0.37 * (2D^3 - d^3)] \tag{7}$$

Here:

s_{max} is the shear strength (kPa),

T_{max} is the maximum torque (N.m),

K is constant, depending on dimensions and shape of the vane (m^3).

D is the diameter of cylinder rotation swept out by the vane (cm)

H is the height of the cylinder of rotation swept out by the vane (cm)

It should be noted that *D* and *H* are taken to be the dimensions of the vane itself under the assumption that the shear band observed upon slow rotation of the vane does not extend appreciably beyond the vane paddles.

The distance between the vane and the inner surfaces of the sample container as well as to the free surface of the sample solids is an important factor that can affect the shear strength results. Therefore, it is important that this factor is taken into account for the test to be considered independent of geometry of the container. These constraints are outlined in Table 5 with dimensions for a 7 mm × 21 mm vane tool, which is employed in this study.

ASTM D2573 expands on the procedure and protocol for the standard test method for field vane shear testing in cohesive soil. The procedure was chosen mainly because MFT of

various solid content as well as kaolinite slurries possess similar rheological characteristics to that of cohesive soil.

Table 5: Constraints for using vane tool using shear strength measurements

Constraints	Criterion	For 7x21mm (rxH) vane	Measurement conditions used
Vane height (H) to radius (r)	$H \leq 7r$	$H \leq 49$ mm	H = 21 mm
Container radius (R) to vane radius (r)	$R \geq 2r$	$R \geq 14$ mm	R = 140 mm
Immersion depth to vane height	$h \geq H$	$h \geq 21$ mm	h = 195 mm

One of the important aspects of the standard stipulates that the torsional torque be measured at a rotational rate of not more than 0.1°/s. Furthermore, depending on the nature of the soil, the test should take up 2 to 5 minutes for failure, except in very soft clays where the time to failure may be as much as 10 min. In harder materials, it is advisable to reduce the rotational speed to obtain a more resolved stress against time curve. It has also been recommended to record intermediate values of torque at intervals of 15 s or at lesser frequency if conditions require (ASTM Standard D2573, 2002).

Furthermore, it is important to consider the friction of the vane rod and instrument to avoid the friction to be improperly recorded as soil strength. Friction measurements under no-load conditions can be carried out using blank stem instead of the vanes. The vane rod should also have sufficient rigidity so that it does not twist under full load conditions. Correspondingly, corrections for rod deformation must be made for plotting torque rotation curves.

The shear strengths of MFT and kaolinite samples were measured using the Malvern Kinexus Lab+ rheometer which is a modular, highly intelligent and robust rotational rheometer.

The rSpace software installed on a computer is used to remotely control the rheometer and acquire data. The rSpace software serves as a central program for obtaining, processing, and recording the data from Kinexus Lab+ measuring system. rSpace automatically converts the torque into shear stresses based on the appropriate K constant and provides the user with a stress versus time plot.

On attaching the shear vane to the rheometer, the rSpace software automatically detects the geometry, using the unique microchip present within the vane tool, and prompts the user to load the sample. For convenience shear strength measurements for this study were carried out directly in the sample container in which the sample is prepared. Figure 14 shows the setup used to do shear strength measurements. Shear strength measurements employed a 7 mm × 21 mm tapered shear vane tool.

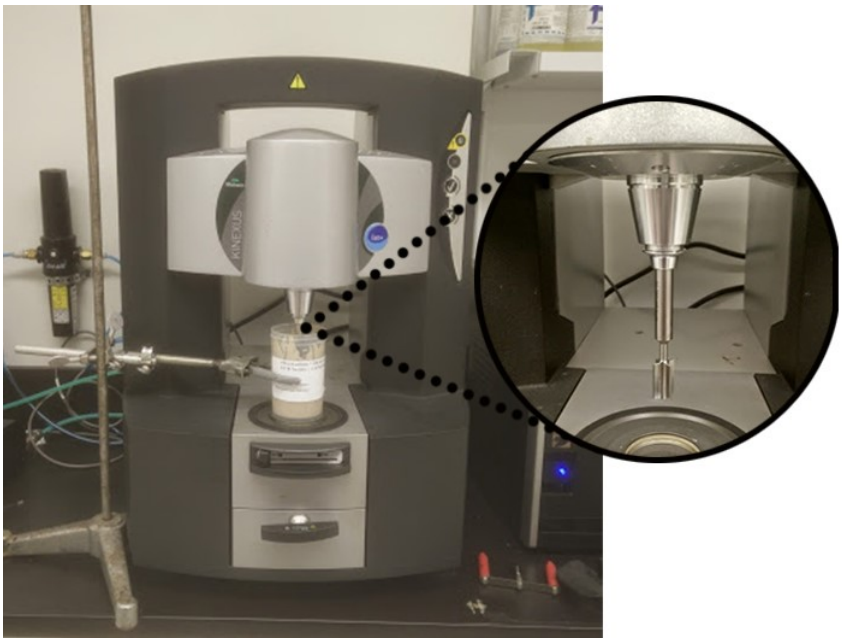

Figure 14: Shear strength measurement setup using Malvern™ Lab^{+} rheometer

The rSpace software also allows post-measurement processing and interpretation of the collected data. Specifically, it can be used to obtain maxima point in shear stress versus time curves, i.e. the shear strength. Shear strength of all the samples was tracked using the Malvern Kinexus Lab^{+} rheometer with 7 x 21mm vane tool. Measurements were done using the procedures described in the ASTM D2573. Samples were sheared at the rate of 0.01 s^{-1} under the assumption that the samples were characteristic to soft clay.

3.3.2 Fourier transform infrared spectrometry (FTIR)

Variations in the kaolinite microstructure were examined using the Thermoscientic Nicolet 6700 Fourier Transform Infrared (FTIR) spectrometer. Kaolinite sample was mixed with KBr in the range of approximately 0.5 wt% of the sample and ground with a mortar and pestle to obtain a homogenous solid mixture. Using hydraulic press the mixture was then made into a disc, which was then mounted onto the sample holder of the FTIR. It is important to not use high concentration of sample since it can cause difficulties in obtaining clear pellets. Cloudy pellets completely absorb or scatter the IR from the sample resulting in very noisy spectra (Northern Illinois University - Chemistry Analytical Lab, 2007).

Reacted kaolinite samples were centrifuged at 5000 rpm for 60 minutes. The supernatant was decanted and the solids were kept for overnight vacuum drying at 70°C to remove moisture. The dried samples were prepared for FTIR using the procedure mentioned above. The infrared spectra of the ground samples were recorded using the OMNIC software with scan speed of 2.5 kHz and 256 scans were run.

3.3.3 Particle size distribution by laser diffraction

The particle size distributions of kaolinite and reacted samples was measured using Malvern's Mastersizer™ 3000. Particle size analysis by laser diffraction can denote if a reaction has taken place, specifically dissolution, showing a reduction in particle size.

Dry kaolinite or centrifuged and dried reacted sample were mixed with deionized water at a concentration of approximately 1 wt% particle. The suspension was analyzed by the Mastersizer™ 3000 and the data obtained is further analyzed using the Mastersizer™ 3000 software.

3.3.4 Inductively coupled plasma optical emission spectrometry (ICP-OES)

The ionic concentration of the liquid phase of the sample represent the amount of the Al-Si source minerals leached by the addition of alkali activators. To analyze the ionic concentration of the liquid, samples were centrifuged at 5000 rpm for 60 minutes and the supernatant was analysed by a Perkin Elmer Optima 3000 inductively coupled plasma spectrometer (ICP-OES). Spectral lines used were Si: 251.607 nm; Al 308.215 nm; Na: 588.983 nm; Fe: 259.933 nm (Sarojam, 2010) .

3.3.5 Powder X-ray diffraction (XRD) & quantitative XRD

Kaolinite samples and MFT solids were analyzed by X-ray diffraction (XRD) for the identification of their crystalline phases and amount of minerals present. For quantitative XRD of the minerals present in MFT, the method proposed by Omotoso and Eberl (2009) was used. MFT sample was dried at 75°C in a vacuum oven for 12 hours to remove all moisture. The dried solids were passed through 250 μm sieve to obtain uniform grain sizes. 1.000 g of the solids was

then mixed with 0.250 g conundrum and ethanol and wet milled using McCrone micronizing mill. The slurry was then left for overnight drying at 80ºC and vertrel was then added to the dried solids before it was sieved again. The sample was finally side loaded in a modified sample holder against frosted glass and examined from 5 to 65 degrees 2θ using Cu $K\alpha_{1,2}$ radiation, with the step size of 0.02 degrees 2θ and scan rate of 2°/minute. The characterization results were entered into RockJock™ and analyzed to give the weight percent of the minerals present in the sample.

Kaolinite and reacted kaolinite samples were prepared using the above mentioned sample preparation procedure. Quantitative X-ray diffraction results of the kaolinite samples were recorded and compared before and after the geopolymerisation reactions to observe any changes in the crystal structure. The obtained spectra were analyzed using Material's Data Inc. (MDI) JADE™ software with ICDD® database. All the samples were characterized by Rigaku Ultima IV X-Ray Diffractometer with Cu tube as X-ray source operating at 40 kV and 44 mA.

3.3.6 Transmission electron microscopy/ Energy-dispersive X-ray/ Selected area electron diffraction (TEM/EDX/SAED)

The geopolymers formed in this work are mixtures of amorphous phase and crystalline particles, and traditional XRD methods are not effective in studying these phases. Hence TEM/SAED is applied to identify the crystalline particles and to gauge the extent to which reaction has taken place. Furthermore, TEM/EDX is used for carrying out elemental analysis of the formed geopolymers. Sample preparation for TEM analysis involves grinding the sample and depositing it from an alcohol suspension on carbon covered copper grids. TEM/SAED and

TEM/EDX analyses are conducted using a Philips CM20 FEG TEM/STEM transmission electron microscope at an accelerating voltage of 200 kV.

The quality of TEM results is highly dependent on sample preparation. There are certain factors that must be accounted for while preparing clay minerals like kaolinite for TEM analysis. These include their property of electrical insulation and their corrosion resistance which limits their possibility of using chemical polishing during preparation. Also, to keep interlayer spacing homogenous in the kaolinite sample, it is important that samples prepared for TEM analysis are homoionic with only one type of cation present in the interlayer. This can be achieved by repeatedly washing the sample with 1.0 M solution of NaCl and then deionized water to remove the excess chloride. For more details on sample preparation of clay minerals for TEM the reader is referred to article by Buseck and Iijima (1975). In any case, interpreting TEM images of clay minerals can be a difficult task, as demonstrated by O'Keefe et al. (1978) through simulation.

Unreacted kaolinite and reacted solids were centrifuged and dried overnight before they were sent to Alberta Center of Surface Engineering and Science (ACSES) for TEM/EDX/SAED analysis.

3.3.7 Moisture analyzer

Moisture measurements in MFT samples were carried out using a Mettler Toledo HB43-S Halogen Moisture Analyzer. Approximately 3 g of the wet sample are placed onto the aluminum pan that fits inside the instrument. The analyzer weighs the samples and heats using the integral halogen heating module. During the drying process, the mass of the sample is constantly measured and the amount of reduction in moisture is directly reported in the display. On completion of the run, the final moisture content of the sample is displayed.

3.3.8 Dean-Stark analysis

Dean-Stark analysis is a method used for determining the amount of bitumen, solid and water in a sample by extraction through toluene (Starr & Bulmer, 1979). A setup similar to soxhlet extractor is used, in which toluene is heated so that the vapours wash over the sample placed in a thimble and extract the bitumen and water from the sample. The solids remain in the thimble while the water collects in a water trap. The extracted bitumen remains mixed with the toluene. The extraction process is complete when clear colorless liquid drips off from the bottom of the thimble (Barber, 2004).

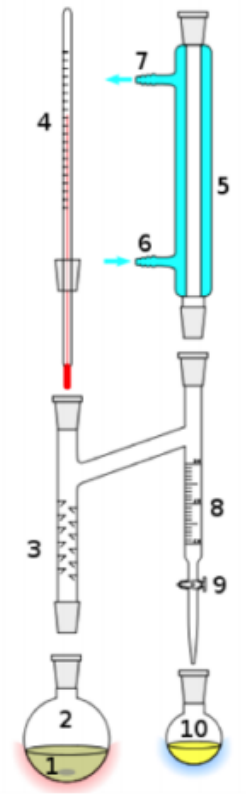

Figure 15: Illustration of Dean Stark Apparatus. (1) Toluene (2) Round-bottomed Flask (3) Holder for Froth Thimble (4) Thermometer (5, 6, 7) Reflux Condenser (8, 9) Reflux Collector (10) Receiver flask to collect water (Dean & Stark, 1920)

Figure 15 illustrates a schematic of a typical Dean Stark analysis setup. Approximately 200 mL of toluene is used in the analysis and heated above the boiling point (110.6 °C). One of the important considerations during this process is to regularly drain the water from the trap.

After the extraction process, the amount of water collected is weighed and so is the solids remaining in the thimble. The amount of bitumen is determined from the toluene remaining in the flask. This analysis has specifically been employed to measure the solid content in the MFT sample.

3.3.9 Capillary suction time

Capillary suction time (CST) of MFT was measured using a Triton Type 319 Multi-purpose capillary suction timer with 5 single radius test heads. CST assesses the resistance of MFT samples to filtration and gives an idea of the reacted MFT samples' dewatering capability. Higher CST denotes more resistance and lower CST denotes otherwise.

In theory, the capillary suction time (CST) apparatus measures the time taken for water from the sample to travel a fixed radial direction through a porous filter paper. This is achieved using electrodes arranged in triangular manner. The time starts when the fluid reaches the first two electrodes and it stops when it reaches the third. The measured time is the capillary suction time. MFT samples were placed inside single radius cell heads with 10 mm diameter and 7x9 cm Triton filter paper was used to gauge the dewaterability of different types of MFT.

Chapter 4

Results and Discussion

4.1 Kaolinite

4.1.1 Shear strength measurement

The shear strengths were measured 90 days after the samples were mixed with the alkali activators. The shear strengths of the kaolinite and centrifuged MFT samples in the different series of tests are summarized in Table 10. Figure 16 shows the change in shear strength with the changing Na_2SiO_3 concentration while NaOH concentration has been kept constant.

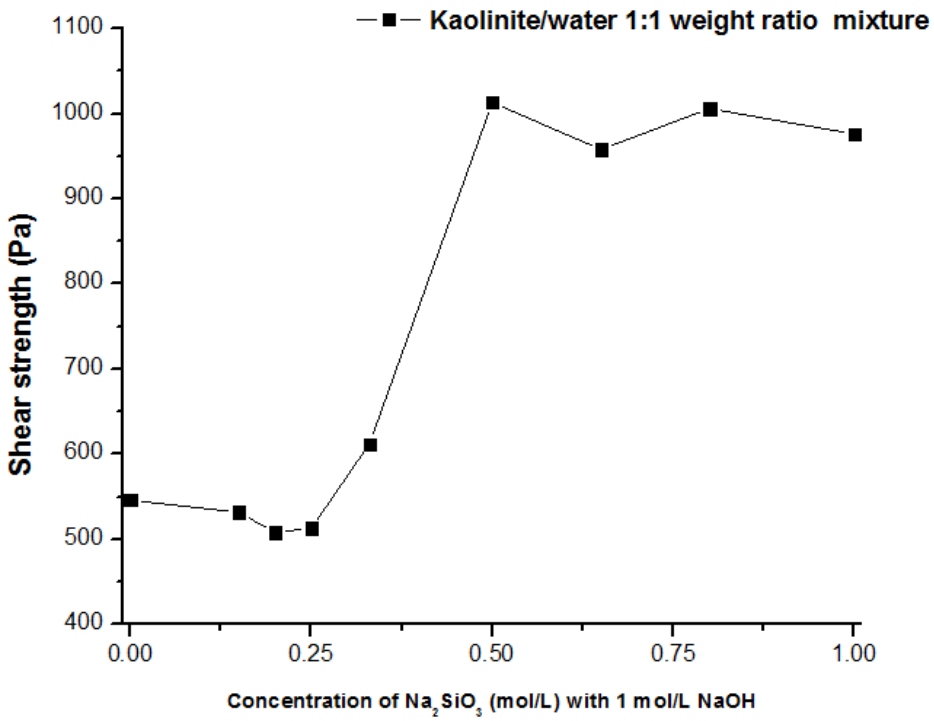

Figure 16: Shear strength of kaolinite with varying concentrations of Na_2SiO_3 and 1 mol/L of NaOH.

It should be noted that the optimum concentration refers to the concentration of alkali activators, NaOH and Na_2SiO_3, at which the highest shear strength of sample is obtained. The optimum molar ratio of Na_2SiO_3 to NaOH for kaolin/water mixture was found to be 0.5 to 1. This concentration was used for sample A-1-6 (refer to Table 4).

The literature reports a variety of optimum ratios. While many sources have pointed out the optimum mass ratio of Na_2SiO_3 to NaOH to be 1 or higher, some studies claim values to be below 1. For instance, Chindaprasirt et al. (2007) and Khale and Chaudhary (2007) stated that a mass ratio for Na_2SiO_3:NaOH of 0.67-1 gives the best compressibility, whereas Hardjito and Wallah (2004) published experimental results that denote the optimum mass ratio as high as 2.5. Our test results indicated an optimum molar ratio of Na_2SiO_3 to NaOH to be 0.5 to 1, or an optimum mass ratio of 1.5 to 1. Our results were more in line with those of Hardjito and Wallah (2004).

The B-1 series, as mentioned in Chapter 3, was set up to gauge the effect of increasing concentration of the alkali activators on shear strength of the samples while maintaining the same ratio of sodium silicate to sodium hydroxide. The results of this experimental series are illustrated in Figure 17.

The concentration multiplier, M, refers to a certain concentration of the alkali activators. For instance, when M is equal to 0.5, the concentration of NaOH is 0.5 mol/L and that of Na_2SiO_3 is 0.16 mol/L. The results from this series illustrate that the shear strength does not increase with the increasing concentration of alkali activator. The shear strength at the highest concentration was lower than that recorded at M of 0.5. Besides, a strange behavior was noted at M of 0.1, which will be discussed further in this chapter.

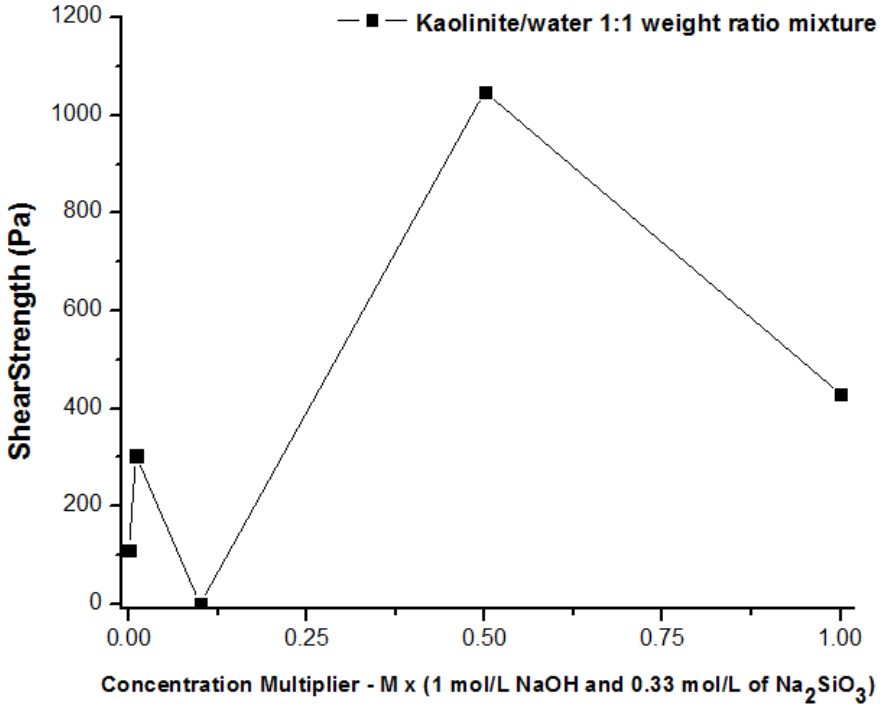

Figure 17: Shear strength of kaolinite with varying concentration of Na_2SiO_3 and NaOH. M is the concentration multiplier with M = 1 at 1 mol/L NaOH and 0.33 mol/L Na_2SiO_3.

In order to study the change in shear strength with time, 12 samples were prepared at the optimum concentration, and the shear strength of these samples were measured separately over a span of 90 days. The results are shown in Figure 18.

The shear strength is observed to increase with time, with the maximum increase occurring in the first twenty days after the start of the experiment then slacken after 20 days. This indicates that most of the reactions take place in first few days after the addition of the activators. The reaction is observed to slow down as the increase in shear strength gradually flattens. However, based on the trend, an increase is expected 90 days after the experiment was begun.

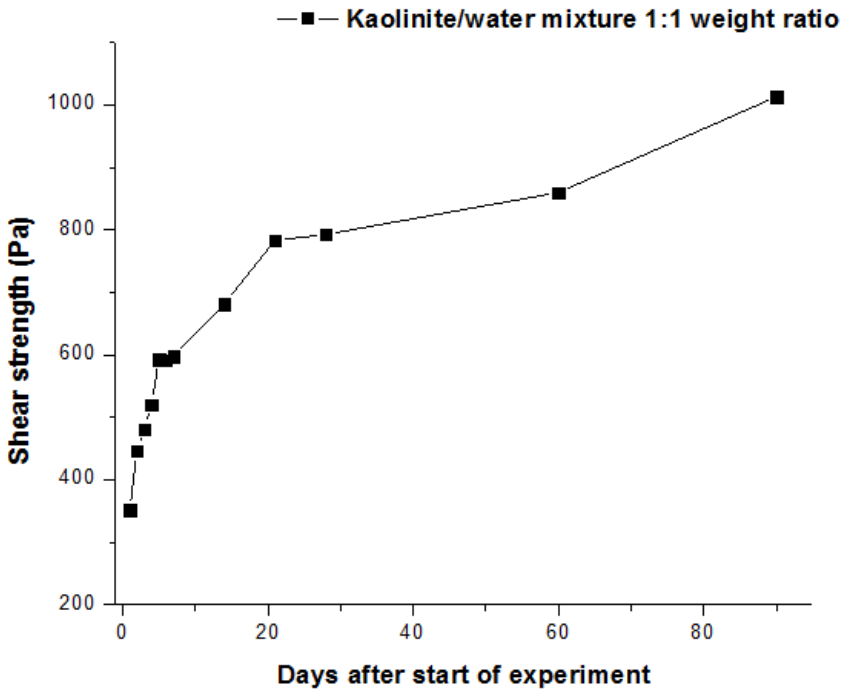

Figure 18: Change in shear strengths of kaolinite/water samples over a period of 90 days after being treated with optimum molar ratio of Na_2SiO_3:NaOH of 0.5:1. The NaOH dosage was 4 wt%.

4.1.2 Characterization results

The results of ICP-OES analysis of the supernatant of sample A-1-6 for kaolinite are shown in Table 6, together with the theoretical composition of a solution containing 1.0 mol/L NaOH and 0.5 mol/L Na_2SiO_3. The results show that the concentration of aluminum ions increased from 0 to 109 ppm, clearly due to the dissolution of the kaolinite sample. Interestingly, while the solution of 1.0 mol/L NaOH and 0.5 mol/L Na_2SiO_3 should contain 14,000 ppm of Si and 46,000 ppm of Na, the actual measured concentrations of Si and Na in sample A-1-6 were 2,915 ppm and 23,651 ppm, respectively. The results seem to indicate that there was indeed the dissolution of the kaolinite sample, but the dissolved ionic species must have re-solidified which consumed the Si and Na ions.

Table 6: Comparison of ionic concentration in a solution mixture of 1 mole/L NaOH and 0.5 mol/L Na_2SiO_3 with the supernatant of sample A-1-6 as measured by ICP-OES.

	Al	Si	Na
A-1-6 Supernatant (ppm)	109	2,915	23,651
Expected amount if no reaction takes place (ppm)	0	14,000	46,000

Zaman and Mathur (2004) studied the solubility of kaolinite under various pH conditions. The following reactions illustrate the dissolution in acidic and basic conditions respectively:

Acidic

$$Al_2Si_2O_5(OH)_4 + 6H^+ \rightarrow 2Al^{3+} + 2H_4SiO_4 + H_2O \quad (8)$$

Basic

$$Al_2Si_2O_5(OH)_4 + 2OH^- + 5H_2O \rightarrow 2Al(OH)_4^- + 2H_4SiO_4 \quad (9)$$

Zaman and Mathur (2004) pointed out that while the silicon concentration decreases with increasing pH, aluminum ion concentration was comparatively low in the solution over the entire range of the pH studied. This may be a result of the formation of $Al(OH)_3$ precipitate which is amphoteric and has low water solubility in the pH range of 4.5-8.5. Also, an aluminosilicate gel can form which can further decrease the concentration of Al^{3+} in the supernatant. They also observed further dissolution of kaolinite to release Al^{3+} and Si^{4+} ions in the presence of sodium silicate as a dispersing agent.

In another detailed study, Zaman et al. (2003) have elaborated how the dissolution of kaolinite and the release of Al^{3+} and Si^{4+} is dependent on the types of dispersing agents, dispersant dosages and pH. Hence, this explains the deduction from the results obtained from the ICP-OES about the dissolution of silicon and aluminum from the kaolinite structure. To further study ion content of the samples, the samples that were prepared for separate shear strength measurements were centrifuged and the supernatant was decanted and its ion content was analyzed by ICP-OES.

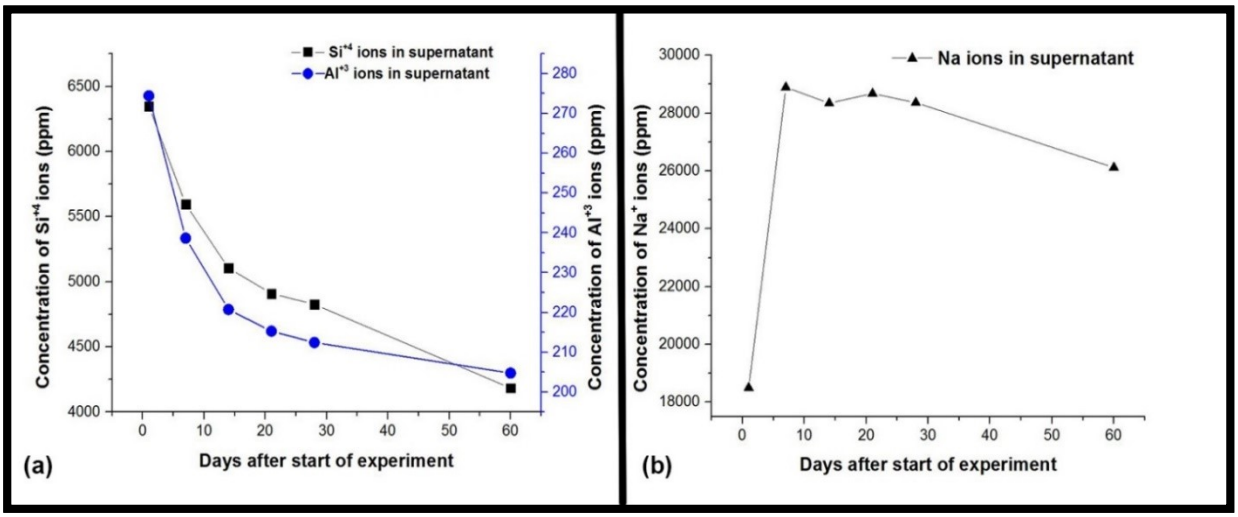

Figure 19: Change in supernatant ion concentration of sample A-1-6 with time of (a) Silicon & Aluminum (b) Sodium

The concentration of the ions are seen to decrease indicating that Si and Al ions might be re-solidifying, forming the geopolymeric species. Decrease in the ionic concentration of Na^{+} further denote to the formation of a polysialate molecule hypothesized by Davidovits (2011). Due to the negative charge on tetrahedral aluminate, the polysialate molecules need monovalent cation to balance the net charge as denoted by reaction mechanism of kaolinite with NaOH in Figure 20.

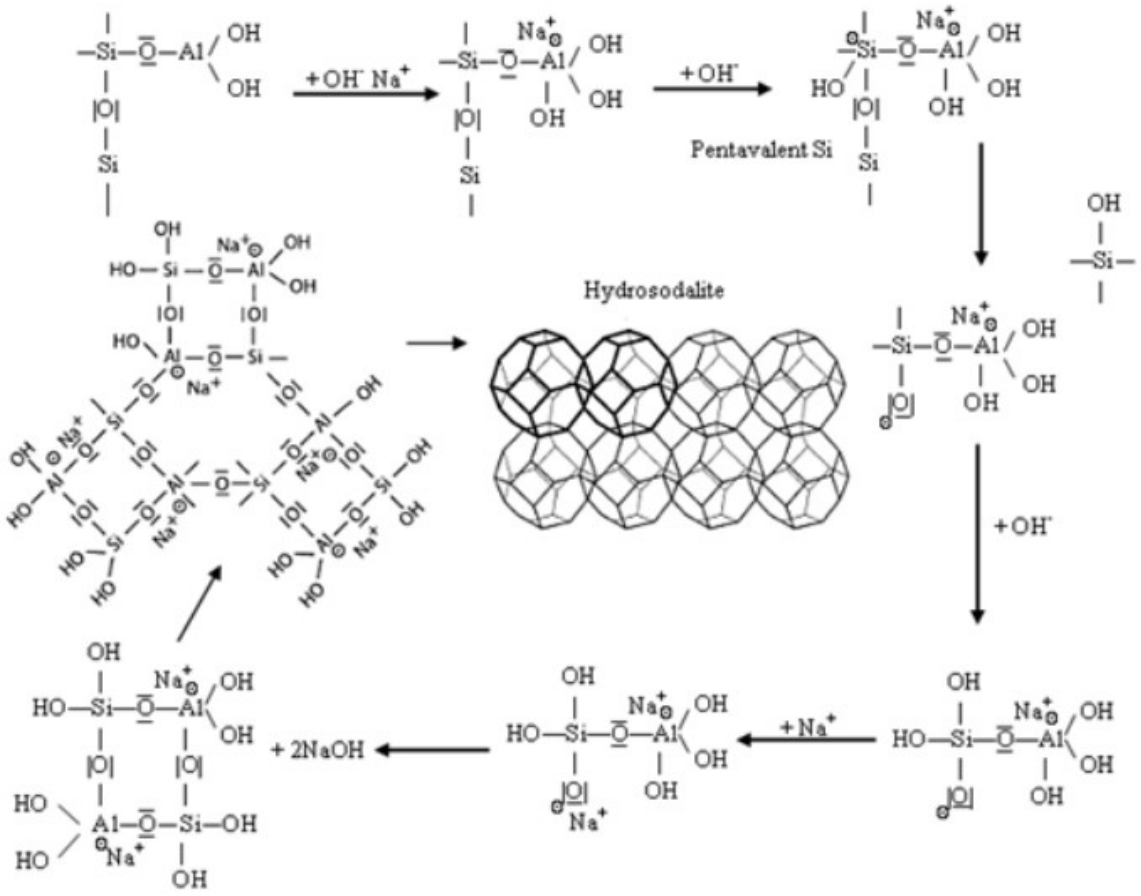

Figure 20: Reaction mechanism of kaolinite with NaOH (Cheng & Hazlinda, 2011)

However, the initial low concentration of Na^+ ions could be attributed to the high adsorption of Na^+ to the surface of kaolinite, which is reported to have negative surface charge in alkaline pH (Yukselen & Kaya, 2003; Yukselen-Aksoy & Kaya, 2011).

Figure 21 shows the FTIR spectrum of kaolinite sample superimposed with the spectrum of sample A-1-6. Following the analysis of Davidovits (2011) who defined every peak expressed by kaolinite in the FTIR spectrum, it can be seen that the kaolinite tested in this work has a high purity. Similarly, the FTIR spectrum of the bulk A-1-6 sample shows that it is mainly kaolinite. The only discernible difference between the two spectra is the peak at 1440 cm^{-1} which corresponds to the very strong intensity exhibited by sodium carbonate (Miller and Wilkins,

1952). The presence of sodium carbonate is indicative of unreacted sodium hydroxide. Sodium hydroxide might have reacted with the atmospheric carbon dioxide to produce the sodium carbonate during the drying stage of sample preparation for FTIR (Jaarsveld & Deventer, 1999). The low intensity points out that sodium hydroxide is present in very small quantities. Most of the peaks associated with sodium carbonate could have been overlapped by strong kaolinite signals. Also, the peaks exhibited by the formed geopolymeric product might also been overlapped by kaolinite for the same reason.

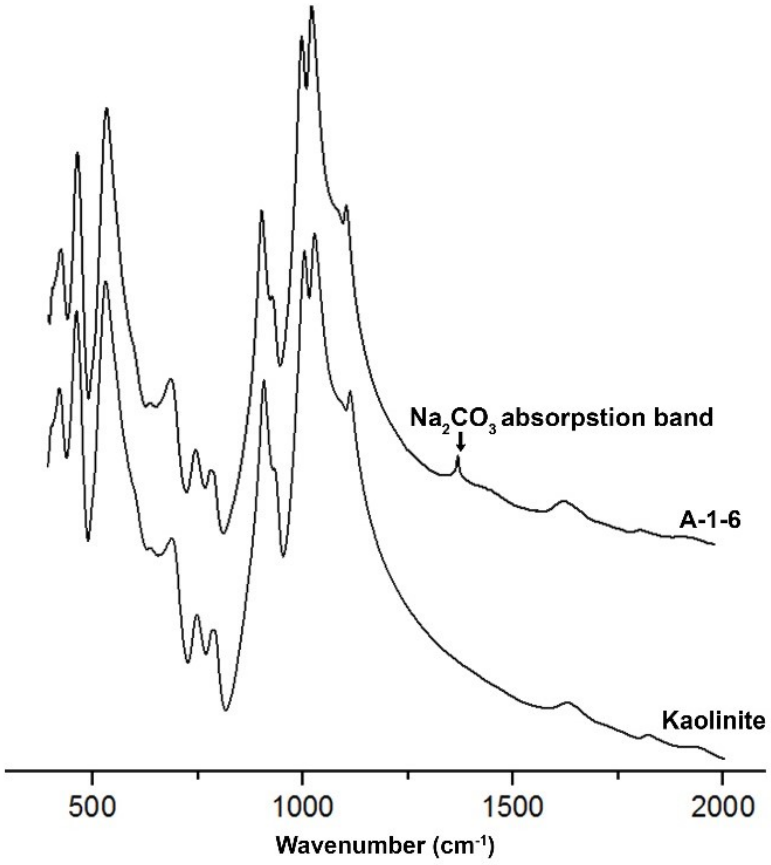

Figure 21: FTIR spectra of kaolinite and sample A-1-6. The latter exhibits a peak typically pronounced by sodium carbonate which denotes the presence of unreacted sodium ions on the surface

Figure 22 depicts the XRD patterns of kaolinite and sample A-1-6. Like the FTIR results, the XRD spectrum shows that sample A-1-6 is mainly unreacted crystalline kaolinite. However, the results from the quantitative XRD analysis done by RockJock™ shows a decrease in crystallinity. The amount of the ordered and branched kaolinite has decreased by 2.8 and 5 percentage points, respectively, denoting modification of the kaolinite crystal structure on addition of the activators. About 7.8% of the kaolinite has been converted to an amorphous species which cannot be detected by XRD.

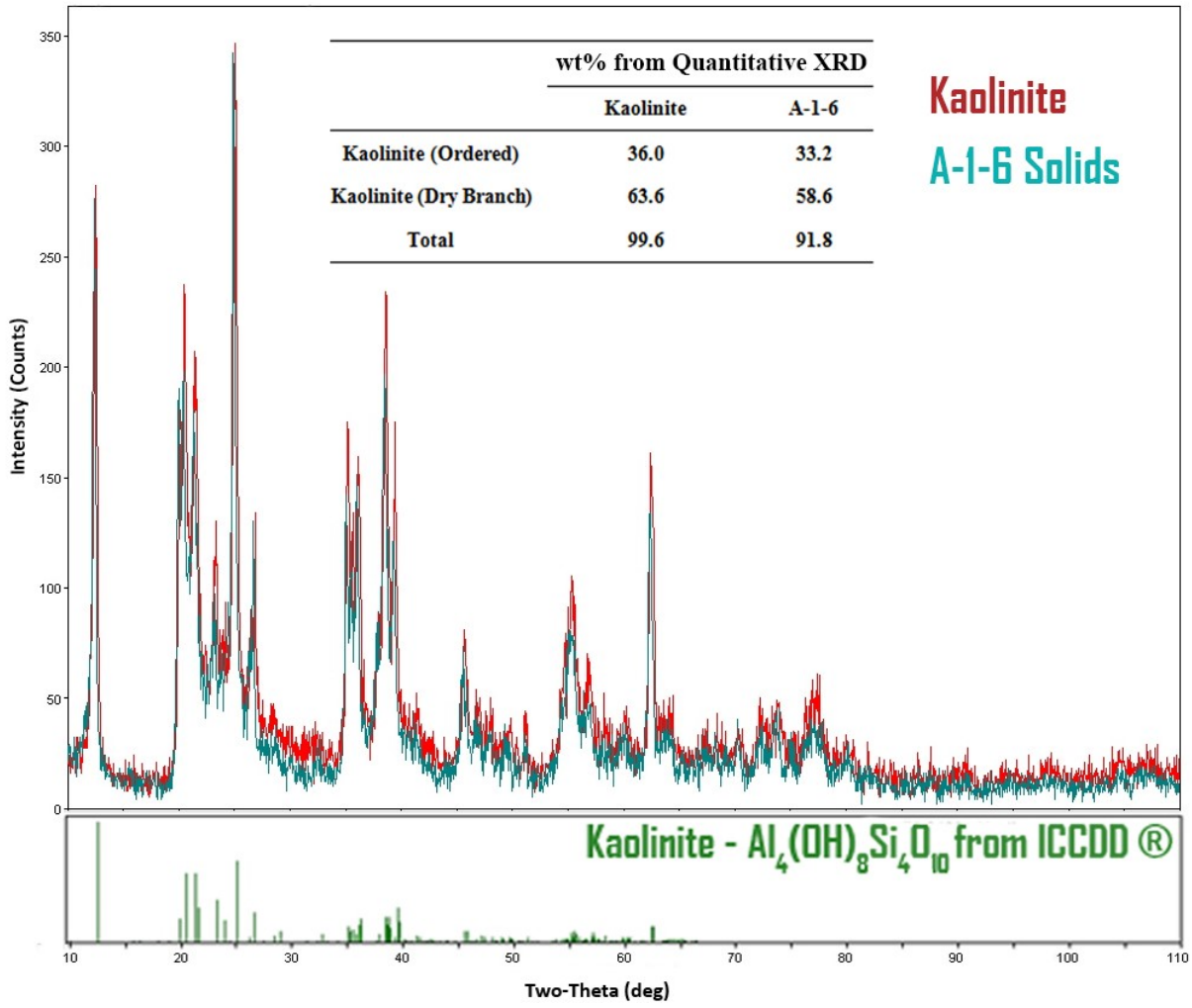

Figure 22: Quantitative XRD results of sample kaolinite and sample A-1-6 generated from JADE™. Results indicate a decrease in the quantity of crystalline kaolinite in A-1-6.

This hypothesis is further supported by results from TEM results as seen in Figure 3a. While the bulk of the material has remained in the crystalline state, the selective area electron diffraction shows the presence of amorphous grains on the periphery of the A-1-6 sample.

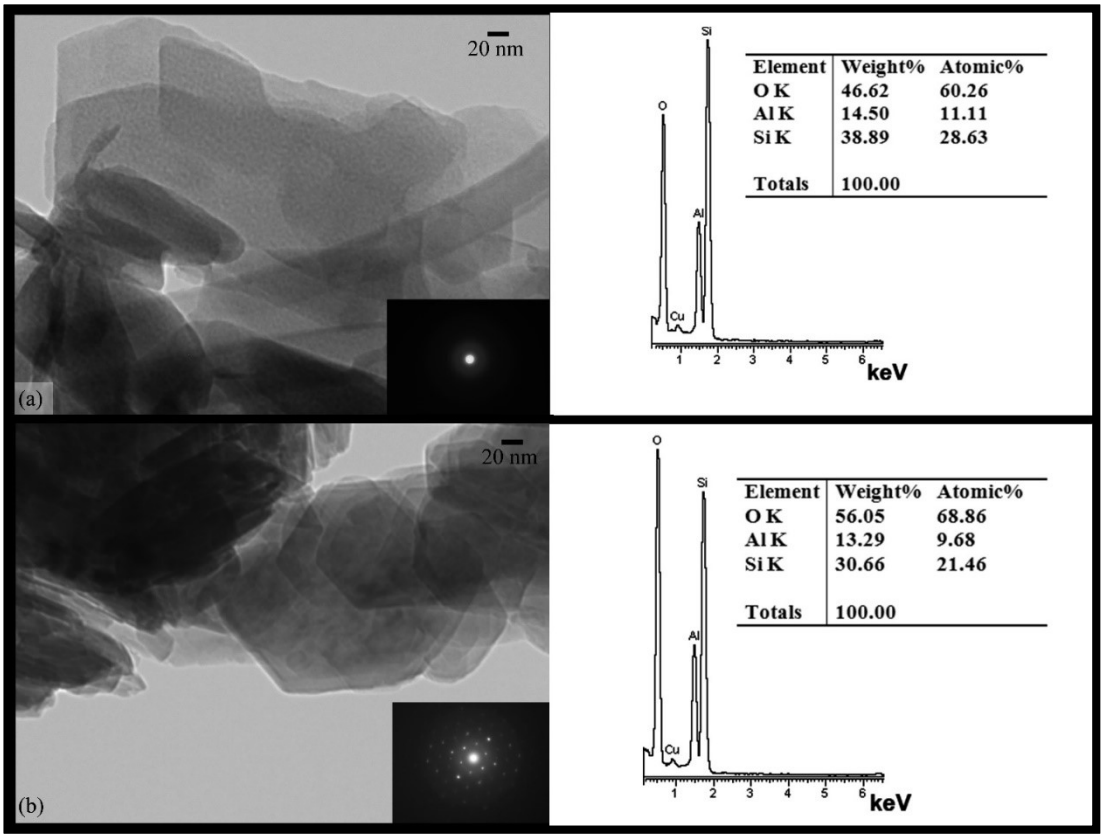

Figure 23: Transmission electron microscopy, selective area electron diffraction and energy dispersive X-ray of reacted and unreacted kaolinite at 200 kV accelerating voltage with (a) amorphous aluminosilicate grains characteristic of geopolymer found on the periphery of grain clusters in the reacted sample (b) characteristic hexagonal shaped grains and high crystallinity observed in unreacted kaolinite structure.

Furthermore, energy dispersive x-ray (EDX) spectroscopy indicated that these grains were aluminosilicate in nature. It should be noted that the appearance of copper in the EDX is due to the copper grid on which the samples were mounted. Amorphous grains have been

reported to be characteristic to geopolymers (Davidovits, 2011). The presence of these amorphous grains was repeatedly seen on the edges of the bulk crystalline material.

The TEM/EDX/SAED, coupled with ICP-OES and XRD results, indicate that the kaolinite has undergone chemical changes even at much lower concentration of the 'alkali activators' used in this work than reported in the literature. The presence of geopolymer grains further corroborate in explaining the increase in shear strength of kaolinite.

Hence it is seen that at this concentration of alkali activators, the geopolymerzation reactions are only taking place on the surface of the aluminosilicate minerals. Nevertheless, the newly formed geopolymer grains act like a matrix holding the crystalline clay particles together.

4.1.3 The Anomaly of B-1-3

In sample series B-1, sample B-1-3 did not strengthen during the geopolymerisation treatment. This sample was a 50 wt% kaolinite suspension mixed with the alkali activators at concentrations of 0.1 mol/L sodium hydroxide and 0.033 mol/L sodium silicate. On mixing the alkali activators with kaolinite, the resulting suspension immediately turned serous, showing negligible mechanical strength. This condition remained as such indefinitely even after the sample was kept untouched for several weeks. Therefore, to understand this behavior, characterization techniques of ICP-OES, particle size distribution, and XRD were carried out on B-1-3.

The B-1-3 sample was first centrifuged to separate the solids from the supernatant. The supernatant was then decanted and kept aside for ICP-OES analysis while the solids were divided into two equal portions. One portion of the solids was characterized for particle size

distribution by laser diffraction and the results were compared to a control kaolin sample. The results are summarized in Table 7.

It was found that B-1-3 solids possessed slight smaller particle size distribution than unreacted kaolinite solids. Sonication was required for the kaolinite control sample, which otherwise showed a higher average particle size possibly due to aggregation. This was not observed for the B-1-3 solids which showed a consistent particle size distribution even after sonication.

Table 7: Particle size distribution of kaolinite and dried solids of sample B-1-3. The table shows how the particle size distribution dropped for kaolinite sample after sonication.

		Kaolin	Sample B-1-3
Without Sonication	**D_v (10)**	1.74 µm	0.556 µm
	D_v (50)	12.8 µm	4.38 µm
	D_v (90)	43.9 µm	23.1 µm
After Sonication	**D_v (10)**	0.881 µm	0.561 µm
	D_v (50)	5.45 µm	4.38 µm
	D_v (90)	24.0 µm	21.2 µm

The other portion of solids was vacuum dried and was sent for XRD analysis. The obtained results were compared to the spectrum of the of kaolin sample that was initially used for preparing B-1-3. The results generated from JADE™ software are shown illustrated in Figure 9.

The XRD results denote that B-1-3 solids are mainly unreacted. The ICP-OES analysis of the supernatant showed the presence of aluminum ions which were not initially present in the solution. Also, the amount of silicon ions were seen to be much higher than predicted from the

added sodium silicate. Hence, there is a possibility that some amount of dissolution of kaolinite has taken place on addition of the alkali activators. The characterization results from the ICP-OES are illustrated in Table 8.

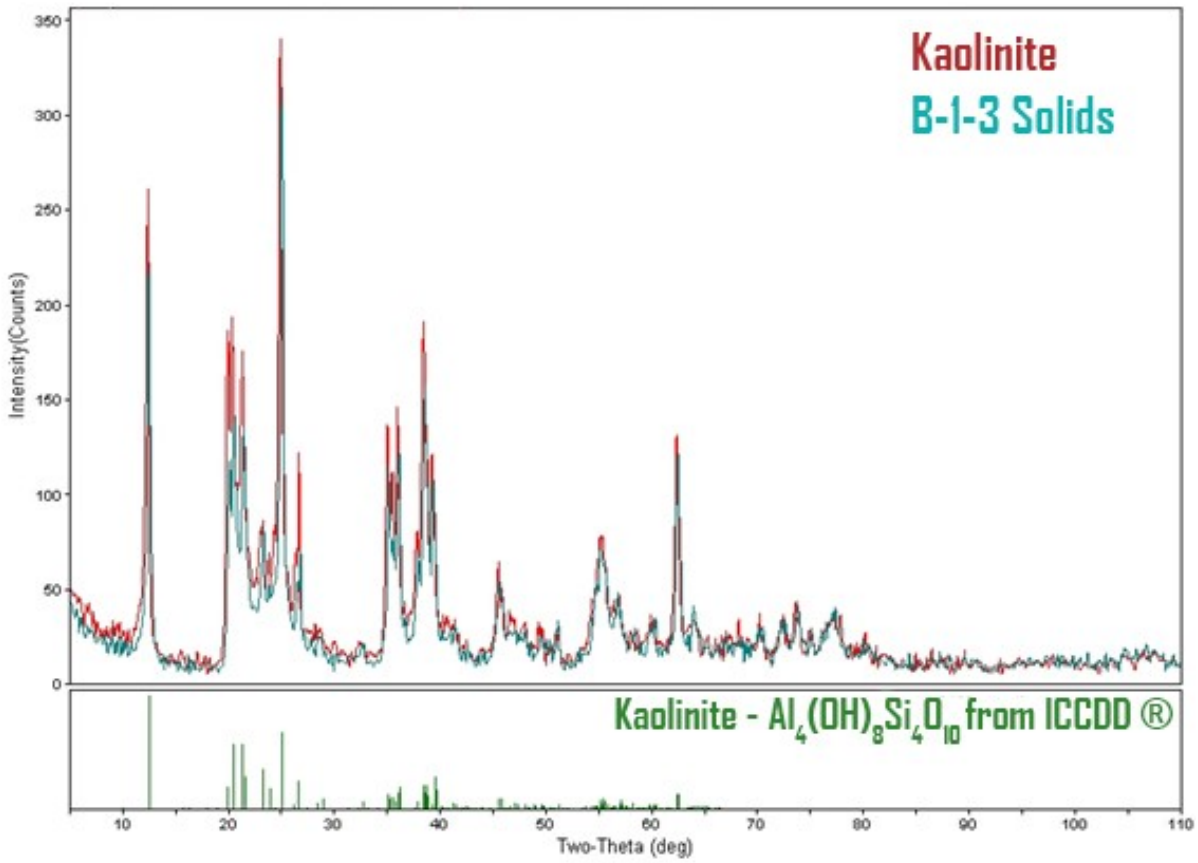

Figure 24: XRD pattern of the sample B-1-3 solids (Green) and kaolinite (Red) generated from JADE™. The two spectra have similar peaks denoting that B-1-3 solids are quite similar to unreacted kaolinite.

From the results of the characterization, it can be concluded that the phenomenon exhibited by B-1-3 is deflocculation. Commercial 'deflocculants', or 'dispersants', are used in the ceramic industry to reduce the attraction forces between clay particles in a suspension so that

the resulting 'slip' can be easily pumped (Andreola et al., 2006; Rodrigues et al., 2002). Such 'deflocculants' includes silicates, sodium tripolyphosphates and polyacrylate.

Table 8: Results of ICP-OES of the supernatant of sample B-1-3 compared to the amount of ions initially present in the solution mixture contributed by added sodium silicate and sodium hydroxide.

	Al	Fe	Na	Si
Expected amounts from solution (ppm)	0	-	5316.4	919
ICP-OES of Supernatant (ppm)	1549	153.8	1161	1880

Rodrigues et al. (2002) pointed out that deflocculation of clay can be achieved by one or more of the following mechanisms: electrostatic repulsion, steric hindrance and cation capture through chelation. The principle mechanism, however, used here is electrostatic repulsion. On the addition of a monovalent salt, with alkali metal ions like Na^+ or Li^+, the zeta potential of the suspended clay increases. The Na^+ ions, which are large and have a small charge, are highly hydratable and adsorb on the clay particle to create a thick double layer. The repulsive forces between the particles have a wide field of action and appear at a distance where the attraction forces are negligible, as per the DLVO theory, causing repulsion. Since, the alkali activators, sodium hydroxide and sodium silicate, used in sample B-1-3 possess Na^+, they both contribute to deflocculation. Besides, an increase in pH caused by hydroxide ions increases the negative charge on the edges of the clay. The highly charged surface of the clay causes strong long-range repulsion further aiding in deflocculation.

The role of sodium silicate in deflocculation can also be explained by work done by Diz et al. (1989). In their study, they elucidated the deflocculation mechanism of kaolinite by polyanions like sodium silicate, sodium pyrophosphate and sodium polyacrylate. The silicate

species, as they postulated, is first adsorbed on the kaolinite surface in one or more of the following ways:

- Electrostatic attractive interaction between negatively charged ions and positive edges (possible only at low pH in kaolinite)
- Intermolecular interactions, like hydrogen bonds and van der Waals bonds between the ions and the basal plane or the edge surface atoms
- Condensation reaction between silanol group of silicate and kaolinite surface hydroxyls

Once the silicate species has been adsorbed, the increased stern potential results in a larger energy barrier to aggregation of clay particles. But again, slight variation in the conditions can lead to desorption and decrease in the stern potential, eventually leading to aggregation.

In order to study as to which of the two reagents are more effective in 'deflocculation', two different samples were prepared. One containing kaolinite in 0.033 mol/L of sodium silicate, while the other containing kaolinite in 0.1 mol/L sodium hydroxide. It was observed that both the samples showed consistencies quite similar to B-1-3. This denotes that a change in pH alone can also cause deflocculation and it is consistent with the results provided by Yukselen-Akdoy and Kaya (2011) who clearly demonstrate that the surface charge of kaolinite becomes increasingly negative above pH 7. Also, a summary of various zeta potentials studies of kaolinite at high pH indicate that kaolinite surface is negative at alkaline pH (Yukselen & Kaya, 2003). Not surprisingly, the 0.033 M sodium silicate sample alone also caused the deflocculation and this result matches the one obtained from the study done by Diz et al. (1989) in which a concentration of 0.04 mol/L of sodium silicate was considered to be a critical point beyond which aggregation of the clay particle was observed. This is because high silicate concentration increases the ionic strength of the solution, causing the electrical double layer of the kaolinite

particle to compress. Eventually, the short range attractive forces, like van der Waals, become dominant and cause aggregation. It should be noted that sample B-1-3 did not need sonication for particle size distribution analysis which further supports the idea of deflocculation.

ICP-OES results showed significant amounts of silicate and aluminum ions in the supernatant. This can be supported by the explanation on dissolution provided in the previous section. To further elaborate on this, Figure 25 displays surface response plots showing how the dissolution of Al^{3+} and Si^{4+} from kaolinite is dependent on the dosage of sodium silicate and pH of the solution (Zaman et al., 2003).

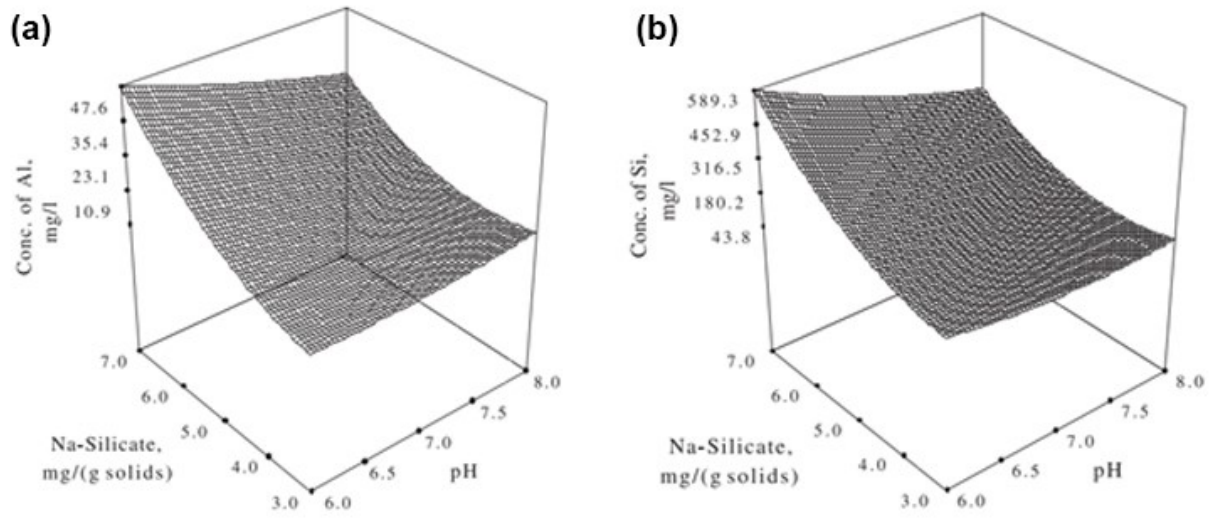

Figure 25: (a) Surface response plot for the effects of pH and Na-silicate dosage on solubility of (a) aluminum (b) Silicon from kaolin (time = 13 h, wt% solids = 35) (A. Zaman et al., 2003)

In brief, sample B-1-3 helps in pointing out sodium hydroxide and sodium silicate as dispersants, which are conflicting roles to the ones they play in geopolymerisation. Dispersion is seen to be quite dominant in sample B-1-3, even though dissolution of kaolinite particle, which is the first stage of geopolymerisation, is also observed. The presence of hydroxide ions increases

the pH of the system, while the sodium ions and silicate polyanion get adsorbed on the kaolinite surface, leading to dispersion by electrostatic repulsion. This prevents the clay particles from approaching each other to propagate geopolymerisation reaction.

Hence, it is crucial to understand the balance between dispersion and geopolymerisation reaction, especially in this context since low concentrations of the alkali activators are being used. The optimum concentration found in this study, however, is significantly above the deflocculation concentration. Increased shear strength was observed at the optimum concentration and geopolymeric species were also found to be formed. While the prime function of alkali activators should be to initiate geopolymerisation in clay minerals, it is imperative to note that the same reagents can be used to deflocculate clays and particular importance should be placed in controlling dosage for achieving surface geopolymerisation.

4.2 Mature fine tailings

4.2.1 Preliminary test series

Centrifuged MFT samples with 51 wt% solids were prepared, treated with alkali activators, and kept for 90 days before shear strength measurements were carried. Figure 26 shows the results of the preliminary series, A-2 (see Table 4), prepared to find the optimum concentrations of the alkali activators.

The optimum concentration for Na_2SiO_3 and NaOH was found to be 0.5 mol/L and 1 mol/L, or an optimum mass ratio of 1.5 to 1. This is the same concentration which was found for kaolinite/water samples as mentioned previously.

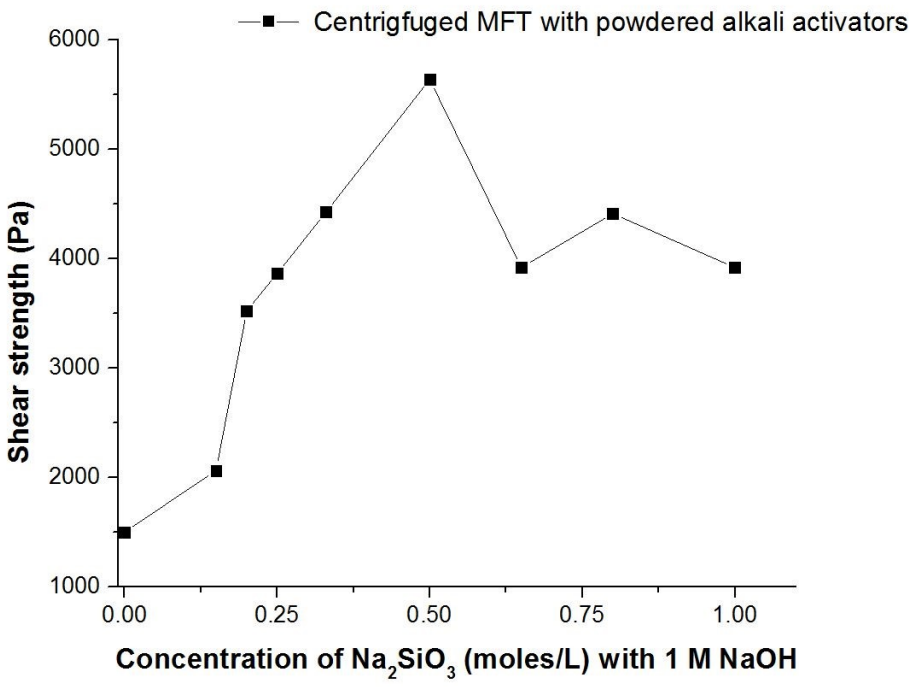

Figure 26: Shear strength of centrifuged MFT (51 wt% solids) with varying concentrations of Na_2SiO_3 and 1 mol/L of NaOH

Nevertheless, the B-2 series (see Table 4), which was prepared to determine the effect of increasing concentration on shear strength while maintaining a fixed ratio of sodium silicate versus sodium hydroxide, displayed a different trend from the kaolinite/water mixture series of B-1. The results of the B-2 series are shown in Figure 27. In series B-1, deflocculation was observed at M of 0.1 and the maximum shear strength was obtained at M of 0.5. However, in the B-2 series the shear strength is seen to increase with the increasing concentration of the alkali activators. Moreover, unlike kaolinite/water samples, no deflocculation is observed at any concentration in MFT samples.

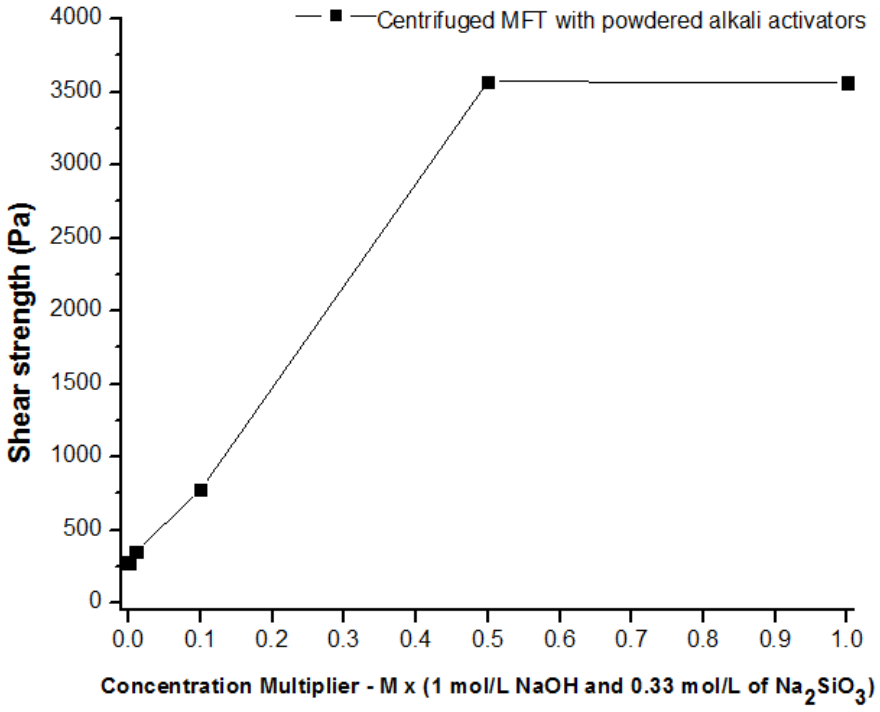

Figure 27: Shear strength of centrifuged MFT (51 wt% solids) with varying concentration of Na_2SiO_3 and NaOH. M is the concentration multiplier with M = 1 at 1 mol/L NaOH and 0.33 mol/L Na_2SiO_3.

It is also observed that the shear strength of the MFT samples is significantly higher than the kaolin/water samples even though the solids contents were similar. This is probably due to the fact that MFT contains a variety of alumninosilicate minerals besides kaolinite, as depicted by Table 2. These alumninosilicates, like quartz, feldspar and other clay minerals, are abundantly present as Al-Si source materials for geopolymerisation reaction to take place. Also, it should be noted that the octahedral aluminum in kaolinite is reported to resist the attack of alkali (Swaddle, 2001). The octahedral aluminate contributes in slowing the dissolution process and, consequently, geopolymerisation as a whole giving kaolinite a lower shear strength. However, the presence of several other aluminosilicate minerals in MFT with aluminum in possibly more

reactive tetrahedral state can give a higher extent of geopolymerisation reactions (Sperinck et al., 2011; Kasperski and Mikula, 2011).

An extra set of samples was prepared for MFT and was named C-1 (see Table 4). This series tracked the increase in shear strength with the increase in the concentration of NaOH in the absence of Na_2SiO_3. The results are illustrated in Figure 28.

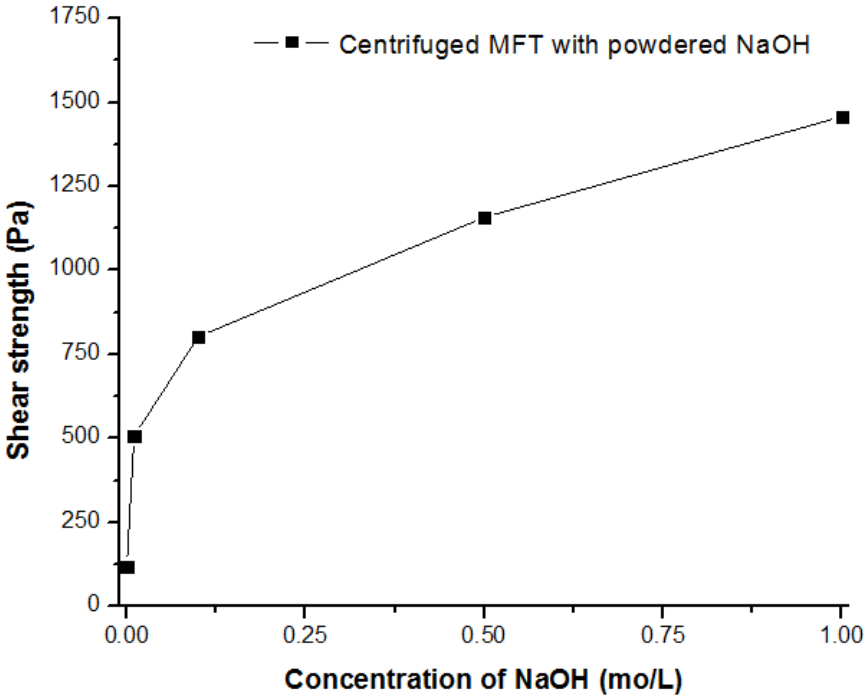

Figure 28: Change of shear strength of centrifuged MFT (51 wt% solids) with varying concentrations of NaOH without the presence of Na_2SiO_3

An increasing trend is observed in shear strength with the maximum strength being observed at 1 mol/L of NaOH. However the maximum shear strength is lower in this series than that observed for the optimum concentration in Series A-2. In addition, 1 mol/L was the highest

sodium hydroxide concentration tested, so that it clearly cannot be considered as the optimum dosage.

The results from the three series, A-2, B-2 and C-1, point out the importance of the synergistic effect of NaOH with Na_2SiO_3 in obtaining high shear strength. While sodium hydroxide is indispensable in initiating the reaction, the presence of Na_2SiO_3 is important in providing additional sodium and silicate ions in progressing the reaction as illustrated by hypothetical reaction mechanism shown in Figure 20.

4.2.2 Shear strength of different MFT at optimum ratio of activators

To observe the evolution of shear strength, the recipe of sample with series A-1 with the highest shear strength, A-2-6, was used for centrifuged MFT (51 wt% solids), polymer (A3335) flocculated MFT (48 wt% solids) and untreated MFT (37.9 wt% solids). Twelve samples were prepared and their shear strengths were measured at different time points over a period of 90 days after the alkali activators were added. Shear strength measurements of different types of MFT recorded over a span of 90 days show an increasing trend with maximum shear strength being recorded at 4,880 Pa for centrifuged MFT. Untreated MFT had a shear strength of 1,244 Pa and MFT treated with polymer flocculant was found to have a shear strength of 3,952 Pa. The results have been displayed by the plot in Figure 29.

The results indicate that the shear strength of untreated MFT sample was higher than that of kaolinite, even when its solid content was lower (37.9 wt% for MFT and 50 wt% for kaolinite). The higher shear strength, as mentioned before, could be attributed to the presence of other sources of aluminosilicate minerals besides kaolinite. These clays provide an adequate

supply of aluminosilicates with active tetrahedral sites required for geopolymerisation, leading higher degree of geopolymerisation (MacKenzie et al., 2008).

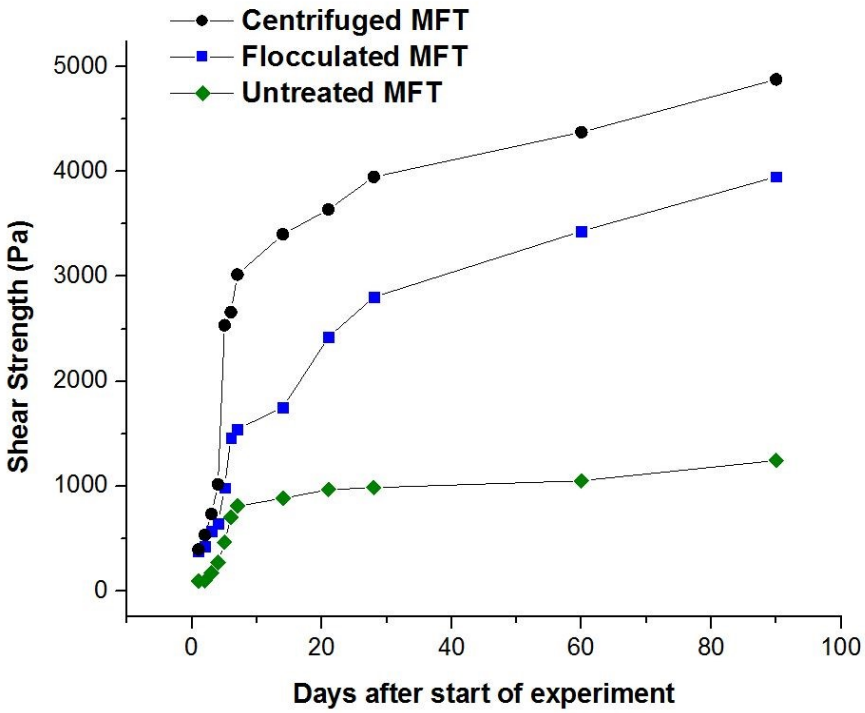

Figure 29: Shear strengths of MFT samples treated with optimum molar ratio of Na_2SiO_3: NaOH of 0.5:1

4.2.3 Hypothesis behind increase in shear strength

By using the deductions from the fundamental study done on the model kaolinite system, the increase in the shear strength in MFT can be explained. Figure 30 gives a graphical description of how the geopolymerisation reactions on the mineral surfaces contribute to an increase in the overall shear strength of MFT. The graphic representation also demonstrates how the geopolymeric species acts as a matrix (glue) and increases the load bearing strength of MFT.

The shear strength also depends on the extent to which the reactions have taken place. In the span of time period over which the measurements were done, an increasing trend is observed. Literature reports an increase in compressive strength of samples over 30 days after the start of the reaction (Lizcano et al. , 2011; Van Riessen et al. , 2013; Wang et al., 2005). In the study by Chen et al. (2011), compressive strength of various geopolymers was reported to increase over a span of 90 days. The shear strength is observed to have increased for 90 days in this study and it seems to be still on the rise beyond 90 days. It is possible that the sodium hydroxide can activate polymerisation of Na_2SiO_3 forming a silica gel structure (Iler, 1979). This gelation of Na_2SiO_3 can itself contribute to increase in shear strength in samples especially if it polymerizes into chains and three-dimensional networks.

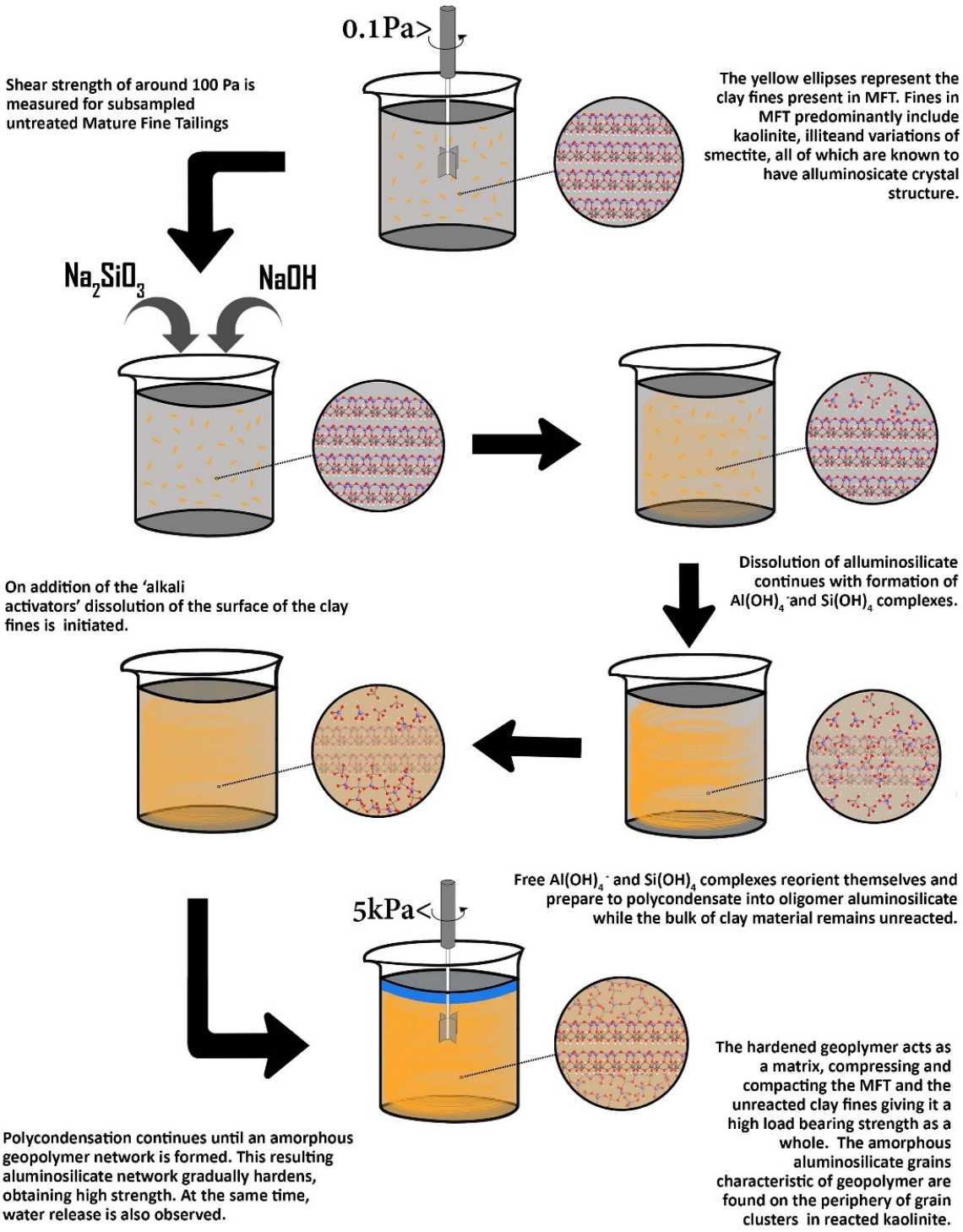

Figure 30: Graphic explanation of the surface geopolymerisation reaction processes upon the addition of alkali activators. The surface geopolymerisation reactions led to the gradual increase in the shear strength of the mature fine tailings.

4.2.4 Differences in shear strength

As denoted by Figure 29, the highest shear strength is observed on centrifuged MFT (51 wt% solids), followed by polymer flocculated MFT (48 wt% solids) and then untreated MFT (37.9 wt% solids). It is understandable why the lowest shear strength is displayed by the untreated MFT due to its high moisture content. Palomo et al. (2003) report the relation between the water to solids ratio and the final strength of geopolymers, with high water to solids ratio contributing to lower strength. Figure 31 displays the results of the study done by Khale and Chaudhary (2007) which points out how the compressive strength of a geopolymeric binder decreases with the increasing water to solid ratio at various curing temperatures. Compressive strength measurement is a good gauge for testing mechanical properties of materials and is preferred over shear strength for very high strength material.

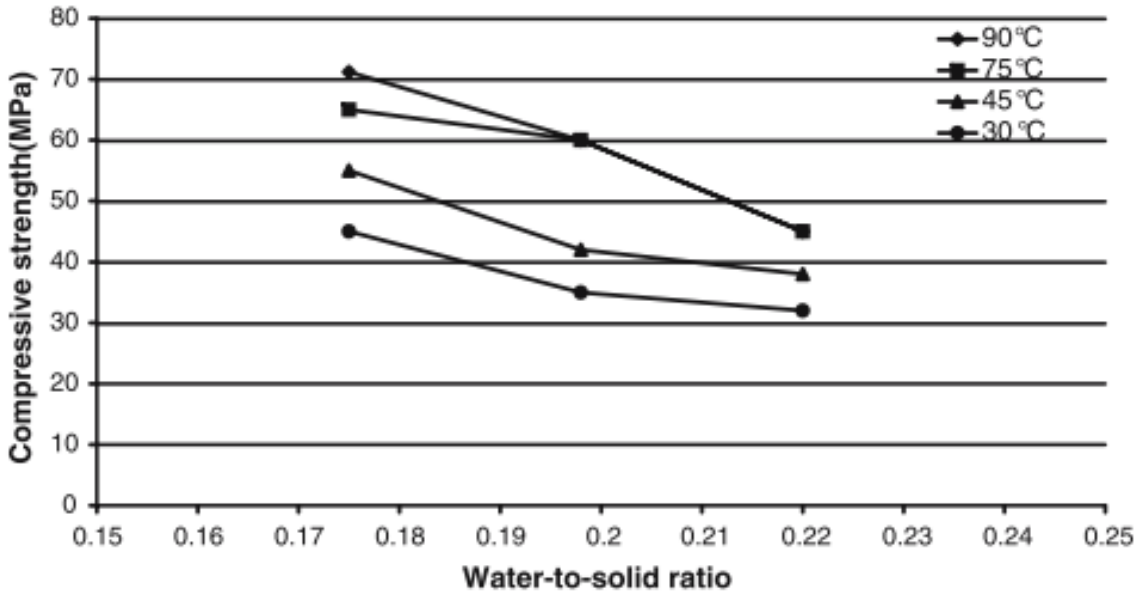

Figure 31: Effect of water to solid ratio on compressive strength at differing curing temperature (Khale & Chaudhary, 2007)

Geopolymers produced from metakaolin and cured at different temperatures showed the same behavior of low compressive strength at high water to solid ratio. It also explains why the initial shear strength of untreated MFT was recorded to be the lowest among the different categories of MFT.

On the other hand, the initial shear strength of polymer flocculated MFT was measured to be highest among the three groups but the final value was recorded to be much lower than centrifuged MFT even though centrifuged MFT and polymer flocculated MFT had similar water to solid ratio. The initial strength of polymer flocculated MFT was measured to be 395 Pa, whereas 115 Pa was measured for centrifuged MFT and 19 Pa for untreated MFT.

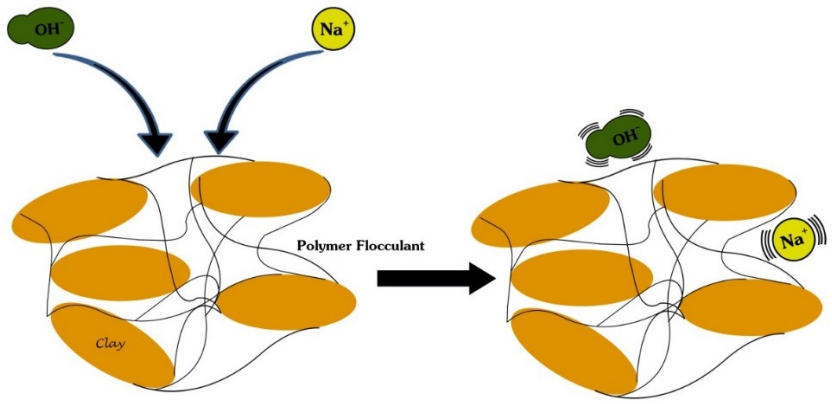

Figure 32: The presence of polymer flocculant on the surface of the clay particles hinders the alkali activators from reaching the clay mineral surface and initiating the geopolymerisation reactions

High initial shear strength of the polymer flocculated MFT is mainly due to the polymer bridge between clay particles, which clump the particles together and increase the overall strength. However, the final lower shear strength could be attributed to the polymer flocculant covering the surface of the clay minerals and hindering the alkali activators from propagating the geopolymerisation process. It is also possible that the addition of polymers flocculant yields flocs

of MFT instead of dispersed clay particles, which blocks some reactive sites to geopolymerisation. This leads to low degree of geopolymerisation. Since geopolymerisation, as a whole, is affected by the addition of the polymer flocculant, the final shear strength is lower than when the polymers were absent – i.e., the centrifuged MFT samples. Figure 32 graphically depicts this hypothesis.

4.2.5 Dewaterability

The dewaterability of the samples was tested using the capillary suction time apparatus. CST tests were carried out only on the MFT samples with the optimum concentration of the alkali activators. The results are summarized in Table 9.

Table 9: CST results of three types of MFT

Sample	Average CST (seconds)
Centrifuged MFT	3604
Flocculated MFT	574
Untreated MFT	2573

The results from CST tests clearly indicate that polymer flocculated MFT treated with alkali activators has the best dewatering capabilities. This is in line with the fact that formation of flocs increases the hydraulic conductivity of MFT allowing faster consolidation and water release. The addition of the akali activators after flocculation of MFT could help with increasing the shear strength of the consolidated solids, thus increasing the strength of the pores in the sediments, which facilitates water release. Hence, the synergy of flocculation and geopolymerisation can prove to be quite viable in the reclamation process of tailings ponds but assessing the implications of such technology is beyond the scope of this thesis.

Chapter 5

Conclusions

1. Preliminary tests were carried out on kaolinite/water mixture with 1:1 weight ratio and MFT centrifuged to 51 wt% solids. Two series for kaolinite/water and three series for centrifuged MFT were set up:
    - A-1 series: Kaolinite/water mixture with increasing Na_2SiO_3 concentration and 1 mol/L of NaOH to determine the optimum ratio of the alkali activators
    - B-1 series: Kaolinite/water mixture with increasing concentration of Na_2SiO_3 and NaOH at a fixed molar ratio of 0.33:1, or mass ratio of 1:1
    - A-2 series: Centrifuged MFT with increasing Na_2SiO_3 concentration and 1 mol/L of NaOH to determine the optimum ratio of alkali activators
    - B-2 series: Centrifuged MFT with increasing concentration of Na_2SiO_3 and NaOH at a fixed molar ratio of 0.33:1, or mass ratio of 1:1
    - C-1 series: Centrifuged MFT with increasing concentration of NaOH in the absence of Na_2SiO_3
2. The combination of 1 mol/L NaOH and 0.5 mol/L of Na_2SiO_3 was found to be the optimum concentration for both kaolinite/water mixture and centrifuged MFT as determined by series A-1 and A-2 respectively. The shear strength increased from 115 Pa to 4,880 Pa for centrifuged MFT (51 wt% solids) at the optimum activator concentrations. At the same activator concentrations, the original un-centrifuged MFT (37.9 wt% solids) only saw an increase of its shear strength from 19 Pa to 1,245 Pa.
3. The optimum concentration of the activators were added to MFT sample flocculated by adding 1000 g/t of A3335 polymer flocculant. While the solid content of the flocculated

MFT after 48 h sedimentation increased to 48 wt%, its shear strength increased from 395 Pa (without adding alkali activators) to 3,950 Pa (90 days after adding the alkali activators).

4. Fundamental studies conducted on kaolinite sample using quantitative X-ray diffraction, transmission electron microscopy coupled with selected area electron diffraction and energy dispersive X-ray spectroscopic analyses showed that under the test conditions, the geopolymerisation reactions only occurred on the surface of the kaolinite mineral. The "surface geopolymers" held the kaolinite particles together leading to an increase in shear strength from 110 Pa to 1,010 Pa at 50 wt% solids at the optimum alkali activator dosages (1 mol/L sodium hydroxide and 0.5 mol/L sodium silicate). ICP-OES analyses done on the supernatant of geopolymerised sample showed that Al, Si and Na species dissolved and re-solidified.
5. The addition of polymer flocculant such as A3335 impedes the geopolymerisation process and reduces the final shear strength of MFT, compared with centrifuged MFT. The presence of the polymers on the surface of the clay particles may hinder the functions of the alkali activators on the clay surfaces.
6. A method of using surface geopolymerisation reactions to strengthen oil sands mature fine tailings (MFT) was proposed.

Chapter 6

Scope of Further Study

In most studies done on geopolymerisation, metakaolin has been the main focus of research interest. Metakaolin is the dehydroxylated amorphous derivative of kaolinite that has shown a lot of promise in producing construction grade products in the recent years. Studies on geopolymerisation involving only kaolinite, however, has been quite limited. It is integral to delve deeper into exploring this process to have sound understanding of mechanisms involved in the increase of strength in kaolinite at such a low concentration of alkali activators.

Since geopolymerisation on tailings sludge is an innovative approach to solve the tailings problem, there are many aspects that are yet to be explored. Some of the aspects include the study of:

- Activators other than NaOH and Na_2SiO_3 on the initiation of the geopolymerisation process and how their concentration can affect the process;
- Long range and short range forces that affect the strength of the geopolymer and a detailed account of the underlying colloidal chemistry during the geopolymerisation processes;
- The effect of the presence of species other than aluminosilicates on the surface geopolymerisation reaction.

Furthermore, to commercialize the process, this understanding needs to be safely translated into mature fine tailings to allow optimization of the necessary parameters involved in geopolymerisation reactions. Such parameters include different Si/Al ratios etc.

Some studies also pointed out the importance of cations in the geopolymerisation process (Komnitsas and Zaharaki, 2007; Silva et al., 2007). Although the majority of them assumed that cations are the main part of the process, their importance in the reaction process has not been well understood. While some studies report on cations acting as a charge balancer for the tetrahedral aluminate, others illustrate their importance as precursors of certain steps in the reaction mechanism (Lee and van Deventer, 2002; Gastuche et al., 1963; Cheng and Hazlinda, 2011). Understanding the roles of cation is further necessitated by their inherent presence in MFT, especially sodium ions. Clark Hot Water Extraction process, used in obtaining bitumen from tar sands, leaves significant quantities of sodium hydroxide in the tailings rejects.

Preliminary experiments were also carried out to assess the synergistic effect of surface geopolymerisation with polymer flocculation followed by filtration. The feasibility of this project can be further examined. Polymer flocculation with filtration is a relatively new process for dewatering oil sands tailings that can be quite promising (Alam et al., 2011;Wang et al., 2010; Y. Xu et al., 2008). However, there is still a lot of scope for improvement in this technology. Xu et al., (2008) point out the importance of specific filtration resistance in obtaining best results in dewatering of oil sands tailings with filterability decreasing with the increasing specific resistance. Flocculation has been reported to considerably decrease the specific resistance of tailings. High filtration pressure, however, can crack the cake during the filtration process and hamper the dewatering process. Hence flocculation, coupled with surface geopolymerisation, can be used to considerably decrease the specific resistance while retaining enough mechanical strength at high filtration pressure to obtain the recommended high solid content in the consolidated mature fine tailings.

Bibliography

AER. (2014). *ST98-2014 Alberta' s Energy Reserves 2013 and Supply/Demand Outlook 2014-2023*. Alberta Energy Regulator (AER). Retrieved April 20, 2015 from http://www.aer.ca/data-and-publications/statistical-reports/st98

Alam, N., Ozdemir, O., Hampton, M. A., & Nguyen, A. V. (2011). Dewatering of coal plant tailings: Flocculation followed by filtration. *Fuel*, *90*(1), 26–35.

Alberta Chamber of Resources. (1996). *Mineral developments agreement co-products study : final report.* Alberta: H.A. Simons.

Alberta Energy Regulator. (2009). Directive 074: Tailings Performance Criteria and Requirements for Oil Sands Mining Schemes, Energy Resources Conservation Board, Calgary, AB.

Allen, E. W. (2008). Process water treatment in Canada's oil sands industry: I. Target pollutants and treatment objectives. *Journal of Environmental Engineering and Science*, *7*(2), 123–138.

Andreola, F., Romagnoli, M., Castellini, E., Lusvardi, G., & Menabue, L. (2006). Role of the Surface Treatment in the Deflocculation of Kaolinite. *Journal of the American Ceramic Society*, *89*(3), 1107–1109.

ASTM Standard D2573. (2002). Standard Test Method for Field Vane Shear Test in Cohesive Soil. West Conshohocken, PA: ASTM International.

ASTM-IP petroleum measurement tables : ASTM designation D1250, IP designation 200. (1952). Philadelphia : American Society for Testing Materials.

Atkins, P. W. (2010). *Shriver & Atkins' inorganic chemistry.* New York : W. H. Freeman and Co.

Barber, M. (2004). *AST Dean Stark procedure : determination of bitumen, water and solids*. Devon, AB: Natural Resources Canada.

Barbosa, V. F. ., MacKenzie, K. J. ., & Thaumaturgo, C. (2000). Synthesis and characterisation of materials based on inorganic polymers of alumina and silica: sodium polysialate polymers. *International Journal of Inorganic Materials*, *2*(4), 309–317.

Barrer, R. M. (1982). *Hydrothermal chemistry of zeolites*. London, England : Academic Press.

BGC Engineering Inc. (2010). Review of Reclamation Options for Oil Sands Tailings Substrates. *OSRIN Report No. TR-2.*, (July), 59 pp.

Bichard, J. A. (1987). *Oil sands composition and behaviour research*. Edmonton, Alta. : AOSTRA.

Brady, P. V, & Krumhansl, J. L. (2001). The Surface Chemistry of Clay Minerals. *Surfactant Science Series*, (103), 281–302.

Burns, C. A., Guaglitz, P. A., & Russell, R. L. (2010). *Shear Strength Correlations for Kaolin / Water Slurries : A Comparison of Recent Measurements with Historical Data*. Oak Ridge.

Buseck, P. R., & Iijima, S. (1975). High Resolution Electron Microscopy of Silicates. *American Mineralogist*, *59*, 1–21.

CAPP. (2015). *Alberta Oil Sands Bitumen Valuation Methodology 2015*. Calgary, Alberta. Retrieved from http://www.capp.ca/publications-and-statistics/publications/261786

CAPP. (2015). *Taling Ponds 2015*. Calgary, Alberta. Retrieved from http://www.capp.ca/publications-and-statistics/publications/261786

Carter, R. A. (2009). Oil sands operators tackle tailings management challenges. *E&MJ - Engineering & Mining Journal VO - 210*, (4), 54.

Chalaturnyk, R. J., Don Scott, J., & Özüm, B. (2002). Management of Oil Sands Tailings. *Petroleum Science and Technology*, *20*(9-10), 1025–1046.

Chastko, P. A. (2004). *Developing Alberta's oil sands. [electronic resource] : from Karl Clark to Kyoto.* Calgary, Alta. : University of Calgary Press, c2004. Retrieved from http://login.ezproxy.library.ualberta.ca/login?url=http://search.ebscohost.com/login.aspx?direct=true&db=cat03710a&AN=alb.4333609&site=eds-live&scope=site

Chen, J.-H., Huang, J.-S., & Chang, Y.-W. (2011). Use of reservoir sludge as a partial replacement of metakaolin in the production of geopolymers. *Cement and Concrete Composites*, *33*(5), 602–610.

Cheng, Y., & Hazlinda, K. (2011). Potential application of kaolin without calcine as greener concrete: a review. *Austrailian Journal of Basic and Applied Sciences*, *5*(7), 1026–1035.

Chindaprasirt, P., Chareerat, T., & Sirivivatnanon, V. (2007). Workability and strength of coarse high calcium fly ash geopolymer. *Cement and Concrete Composites*, *29*(3), 224–229.

Clark, K. A., & Pasternack, D. S. (1932). Hot Water Seperation of Bitumen from Alberta Bituminous Sand. *Industrial & Engineering Chemistry*, *24*(12), 1410–1416.

clay mineral. (2015). In *Britannica*. Retrieved from http://www.britannica.com/science/clay-mineral

Cox, P. A. (1995). *The elements on earth : inorganic chemistry in the environment.* Oxford ; New York : Oxford University Press.

Davidovits, J. (1988). Soft Mineralurgy and Geopolymers. In J. Davidovits & J. Orlinski (Eds.), *Proceedings of the 1st International Conference on Geopolymer '88,* (Vol. 1, pp. 19–23). Compiegne, France.

Davidovits, J. (1991). Geopolymers - Inorganic Polymeric New Material. *Journal of Thermal Analysis and Calorimetry*, *37*(8), 1633–1656.

Davidovits, J. (1994). Geopolymers: Man-Made Rock Geosynthesis and the Resulting Development of Very Early High Strength Cement. *Journal of Materials Education*, *16*(2/3), 91

Davidovits, J. (2011). *Geopolymer chemistry and applications / Joseph Davidovits.* Saint-Quentin : Institut Géopolymère.

Dawson, R., Sego, D., & Pollock, G. (1999). Freeze-thaw dewatering of oil sands fine tails. *Canadian Geotechnical Journal*, *36*(4), 587–598.

Dean, E. W., & Stark, D. D. (1920). A Convenient Method for the Determination of Water in Petroleum and Other Organic Emulsions. *Journal of Industrial & Engineering Chemistry*, *12*(5), 486–490.

Deer, W. A., Howie, R. A., & Zussman, J. (1992). *An introduction to the rock-forming minerals.* Harlow, Essex, England : Longman Scientific & Technical ; New York, NY : Wiley.

Dietrich, R. V., & Skinner, B. J. (1979). *Rocks and rock minerals.* New York : Wiley.

Diz, H. M., & Rand, B. (1989). The variable nature of isoelctric point of edge surface of kaolinite. *British Ceramic: Transactions and Journal*, *88*, 162–166.

Don Scott, J., Dusseault, M. B., & David Carrier, W. (1985). Behaviour of the clay/bitumen/water sludge system from oil sands extraction plants. *Applied Clay Science*, *1*(1-2), 207–218.

Duxson, P., Provis, J. L., Lukey, G. C., & van Deventer, J. S. J. (2007). The role of inorganic polymer technology in the development of "green concrete." *Cement and Concrete Research*, *37*(12), 1590–1597.

Dzuy, N. Q., & Boger, D. V. (1985). Direct Yield Stress Measurement with the Vane Method. *Journal of Rheology*, *29*(3), 335.

Esmaeili, P., Speirs, B. C., Ghosh, M., Lin, C., & Stea, G. (2014). *Canadian Patent No. 2873992*. Canadian Intellectual Property Office.

Ferguson, G. P., Rudolph, D. L., & Barker, J. F. (2009). Hydrodynamics of a large oil sand tailings impoundment and related environmental implications. *Canadian Geotechnical Journal Revue Canadienne de Geotechnique*, *46*(12), 1446–1460.

Flanagan, E., & Grant, J. (2013, July). Losing Ground: Why the problem of oilsands tailings waste keeps growing. *Pembina Institute*, 1–6.

Gastuche, B. M. C., Toussaint, F., Fripiat, J. J., Touilleuax, R., & Meersche, M. V. (1963). Study of intermediate stages in the kaolin to metakaolin transformation, 227–236.

Government of Alberta. (2009). *Environmental Management of Alberta's Oil Sands: Resourceful. Responsible.* Edmonton.

Hardjito, D., & Wallah, S. (2004). On the development of fly ash-based geopolymer concrete. *ACI Materials Journal*, (101), 467–472.

Hepler, L. G., & Hsi, C. (1989). *AOSTRA technical handbook on oil sands, bitumens and heavy oils.* [Edmonton, Alta.] : Alberta Oil Sands Technology and Research Authority.

IFW Dresden. (2015). TEM CM 20 FEG. Retrieved June 20, 2015, from https://www.ifw-dresden.de/?id=311

Iler, R. K. (1979). *The chemistry of silica : solubility, polymerization, colloid and surface properties, and biochemistry.* New York : Wiley.

Jaarsveld, J. G. S. van, & Deventer, J. S. J. van. (1999). Effect of the alkali metal activator on the properties of fly ash-based geopolymers. *Industrial and Engineering Chemistry Research*, *38*(10).

Johnson, R. L. (1993). *Oil sands sludge dewatering by freeze-thaw and evapotranspiration*. Edmonton, Alta.

Kaminsky, H. A. (2009). *Characterization of an Athabasca oil sand ore and process streams*. [Thesis Dissertation] University of Alberta.

Karimi, G., & Macdonald, D. (2013). US Patent No. 20130019780. Google Patents.

Kasperski, K. L. (2001). *A review of oil sands aqueous extraction research : draft.* [S.l.] : CANMET, Western Research Centre.

Kasperski, K. L., & Mikula, R. J. (2011). Waste Streams of Mined Oil Sands: Characteristics and Remediation. *Elements*, *7*(6), 387–392.

Khale, D., & Chaudhary, R. (2007). Mechanism of geopolymerisation and factors influencing its development: a review. *Journal of Materials Science*, *42*(3), 729–746.

Komnitsas, K., & Zaharaki, D. (2007). Geopolymerisation: A review and prospects for the minerals industry. *Minerals Engineering*, *20*(14), 1261–1277.

Lee, J. K., Shang, J. Q., Wang, H., & Zhao, C. (2014). In-situ study of beneficial utilization of coal fly ash in reactive mine tailings. *Journal of Environmental Management*, *135*, 73–80.

Lee, W. K. W., & van Deventer, J. S. J. (2002). The effects of inorganic salt contamination on the strength and durability of geopolymers. *Colloids and Surfaces A: Physicochemical and Engineering Aspects*, *211*(2-3), 115–126.

Liu, Q., Cui, Z., & Etsell, T. (2006). Characterization of Athabasca oil sands froth treatment tailings for heavy mineral recovery. *Fuel*, *85*(5-6), 807–814.

Lizcano, M., Kim, H. S., Basu, S., & Radovic, M. (2011). Mechanical properties of sodium and potassium activated metakaolin-based geopolymers. *Journal of Materials Science*, *47*(6), 2607–2616. 4

Long, J., Li, H., Xu, Z., & Masliyah, J. H. (2006). Role of colloidal interactions in oil sand tailings treatment. *AIChE Journal*, *52*(1), 371–383.

Lowenstein, W. (1954). The distribution of aluminium m the tetrahedral of silicates and aluminates. *American Mineralogist*, *39*, 92–96.

MacKenzie, K. J. D., Komphanchai, S., & Vagana, R. (2008). Formation of inorganic polymers (geopolymers) from 2:1 layer lattice aluminosilicates. *Journal of the European Ceramic Society*, *28*(1), 177–181.

MacKinnon, M. D. (1989). Development of tailings pond at Syncrude's oil sands plant: 1978-1987. *AOSTRA Journal of Research*, *5*(2), 109–133.

Masliyah, J. H., Xu, Z., Czarnecki, J. A., & Dabros, M. (2011a). *Handbook on theory and practice of bitumen recovery from Athabasca Oil Sands.* Cochrane, Alta. : Kingsley Knowledge Pub.

Masliyah, J., Zhou, Z. J., Xu, Z., Czarnecki, J., & Hamza, H. (2004). Understanding Water-Based Bitumen Extraction from Athabasca Oil Sands. *The Canadian Journal of Chemical Engineering*, *82*(4), 628–654.

McFarlane, A., Yeap, K. Y., Bremmell, K., & Addai-Mensah, J. (2008). The influence of flocculant adsorption kinetics on the dewaterability of kaolinite and smectite clay mineral dispersions. *Colloids and Surfaces A: Physicochemical and Engineering Aspects*, *317*(1-3), 39–48.

Mercier, P. H. J., Le Page, Y., Tu, Y., & Kotlyar, L. (2008). Powder X-ray Diffraction Determination of Phyllosilicate Mass and Area versus Particle Thickness Distributions for Clays from the Athabasca Oil Sands. *Petroleum Science and Technology*, *26*(3), 307–321.

Mikula, R. J., Kasperski, K. L., Burns, R. D., & MacKinnon, M. D. (1996). Nature and fate of oil sands fine tailings. *Suspensions: Fundamentals and Applications in the Petroleum Industry*, *251*, 677–723.

Mikula, R. J., Zrobok, R., & Omotoso, O. (2004). The potential for carbon dioxide sequestration in oil sands processing streams. *Journal of Canadian Petroleum Technology*, *43*(8), 48–52.

Mikula, R., & Omotoso, O. (2006). Role of Clays in Controlling Oil Sands Tailings Processing. *Clay Science*, *12*(2), 177–182.

Miller, F. A., & Wilkins, C. H. (1952). Infrared spectra and characteristic frequencies of inorganic ions. *Analytical Chemistry*, *24*(8), 1253–1294.

Mitchell, J. K., & Soga, K. (2005). *Fundamentals of soil behavior.* Hoboken, NJ : John Wiley & Sons Inc.

Moffett, R. H., & Andrin, P. (2013). Canadian Patent No.2684155A1 . Google Patents.

NEB. (2000). *Canada's oil sands: A supply and market outlook to 2015*. Alberta, Canada.

NEB. (2004). *Canada's oil sands: Opportunities and challenges to 2015: an update*. Alberta, Canada.

Ng, S., Warszynski, P., Zembala, M., & Malysa, K. (2000). Bitumen-air aggregates flow to froth layer: II. Effect of ore grade and operating conditions on aggregate composition and bitumen recovery. *Minerals Engineering*, *13*(14-15), 1519–1532.

Northern Illinois University - Chemistry Analytical Lab. (2007). FT-IR sample preparation. Retrieved July 21, 2014, from http://www.niu.edu/analyticallab/ftir/samplepreparation.shtml

O'Keefe, M. A., Buseck, P. R., & Iijima, S. (1978). Computed crystal structure images for high resolution electron microscopy. *Nature*, *274*(5669), 322.

Omotoso, O., Eberl, D., Canmet, E., & US Geological. (2009). Sample preparation and data collection strategies for x-ray diffraction quantitative phase analysis of clay-bearing rocks. In *6th Annual Clay Minerals Society Meeting* (p. 125). Billings, MT.

Omotoso, O., Mikula, R., Urquhart, S., Sulimma, H., & Stephens, P. (2006). Characterization of Clays from Poorly Processing Oil Sands using Synchrotron Techniques TT - Characterization of Clays from Poorly Processing Oil Sands using Synchrotron Techniques. *Clay Science*, *12*(2), 88–93.

Palomo, A., Fernandez-Jimenez, A., & Criado, M. (2003). "Geopolymers": same basic chemistry, different microstructures. *Materiales De Construccion*, *15*(275), 77-91

Phair, J. W., & Van Deventer, J. S. J. (2002). Effect of the silicate activator pH on the microstructural characteristics of waste-based geopolymers. *International Journal of Mineral Processing*, *66*, 121–143.

Proskin, S., Sego, D., & Alostaz, M. (2010). Freeze-thaw and consolidation tests on Suncor mature fine tailings (MFT). *Cold Regions Science and Technology*, *63*(3), 110–120.

Provis, J. L., & van Deventer, J. S. J. (2007). Geopolymerisation kinetics. 2. Reaction kinetic modelling. *Chemical Engineering Science*, *62*(9), 2318–2329.

Rodrigues J B, Oliveira A.P., Alarcon O.E., Pozzi P., A. F. (2002). Comparative Study of Deflocculation Mechanisms in Colloidal Clay Suspensions. *Qualicer 2002*, 283-300.

Sarojam, P. (2010). *ICP-Optical Emission Spectroscopy*. Shelton, CT 06484 USA.

Shaw, R. C., Schramm, L. L., & Czarnecki, J. (1996). Suspensions in the hot water flotation process for Canadian oil sands. *Suspensions: Fundamentals and Applications in the Petroleum Industry*, *251*, 639–675.

Silva, P. De, Sagoe-Crenstil, K., & Sirivivatnanon, V. (2007). Kinetics of geopolymerisation: Role of Al2O3 and SiO2. *Cement and Concrete Research*, *37*(4), 512–518.

Sobkowicz, J. (2012). The Oil Sands Tailings Technology Roadmap and Action Plan: Introduction and Key Recommendations. In *Third International Oil Sands Tailings Conference* (pp. 13–22). Oil Sands Tailings Research Facility, University of Alberta.

Sobkowicz, J. (2013). *Oil sands tailings technology deployment roadmaps. [electronic resource]*. Alberta Innovates, Energy and Environment Solutions, Edmonton. Retrieved from http://login.ezproxy.library.ualberta.ca/login?url=http://search.ebscohost.com/login.aspx?direct=true&db=cat03710a&AN=alb.6177377&site=eds-live&scope=site

Sperinck, S., Raiteri, P., Marks, N., & Wright, K. (2011). Dehydroxylation of kaolinite to metakaolin—a molecular dynamics study. *Journal of Materials Chemistry*, *21*(7), 2118.

Srodon, J. (1999). Nature of mixed-layer clays and mechanisms of their formation and alteration. *Annual Review of Earth and Planetary Sciences*, *27*, 19–53.

Starr, J., & Bulmer, J. T. (1979). *Syncrude analytical methods for oil sand and bitumen processing.* Edmonton : Alberta Oil Sands Technology and Research Authority, 1979.

Swaddle, T. W. (2001). Silicate complexes of aluminum(III) in aqueous systems. *Coordination Chemistry Reviews*, *219-221*, 665–686.

Syncrude. (2012). Tailings Management. Retrieved from http://www.syncrudesustainability.com/2012/environment/tailings-management/

Takamura, K. (1982). Microscopic structure of athabasca oil sand. *The Canadian Journal of Chemical Engineering*, *60*(4), 538–545.

Tsaprailis, H., & Zhou, J. (2013). Properties of Dilbit and Conventional Crude Oils. *Alberta Innovates.* Retrieved from http://www.ai-ees.ca/media/10927/properties_of_dilbit_and_conventional_crude_oils_-_aitf_-_final_report.pdf

Van Jaarsveld, J. G. S., Lukey, G. C., van Deventer, J. S. J., & Graham, A. (2000). The stabilisation of mine tailings by reactive geopolymerisation. *Minprex 2000: International Congress on Mineral Processing and Extractive Metallurgy*, *2000*(5), 363–371.

Van Olphen, H. (1977). *An introduction to clay colloid chemistry for clay technologists, geologists, and soil scientists*. Natl. Acad. Sci., Washington, D.C., United States: John Wiley & Sons.

Van Riessen, A., Jamieson, E., Kealley, C. S., Hart, R. D., & Williams, R. P. (2013). Bayer-geopolymers: An exploration of synergy between the alumina and geopolymer industries. *Cement and Concrete Composites*, *41*, 29–33.

Wang, H., Li, H., & Yan, F. (2005). Synthesis and mechanical properties of metakaolinite-based geopolymer. *Colloids and Surfaces A: Physicochemical and Engineering Aspects*, *268*(1-3), 1–6.

Wang, X. (Tara), Feng, X., Xu, Z., & Masliyah, J. H. (2010). Polymer aids for settling and filtration of oil sands tailings. *The Canadian Journal of Chemical Engineering*, *88*(3), 403–410.

WWF-Canada. (2010). *Tailings , A Lasting Oil Sands Legacy*. Retrieved May 20, 2015 from http://awsassets.wwf.ca/downloads/wwf_tailings_report_october_2010_final.pdf

Xu, H., & Van Deventer, J. S. J. (2000). The geopolymerisation of alumino-silicate minerals. *International Journal of Mineral Processing*, *59*(3), 247–266.

Xu, H., & Van Deventer, J. S. J. (2002). Geopolymerisation of multiple minerals. *Minerals Engineering*, *15*(12), 1131–1139.

Xu, Y., Dabros, T., & Kan, J. (2008). Filterability of oil sands tailings. *Process Safety and Environmental Protection*, *86*, 268–276.

Yao, X., Zhang, Z., Zhu, H., & Chen, Y. (2009). Geopolymerisation process of alkali–metakaolinite characterized by isothermal calorimetry. *Thermochimica Acta*, *493*(1-2), 49–54.

Yukselen, Y., & Kaya, A. (2003). Zeta potential of kaolinite in the presence of alkali, alkaline earth and hydrolyzable metal ions. *Water, Air, and Soil Pollution*, *145*, 155–168.

Yukselen-Aksoy, Y., & Kaya, a. (2011). A study of factors affecting on the zeta potential of kaolinite and quartz powder. *Environmental Earth Sciences*, *62*(4), 697–705.

Zaman, A., Demir, F., & Finch, E. (2003). Effects of process variables and their interactions on solubility of metal ions from crude kaolin particles: Results of a statistical design of experiments. *Applied Clay Science*, *22*(5), 237–250.

Zaman, A., & Mathur, S. (2004). Influence of dispersing agents and solution conditions on the solubility of crude kaolin. *Journal of Colloid and Interface Science*, *271*(1), 124–130.

Zbik, M., & Smart, R. S. C. (1998). Nanomorphology of kaolinites; comparative SEM and AFM studies. *Clays and Clay Minerals*, *46*(2), 153–160.

Zhang, L., Ahmari, S., & Zhang, J. (2011). Synthesis and characterization of fly ash modified mine tailings-based geopolymers. *Construction and Building Materials*, *25*(9), 3773–3781.

Appendix A

Table 10: Shear strengths of kaolinite and centrifuged MFT samples in test series A-1, A-2, B-1, B-2 and C-1.

Sample Name	Test Material	Moisture	NaOH		Na_2SiO_3		Shear strength after 90 days (Pa)
			mol/L of water	kg/t of dry material	mol/L of water	kg/t of dry material	
A-1-1	Kaolinite/Water	50.0%	1	40	0	0	545
A-1-2	Kaolinite/Water	50.0%	1	40	0.15	18.3	532
A-1-3	Kaolinite/Water	50.0%	1	40	0.2	24.4	507.9
A-1-4	Kaolinite/Water	50.0%	1	40	0.25	30.5	513
A-1-5	Kaolinite/Water	50.0%	1	40	0.33	40	612
A-1-6	Kaolinite/Water	50.0%	1	40	0.5	61.0	1013
A-1-7	Kaolinite/Water	50.0%	1	40	0.65	79.3	958
A-1-8	Kaolinite/Water	50.0%	1	40	0.8	97.6	1006
A-1-9	Kaolinite/Water	50.0%	1	40	1	122.2	976
A-2-1	Centrifuged MFT	47.3%	1	37.8	0	0	1501
A-2-2	Centrifuged MFT	47.3%	1	37.8	0.15	17.3	2064
A-2-3	Centrifuged MFT	47.3%	1	37.8	0.2	23.1	3525
A-2-4	Centrifuged MFT	47.3%	1	37.8	0.25	28.8	3865
A-2-5	Centrifuged MFT	47.3%	1	37.8	0.33	37.8	4427
A-2-6	Centrifuged MFT	47.3%	1	37.8	0.5	57.7	5641
A-2-7	Centrifuged MFT	47.3%	1	37.8	0.65	75.1	3920
A-2-8	Centrifuged MFT	47.3%	1	37.8	0.8	92.3	4414
A-2-9	Centrifuged MFT	47.3%	1	37.8	1	115.5	3918
B-1-1	Kaolinite/Water	50.0%	0	0	0	0	329
B-1-2	Kaolinite/Water	50.0%	0.01	0.38	0.0033	0.4	304
B-1-3	Kaolinite/Water	50.0%	0.1	3.8	0.033	3.8	-
B-1-4	Kaolinite/Water	50.0%	0.5	18.9	0.16	18.9	431
B-1-5	Kaolinite/Water	50.0%	1	37.8	0.33	37.8	848
B-2-1	Centrifuged MFT	47.3%	0	0	0	0	114
B-2-2	Centrifuged MFT	47.3%	0.01	0.4	0.0033	0.4	352
B-2-3	Centrifuged MFT	47.3%	0.1	4	0.033	4	777

B-2-4	Centrifuged MFT	47.3%	0.5	20	0.16	20	3564
B-2-5	Centrifuged MFT	47.3%	1	40	0.33	40	3573
C-1-1	Centrifuged MFT	47.3%	0	0	0	0	119
C-1-2	Centrifuged MFT	47.3%	0.01	0.38	0	0	507
C-1-3	Centrifuged MFT	47.3%	0.1	3.8	0	0	803
C-1-4	Centrifuged MFT	47.3%	0.5	18.9	0	0	1158
C-1-5	Centrifuged MFT	47.3%	1.0	37.8	0	0	1458

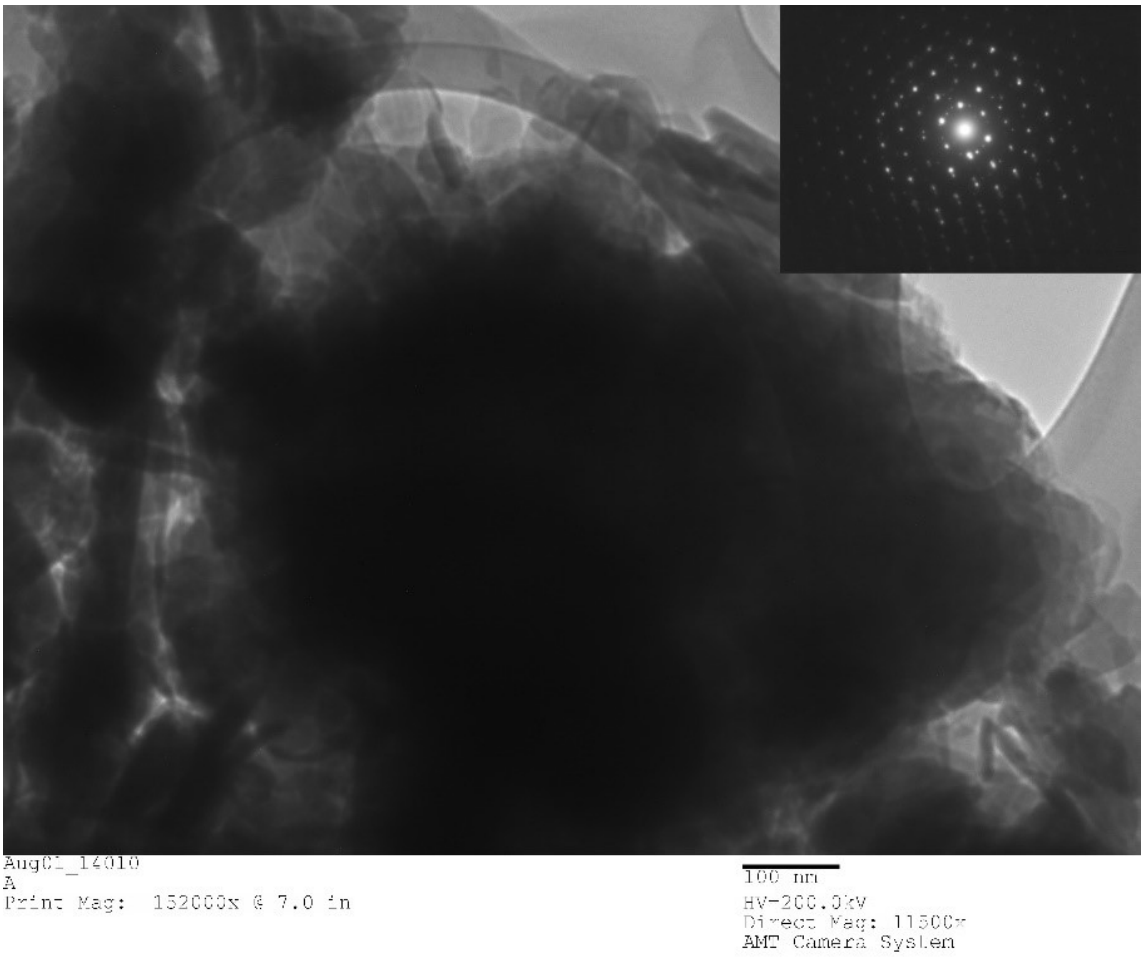

Figure 33: TEM/SAED of kaolinite solids at 200 kV

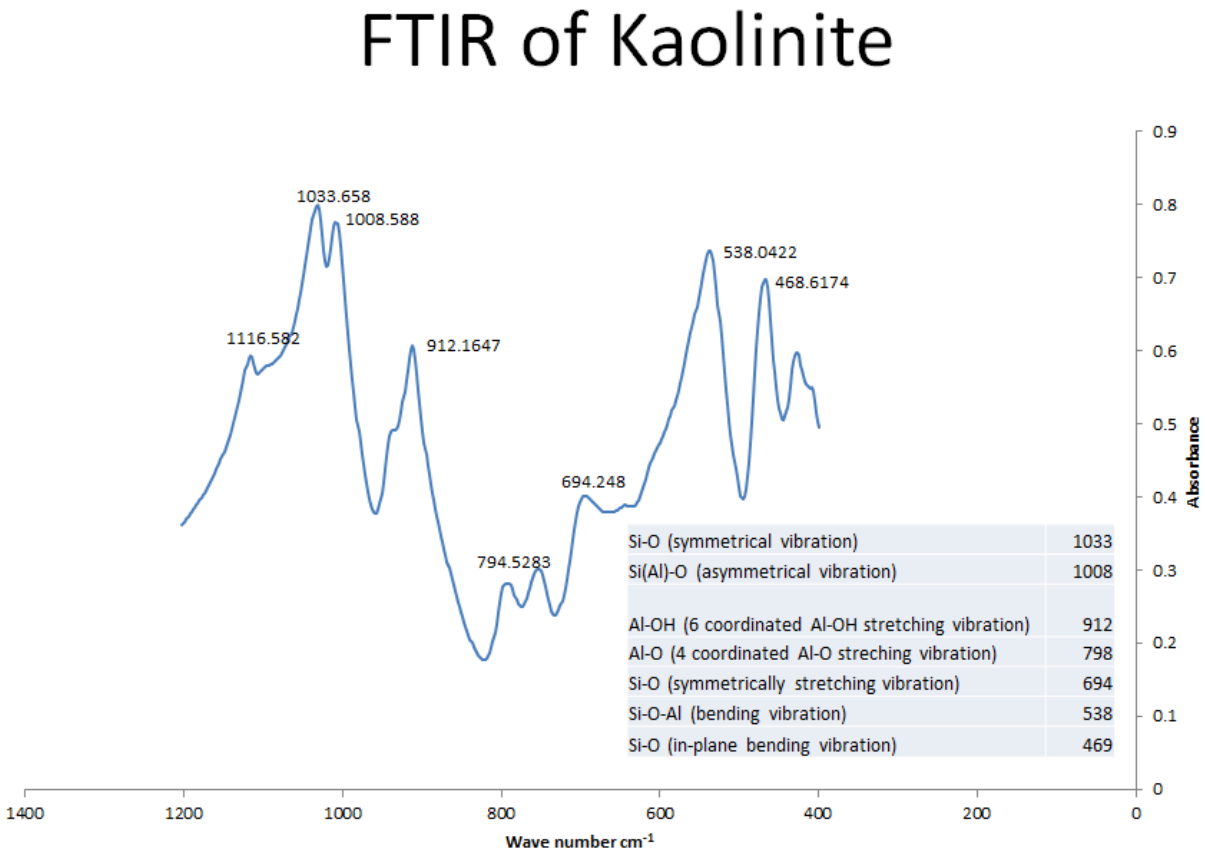

Figure 34: FTIR analysis done on kaolin solids with peak assignments of vibrational modes for kaolinite found in literature

Appendix B - Preliminary Compressive Strength Measurements Using Penetrometer

Compressive strength measurements were carried out on preliminary test series A-1, B-1, A-1, A-2 and C-1 using a field penetrometer shown in Figure 35.

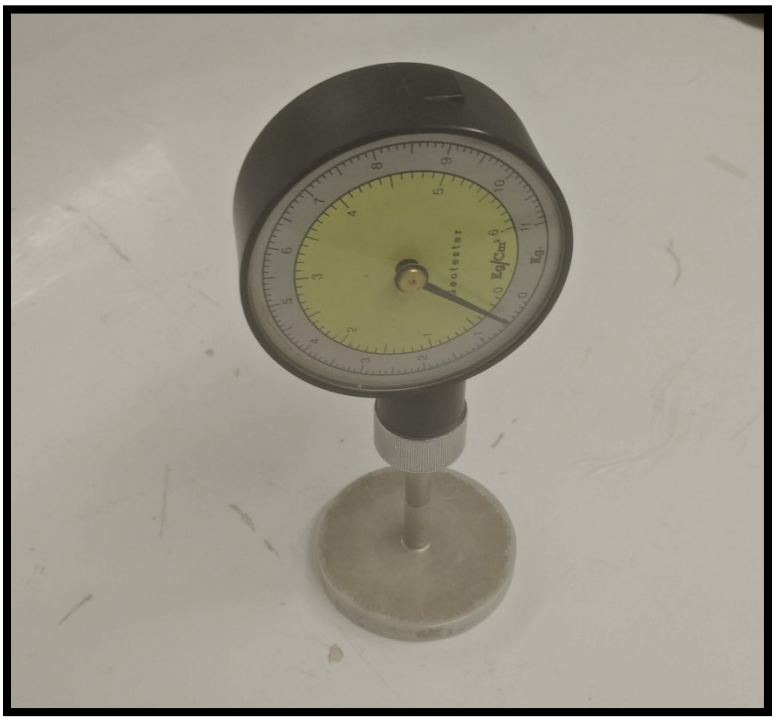

Figure 35: Field Penetrometer

The results of the measurements carried out using this device have been illustrated from Figure 36 to 40. The compressibility was calculated by multiplying the penetrometer reading with gravitational acceleration ($9.8 m/s^2$) and dividing the resultant value by the area of the tip.

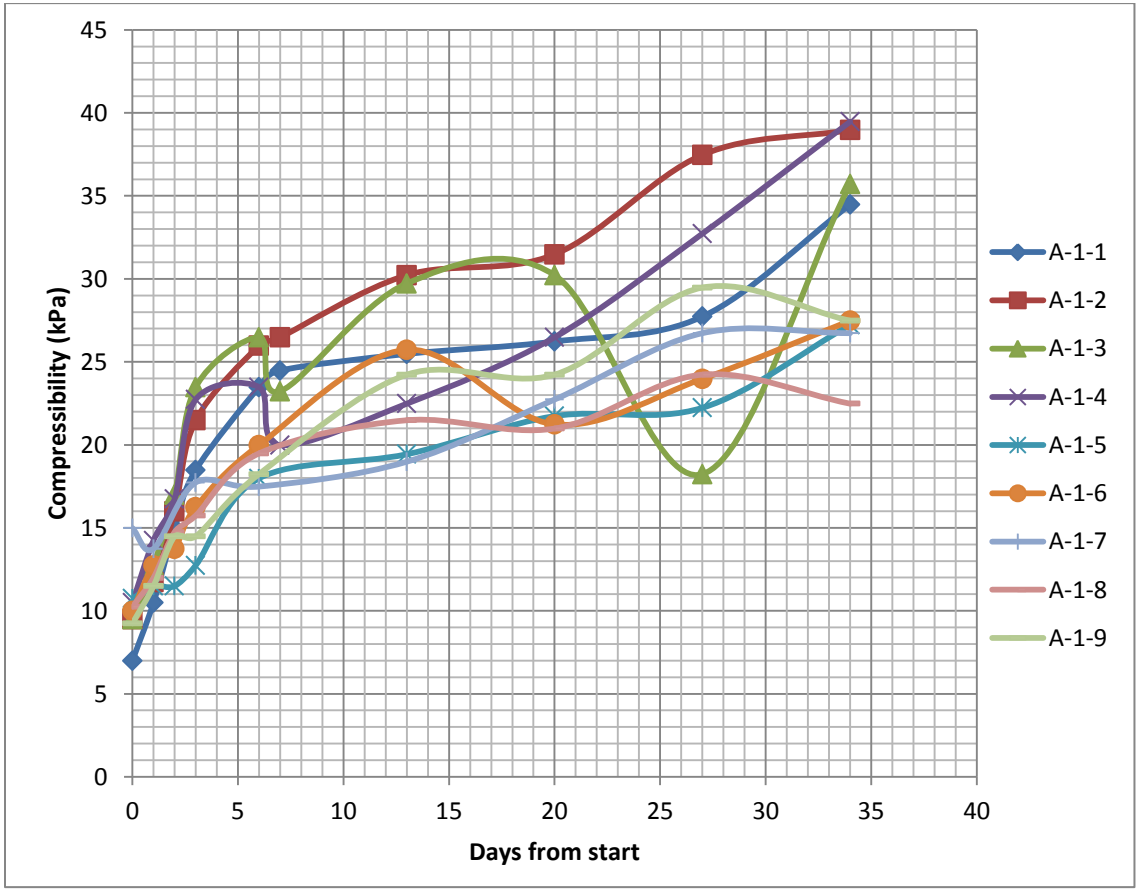

Sample No.	*Na_2SiO_3: NaOH ratio.*
A-1-1	0:1
A-1-2	0.15:1
A-1-3	0.2:1
A-1-4	0.25:1
A-1-5	0.33:1
A-1-6	0.5:1
A-1-7	0.65:1
A-1-8	0.8:1
A-1-9	1:1

Figure 36: Compressive strength of Kaolin/water mixture in different silicate to hydroxide ratio (Sample series A-1) measure over a period of five weeks

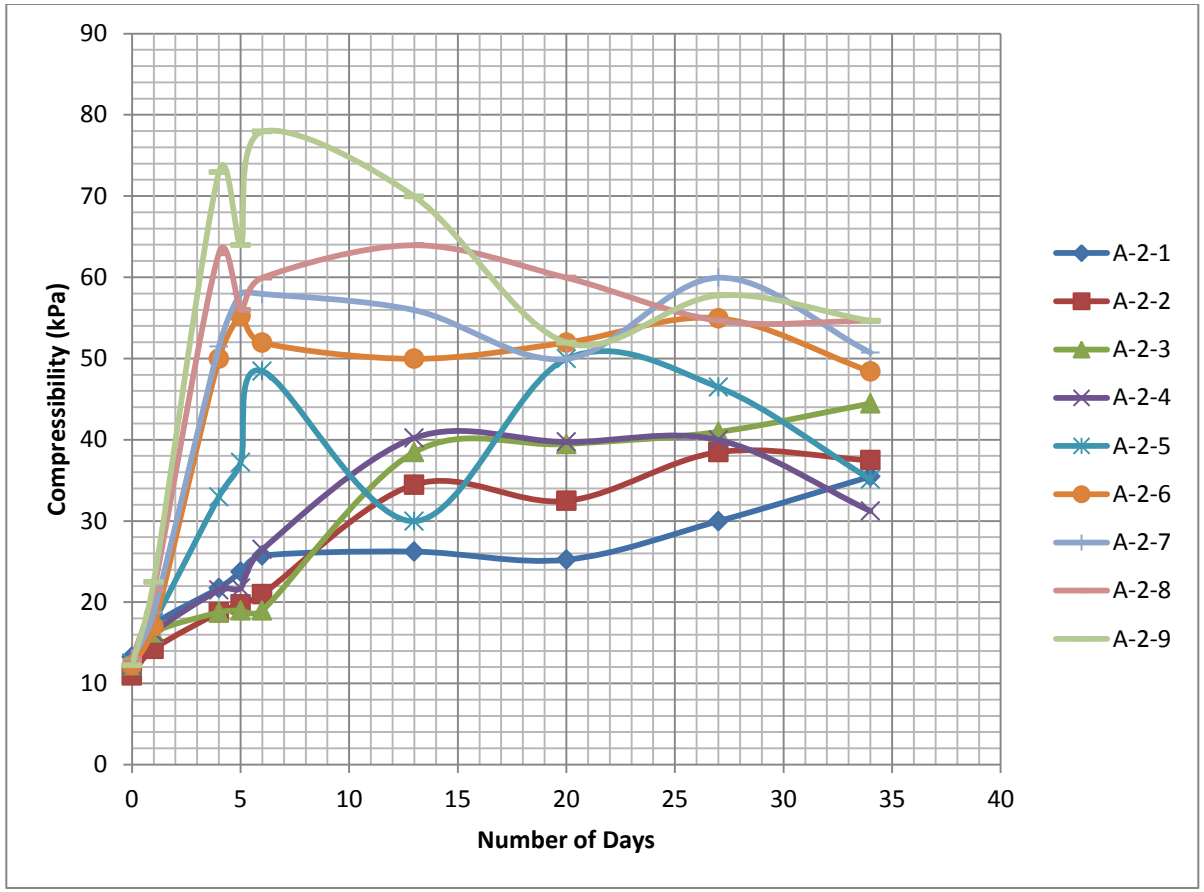

Sample No.	*Molar Ratio – Na_2SiO_3:NaOH*
A-2-1	0:1
A-2-2	0.15:1
A-2-3	0.2:1
A-2-4	0.25:1
A-2-5	0.33:1
A-2-6	0.5:1
A-2-7	0.65:1
A-2-8	0.8:1
A-2-9	1:1

Figure 37: Compressive strength of centrifuged MFT (51 wt% solids) in different silicate to hydroxide ratio (Sample series A -2) measured over a period of five weeks

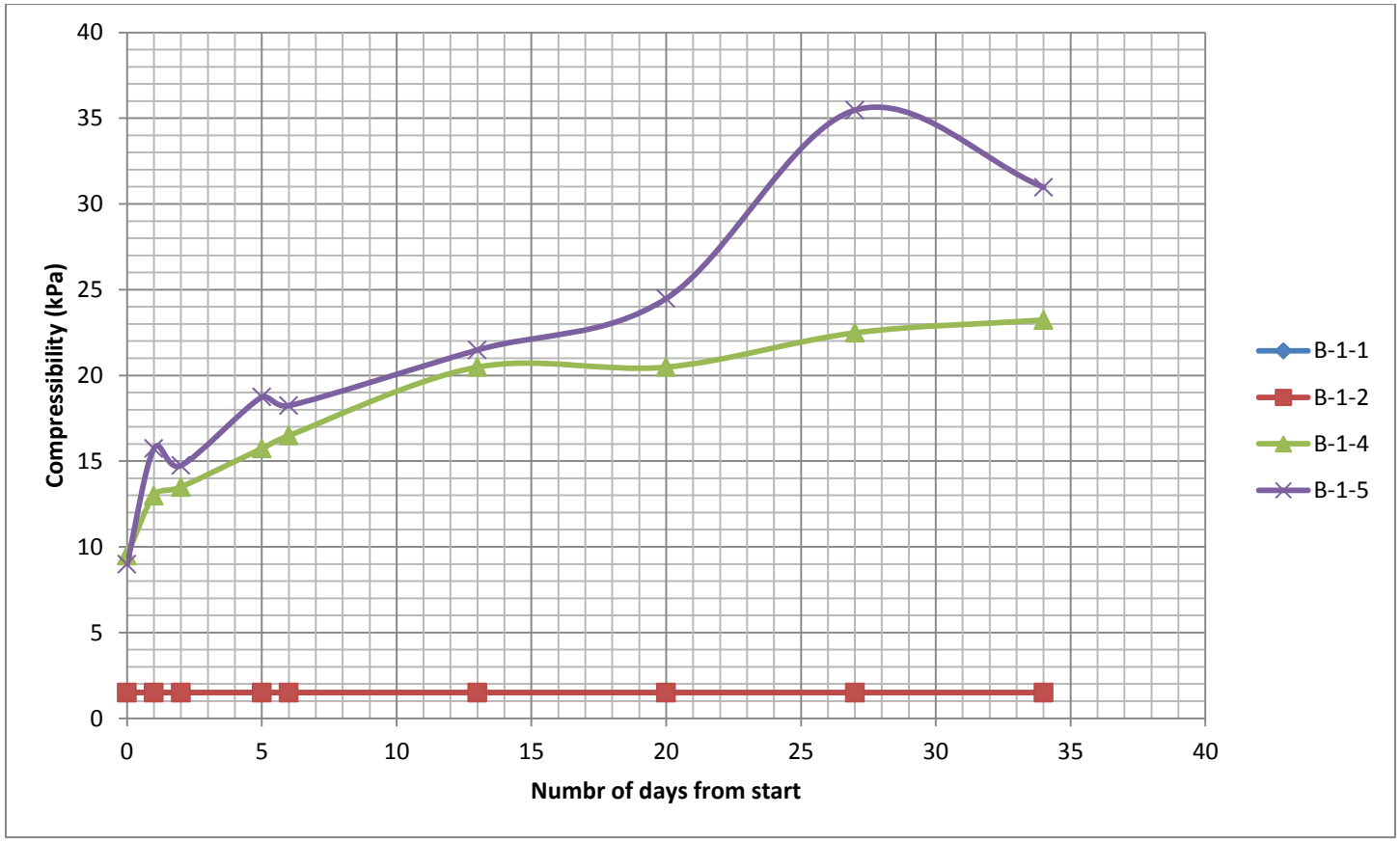

Figure 38: Compressive strength of Kaolin/water mixture in increasing silicate and hydroxide concentration at a fixed ratio (Sample series B-1) measured over a period of five weeks. Samples B-1-1 and B-1-3 had negligible compressive strength and could not be recorded

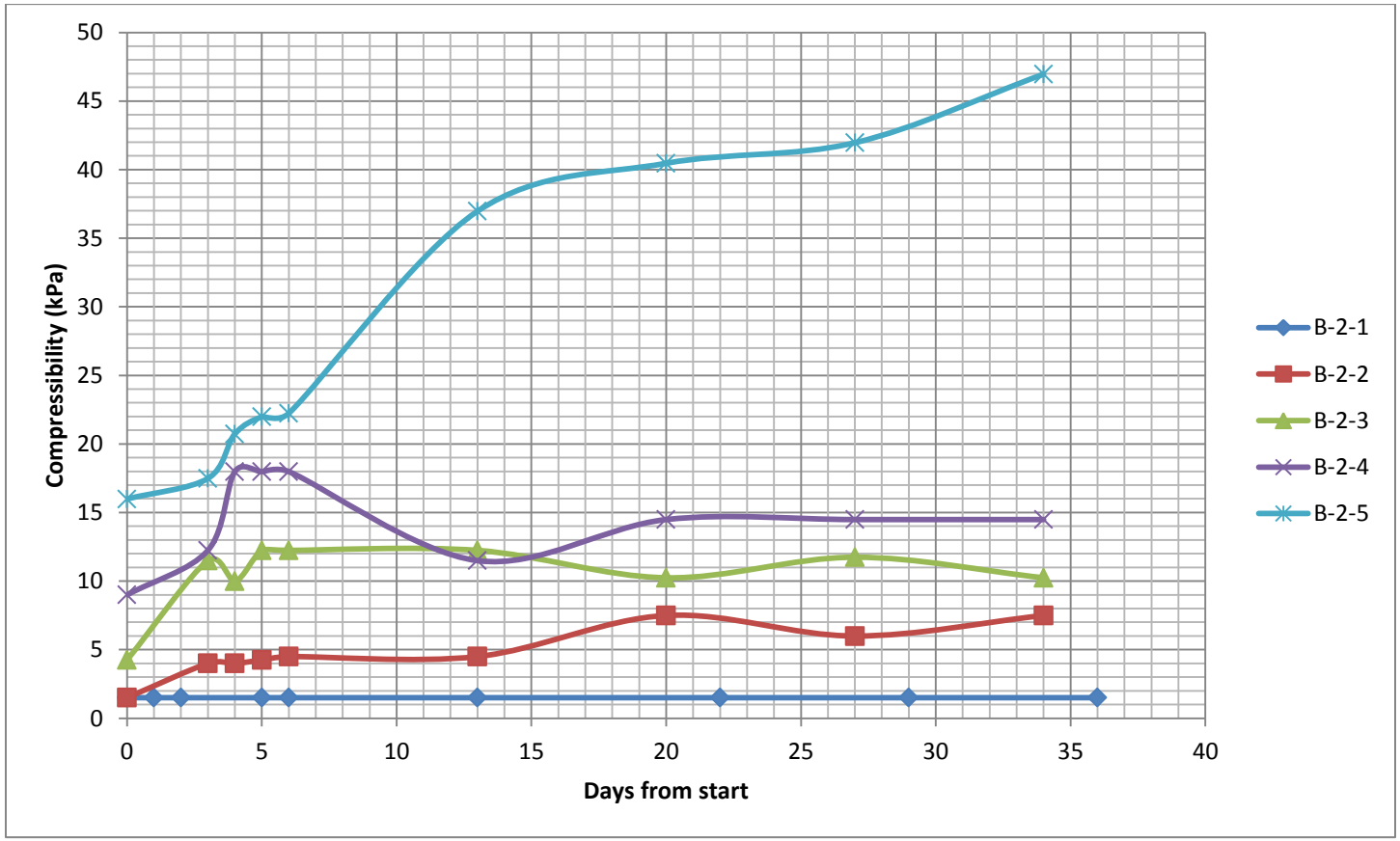

Figure 39: Compressive strength of centrifuged MFT (51 wt% solids) in increasing silicate and hydroxide concentration at a fixed ratio (Sample series B-1) measured over a period of five weeks

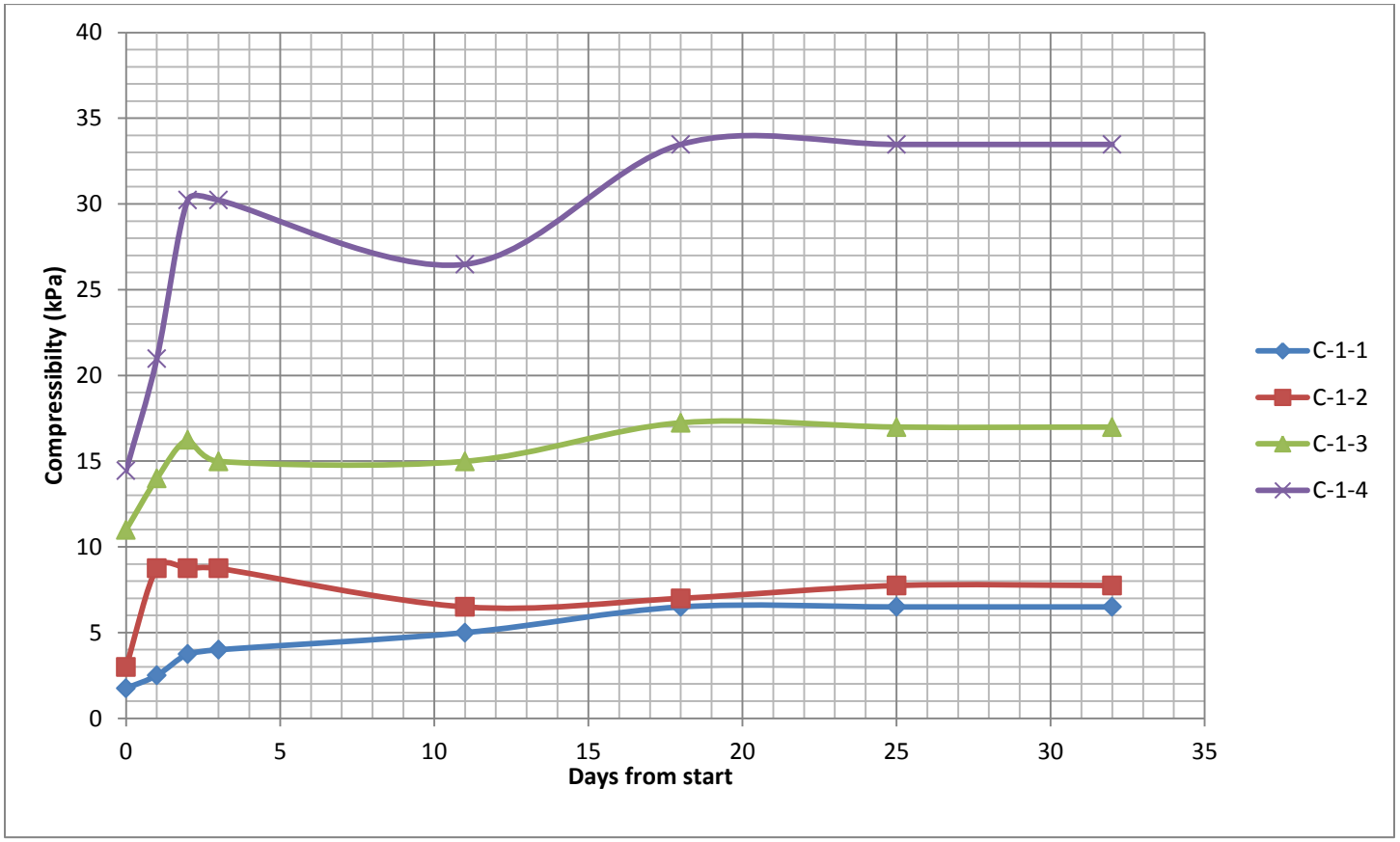

Figure 40: Compressive strength of centrifuged MFT (51 wt% solids) in different NaOH concentrations (w/o Silicate) measured over a period of five week

Appendix C- Photos from the Study

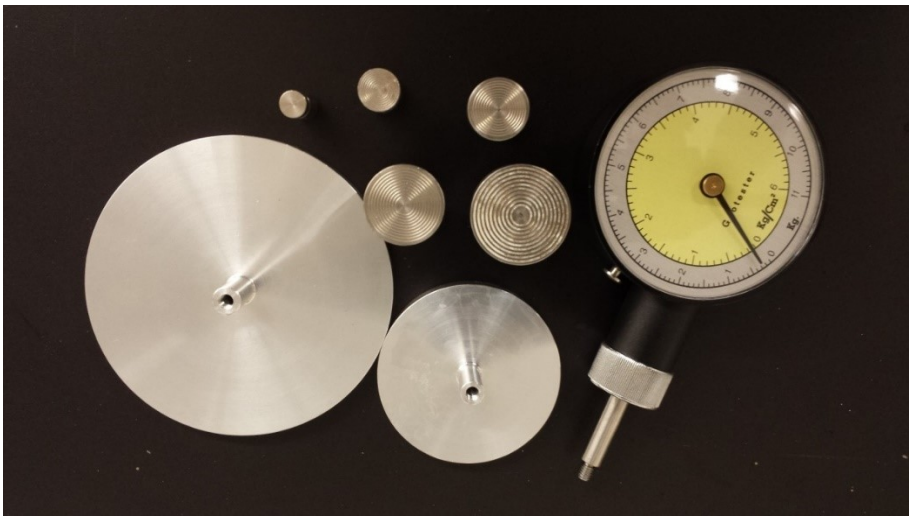

Figure 41: Field penetrometer set

Figure 42: Mastersizer 3000 used for laser particle size analysis

Figure 43: Dean Stark extraction set up for determining bitumen, water and solids content

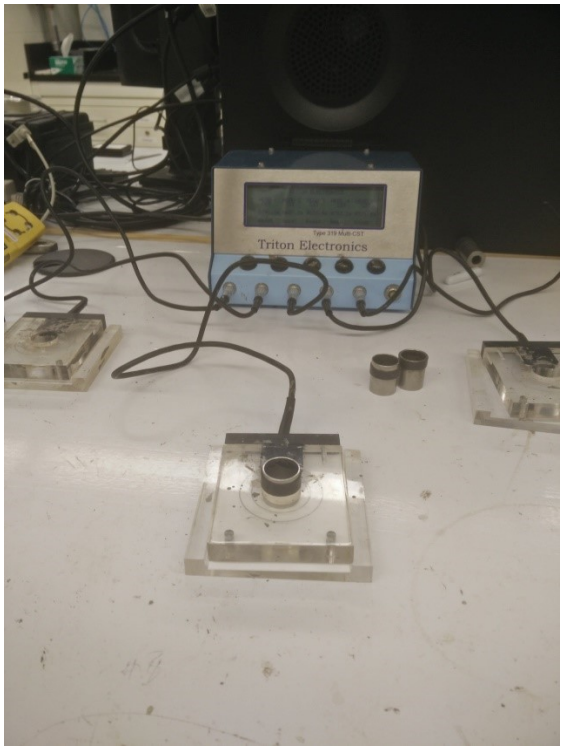

Figure 44: CST apparatus from Triton Electronics

Figure 45: Heidolph™ Electronic Overhead Stirrer (RZR 2052 Control)

Figure 46: Thermoscientic Nicolet 6700 Fourier Transform Infrared (FTIR) spectrometer

Figure 47: Mettler Toledo HB43-S Halogen Moisture Analyzer

Figure 48: Philips CM20 FEG TEM/STEM transmission electron microscope (IFW, 2015)